STRUCTURES AND THERMAL STABILITY OF SELECTED ORGANIC INCLUSION COMPOUNDS

BY:

NIKOLINA JANJIC




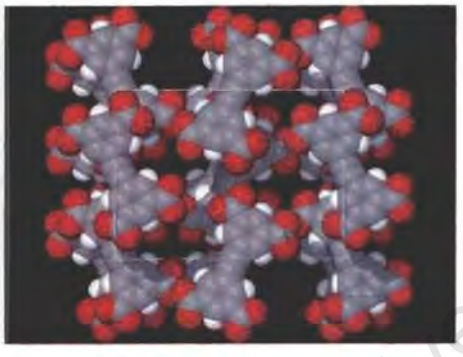

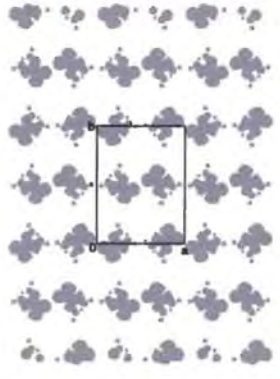

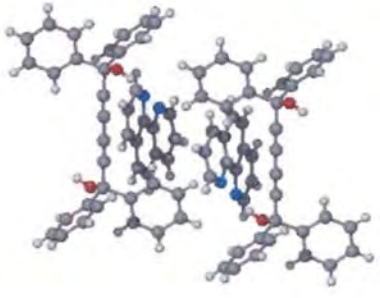


THESIS PRESENTED TO THE UNIVERSITY OF CAPE TOWN FOR THE DEGREE OF MASTER OF SCIENCE

April 2002

ABSTRACT

The crystal structures of 1,1,6,6-Tetraphenyl-hexa-2,4-diyne-1,6-diol and 5-(3,5-Dicarboxyphenylethynyl)-isophthalic acid hosts with various guests have been elucidated. Depending on their structural properties and the way in which the host components pack, the guests may become trapped in spaces or voids, stacked in channels or sandwiched between layers of hosts. The crystal structures are stabilised by hydrogen bonding networks created by host-guest intermolecular interactions. The host hydroxy moieties adopt a *trans* conformation in 1,1,6,6-Tetraphenyl-hexa-2,4-diyne-1,6-diol host-guest inclusion componds. Host-guest hydrogen bonding in 5-(3,5-Dicarboxyphenylethynyl)-isophthalic acid salts occurs *via* the carboxylate group of the host anion. Hydrogen bond formation was the directing force determining the form of a host-guest array.

The crystal structures of four inclusion compounds with 1,1,6,6-Tetraphenyl-hexa-2,4-diyne-1,6-diol host and six hydrated salt structures with 5-(3,5-Dicarboxyphenylethynyl)-isophthalic acid host were solved using the single crystal X-ray diffraction technique. In addition the thermal stability and the structural properties of all compounds were investigated by thermal analysis techniques, including differential scanning calorimetry, thermogravimetry and hot-stage microscopy.

ABBREVIATIONS AND SYMBOLS

Compounds

H_1: 1,1,6,6-Tetraphenyl-hexa-2,4-diyne-1,6-diol

H_2: 5-(3,5-Dicarboxyphenylethynyl)-isophthalic acid

H_1 • TED	**H_1 • Triethylenediamine**
H_1 • TBDA	**H_1 • N,N,N',N'-Tetracyclohexyl-2,2'-biphenyldicarboxamide**
H_1 • PA	**H_1 • 1,10-Phenanthroline**
H_1 • 4PP	**H_1 • 4-Phenylpyridine**
H_2 • RPEA	H_2 • (+)-(R)-1-Phenylethylamine
H_2 • RSPEA	H_2 • (±)-(R,S)-1-Phenylethylamine
H_2 • PEA	H_2 • 2-Phenylethylamine
H_2 • Na	H_2 • sodium
H_2 • Rb	H_2 • rubidium
H_2 • Cs	H_2 • caesium

Techniques

XRD	X-Ray Powder Diffraction
DSC	Differential Scanning Calorimetry
TG	Thermogravimetry
HSM	Hot Stage Microscopy

Symbols

α	The angle between the *b* and *c* unit cell axes
β	The angle between the *a* and *c* unit cell axes
γ	The angle between the *a* and *b* unit cell axes
T_{onset}	Onset temperature
F	Structure Factor
F(000)	Number of electrons in the unit cell
τ	Torsion angle
I	Intensity
G	Guest
H	Host
H:G	Host to guest ratio
Endo	Endothermic
ΔH	Enthalpy Change
e.s.d.	Estimated Standard Deviation
V	Cell Volume
Z	Number of structural units in the unit cell
*	Asymmetric carbon
b.p	Boiling point
m.p	Melting point

TABLE OF CONTENTS

1 INTRODUCTION

"Mankind is divisible into two great classes: hosts and guests."

Max Beerbohm (b. 1872), Hosts and guests

ABOUT HOST-GUEST COMPOUNDS

Molecular assemblies held together by a range of relatively weak intermolecular interactions[1] broadly describe a supramolecular, host-guest complex. Hosts can be described as molecular entities able to form interlayer spaces, channels or closed voids, while guests are molecular entities filling these spaces to achieve high packing efficiency and thermodynamic stability in the crystal.[2,3] The host and guest terminology was introduced in 1974 by D. J. Cram and J. M. Cram[4].

Associations between host and guest molecules, H and G, are usually based on simultaneous non-covalent interactions between single binding sites, A (acceptor) and D (donor).[5] These interactions usually include cations and anions, hydrogen bonding acceptors and donors, or enforced encapsulation of the guest within closed host cavities.

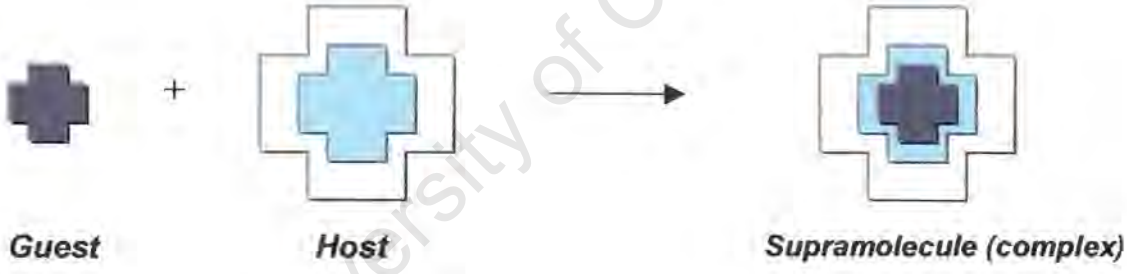

Figure 1.1: Schematic representation of a host-guest relationship

The supramolecular, host-guest complex is characterised by degree of order, interactions between subunits, symmetry of packing and intermolecular interactions[6].

Non-covalent interactions are weak interactions, creating a need for several binding sites to achieve strong and specific complexation (recognition) of a guest molecule. The binding sites of a host molecule are positioned as close to a guest as possible. This causes the overall free energy of host-guest complex formation to be more favourable[7]. Another requirement that dictates the magnitude of any molecular

recognition, occurring for a given supramolecular system, is the degree of electronic and steric complementarity between host and guest. In other words complexation is most efficient when the shapes and arrangements of binding sites in host and guest molecules fit each other. This is the general *lock* and *key* principle of the host-guest relationship.

Clathrate compounds were brought to light by the pioneering work of Powell[8] providing the fundamental insight and the experimental means required to understand the structural and bonding features of inclusion compounds. The word clathrate comes from the Latin word *clathratus,* and it describes something that is enclosed or protected by the crossbars of a grating.

Over the years different terminology has been used to describe inclusion compounds[9]. All of the terms that are given describe the molecules, firmly united to each other without the operation of strong attractive forces between them, kept together through the enclosure of one by the other, of both by each other, or in more complex ways[8]. Confusion over the terminology used for the description of inclusion compounds resulted in a classification of clathrates proposed by Weber and Josel[10,11], according to the host-guest type (charged, polar and neutral), host-guest interaction, topology (layer, ring, channel, pocket, cage) and the number of components forming the host-guest aggregate (two, three, many).

Host-guest interactions include ion-ion, donor-acceptor, van der Waals, steric barrier and are summarised in Figure 1.2.

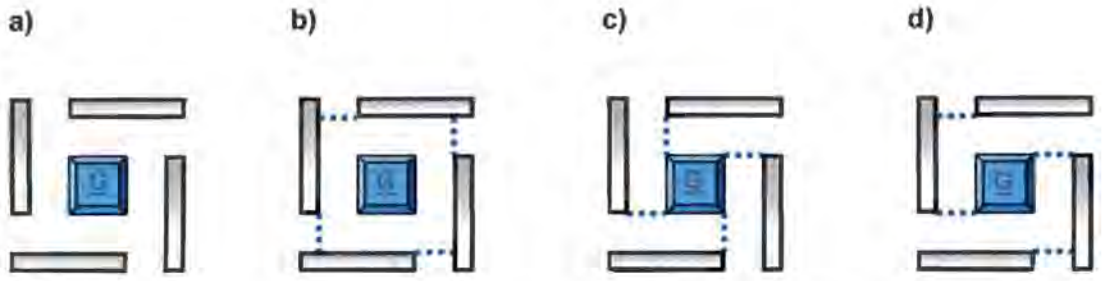

Figure 1.2: Types of host-guest interaction in the lattice[11]

a) Represents a non-coordinative interaction and it is considered to be a true *clathrate*. The guest is enclosed by steric barriers of the host lattice in order to stabilise the crystal structure. In **b)** there is additional stabilisation by host-host interactions. This is called a *coordination-assisted clathrate host lattice*. **c)** Represents *coordinato clathrate* with coordinative host-guest interactions and in **d)** there are both coordinative host-host and host-guest interactions called *coordinato clathrate in a coordination-assisted host lattice*.

Inclusion compounds can be classified into two groups based on the host-guest interaction. The host and guest coordinated together form a *complex* that retains its identity in solution. Examples of host molecules that form complexes are crown ethers[12] and cryptands[13]. On the other hand, the inclusion compounds in which the guest species are retained by steric barriers (voids formed by hosts) are known as *clathrates*. Clathrates tend to decompose on dissolution and some of the clathrate examples include those in which urea[14] and Dianin's compound[15] are the hosts.

Types of voids encountered in clathrate lattices made by host molecules to accommodate guests include different geometries or topologies. These topologies are presented in Figure 1.3 and include a) 2-D layers, b) ring, c) non-intersecting channels, d) intersecting channels, e) cages, f) interconnected cages[16].

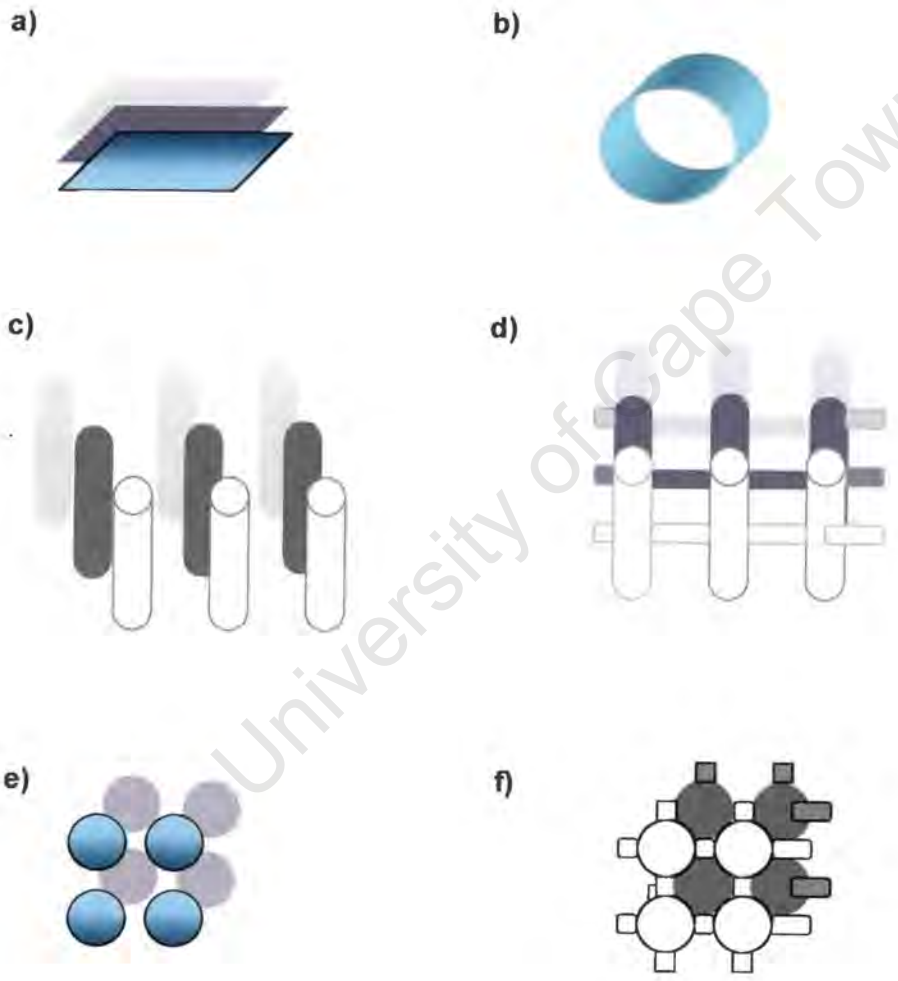

Figure 1.3: Topologies of voids in clathrate lattice

INTERMOLECULAR INTERACTIONS: the glue of supramolecular chemistry

Supramolecular chemistry is chemistry beyond the molecule.[17] It can be described as the chemistry of multicomponent molecular assemblies in which the component structural units are typically held together by a variety of weaker (non-covalent) interactions[18]. This world of supramolecular architecture contains a large number of other self-assembled systems in which metal-donor bonds are employed to 'stitch' together organic components into larger assemblies.

Apart from the special case where metal ions are used as the 'glue', central to the supramolecular field is the use of weaker, non-covalent interactions. Long-range molecular forces are used to describe these non-covalent interactions[19-21]. They are related to the internuclear distance and include van der Waals, electrostatic (including hydrogen bonding) and π-π interactions. These interactions contribute primarily towards supramolecular complexation.

The most important of the 'glues' is the hydrogen bond. The term hydrogen bond was coined in 1920 to describe the internal structure of water, but since then the meaning of the term has been subject to change. Generally it can be described as an attractive interaction between a proton donor and a proton acceptor. Pimentel and McClellan defined a hydrogen bond as a bond that exists between a functional group A (donor)-H and an atom or a group of atoms B (acceptor) in the same or a different molecule[22]. Donor and acceptor atoms have electronegative character, with the hydrogen bond proton being shared between their electron pairs. Hydrogen bonds can be described according to their strengths as weak, medium and strong[22]. They can be the strongest and most directing of the intermolecular interactions, but also weak enough to match van der Waals forces. The range and diversity of hydrogen bonding types is summarised in Figure 1.4[5].

Hydrogen bonding has been described as the 'masterkey interaction in supramolecular chemistry'. In hydrogen bonding C-H, N-H, O-H, S-H, P-H, F-H, Cl-H, Br-H and I-H are the most common donor groups, while acceptor groups include N,

O, P, S, F, Cl, Br and I as well as alkenes, alkynes, aromatic rings and transition metals[23]. Apart from basic requirements for hydrogen bond existence, contraction of bond lengths has been used as a criterion for the existence of hydrogen bonding[24]. It has been suggested that the distance between two atoms involved in hydrogen bonding ~~should be~~ is less than the sum of their van der Waals radii[25].

A recent review by Steiner[26], describes many aspects of the hydrogen-bond in the solid state. In particular, it is pointed out that the energy associated with hydrogen bonds covers a large range. For some gas-phase dimers the calculated energies vary from 39 kcal mol^{-1} in the case of $[F\text{-}H\text{-}F]^-$ to just 0.2 kcal mol^{-1} for $CH_4\cdots F\text{-}CH_3$.

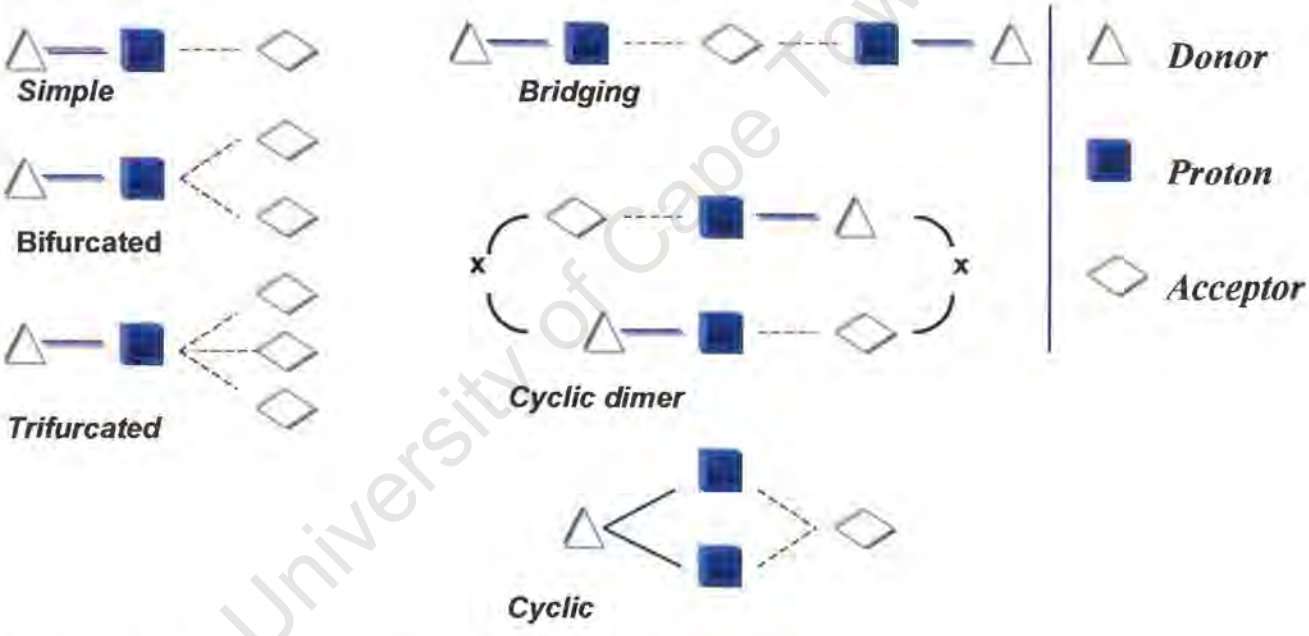

Figure 1.4: Common arrangements of hydrogen bond types

Hydrogen bonding is one of the main characteristics of compounds with –COOH and –OH groups in their structure.[27,28] Accordingly, it also plays a decisive role in the packing pattern of these compounds in the crystalline state.[29]

When acceptor atoms are more electronegative than carbon, the hydrogen bonds are strong enough to match covalent bonds and they correspond to the stongest intermolecular forces found in supramolecular systems. However, it is only recently

that a weaker category of hydrogen bond has been recognised and it is of type C-H···A, where A is F, O, N, Cl, Br or I[23, 30,31]. The reason for this late acceptance was that these interactions do not fall below the respective van der Waals sum values. Systems incorporating weaker (longer) hydrogen bonds exibit a greater tendency to be associated with bond angles showing a greater deviation from linearity.

Another type of hydrogen bond involves π-facial interactions that bear a relationship to both a donor-acceptor hydrogen bond as well as to a π-π bonded system[32,33]. Interactions of this type tend to be weak and usually act in a co-operative manner with other intermolecular interactions; for example, they help to dictate a precise orientation within a given supramolecular system. The π-facial interactions are also considered as C-H···π weak hydrogen bonds. The nature of π-facial interactions has

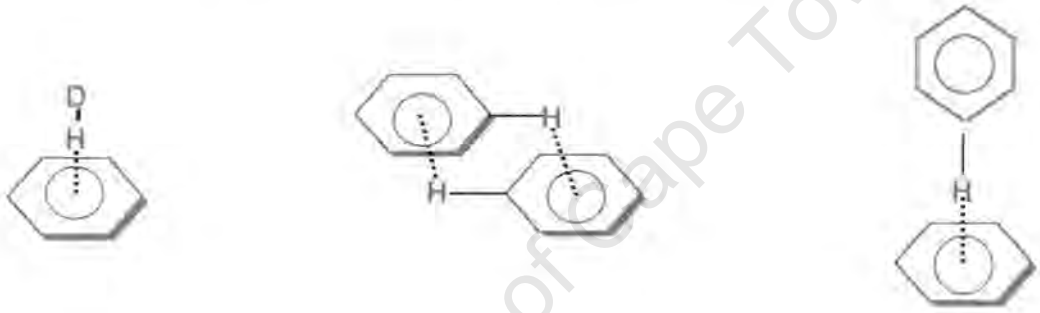

Figure 1.5: Weak hydrogen bond π- facial interactions

been believed to lie in weak electrostatic forces. However, recently it was suggested that London dispersion forces might play a more important role than electrostatic interactions[6].

Solid-state structures have a very small amount of 'empty' space, which is due to their need to achieve a close packed arrangement. Close packing in the solid state, also a significant driving force, is simply a result of maximisation of favourable isotropic van der Waals interactions. In order to achieve efficient packing, Kitaigorodsky has suggested that molecules undergo a shape simplification as they progress towards dimers, trimers, higher oligomers and ultimately crystals[27]. This means that molecules are filling the voids in order to achieve a maximum number of intermolecular contacts.

Non-covalent bonding interactions are used to define and direct the self-assembly processes that lead to new supramolecular systems. However, these forces still continue to govern any dynamic processes once the respective systems are formed. Weak, non-covalent intermolecular interactions are mainly analysed and discussed in supramolecular systems. However, many contain stronger covalent linkages between their individual components. In many systems this involves metal ion co-ordination in which the metal links individual components within the overall structure.

CRYSTAL ENGINEERING STRATEGIES FOR HOST SYSTEMS

A clear understanding of weak intermolecular interactions and the ways in which they coexist in crystals is the key aspect of crystal engineering. A few structural features have been identified as attributes of a good host-guest system and represent desirable goals in the crystal engineering methodology of these substances. They include the host molecules, building a framework independent of the nature of the guest and a possibility to accommodate a wide variety of guest species. Also, altering the host properties should be possible without changing the essential host structure. The goal in the crystal engineering of a host network is to attempt to make the packing of a single species difficult, while the goal in the engineering of a combined host-guest system is to optimise specific intermolecular interactions[34]. These two goals can be summed up in a strategy developed by Weber and co-workers. This so-called strategy of co-ordinato clathration is based on a host system designed to be awkwardly shaped, bulky and highly symmetrical and also containing functional groups that are capable of hydrogen bonding to the guest.[35,36] This is illustrated schematically in Figure 1.6, showing a guest (represented by a circle) that is hydrogen bonded to the host system (hydrogen bonds are represented by dotted lines).

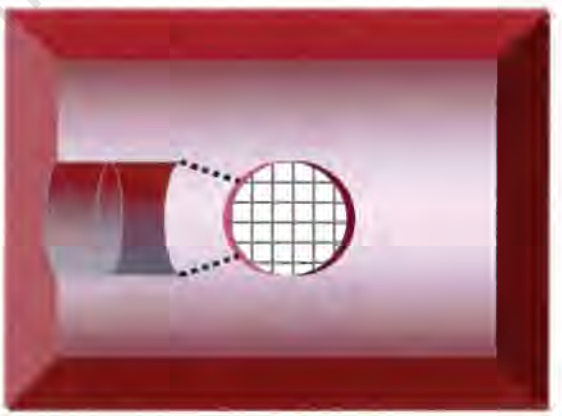

Figure 1.6: Schematic view of a co-ordinato clathrate[37]

HOST DESIGN

In order to design a host that will selectively bind a particular guest, matching of host and guest steric and electronic requirements is necessary. The first step in host design is a clear definition of the host and guest parameters, such as size, charge, character of the donor atoms etc. Since host-guest interactions occur through binding sites, then the number and the type of binding sites of each host and the guest must complement each other. Host binding sites should be spaced apart from each other to minimise repulsions between them, but arranged so that they can all interact simultaneously with the guest. The nature of the organic framework of the host itself plays a fundamental role in host behaviour, determining the solubility characteristics of the host and its complexes.

Up to the early 1980's the majority of the host-guest compounds had been chance discoveries. Simply modifying sections of the known host, new host compounds were created. The host lattice cavity size can be varied as well as selectivity of that host for different guests. An example of this is the modification of Dianin's compound, where the cavity size and geometry changed by simply adding a methyl group[15].

Hexagonal building blocks were identified as the main structural characteristics of such clathrates, observed also in the packing of quinol clathrates. The concept of the hexagon as a template for clathrate formation was used by MacNicol, who designed a new host class, hexa-hosts[38,39]. Hosts of this type are characterised by hexa-substituted benzene rings, where by varying the substituent side arms, the inclusion cavity can be tuned to specific geometric and steric requirements.

An increasing number of new compounds that are unrelated to previous host arrangements have been designed since then, based on the knowledge gained from known crystal structures.

The dictates of crystal close packing suggest that even in the absence of specific, strong attractive interactions, the general effect of dispersion/van der Waals forces will be such as to induce molecules to fill as much space as possible. Organic molecules are frequently of irregular shape and unsymmetrical, but despite this they may pack regularly without the inclusion of solvent molecules. This is due to their conformational flexibility and the 'soft' nature of van der Waals forces. Therefore, a

host molecule possessing bulky groups will be unable to pack efficiently and reach the required energy minimum of crystal formation. It will therefore be energetically favourable to incorporate small 'space-filler' molecules to fill these gaps, in order to achieve a stable crystal structure. In addition to steric features the host should possess enough rigidity to support the clathrate structure.

In 1968 Toda[40] designed host compounds with rigid frame and bulky spacer groups. A linear acetylenic spacer coupled with bulky end groups acts as a solid-state host for a variety of guests. This is due to its need to fill in the empty spaces between the two bulky spacer groups effectively portioned off[41]. The host compounds of this type are called 'wheel and axle' hosts by virtue of their molecular shape (Figure 1.7)[42].

'Wheel and axle'

Figure 1.7: Schematic representation of 'wheel and axle' host.

The empty spaces can be occupied either by a complementary shaped adjacent host molecule or a guest with which the host compound co-crystallises[43]. In order to enhance the selectivity of a geometrically favourable host, directional control in the form of functional groups was introduced. Since host-guest interactions usually occur via hydrogen bond formation, the introduction of functional groups improved inclusion selectivity[44]. Therefore, the functional groups involved in the host-guest inclusion are hydroxyl, carboxyl or amide moieties.

Numerous hydroxy host systems, known as diol hosts, have been synthesised and can be used for rational design of new and more efficient host systems[45-48]. They are able to include a wide variety of guests and form crystalline inclusion compounds. Some of these host systems are represented in Figure 1.8.

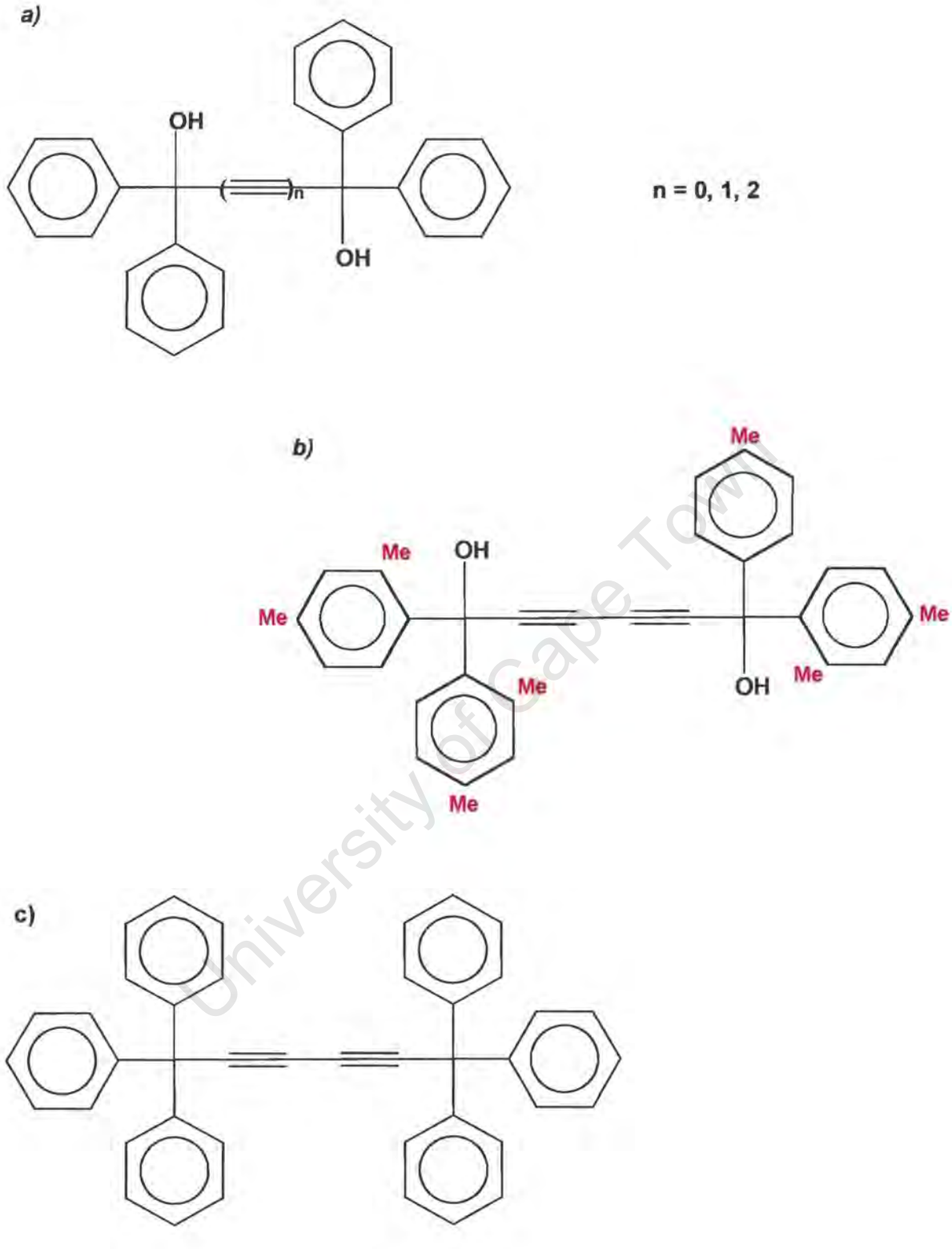

Figure 1.8: Examples of 'wheel and axle' host compounds.

'Wheel and axle' hosts with n = 0, 1 and 2 (Figure 1.8 a)) showed that the increase in alkyne chain length enhances the inclusion ability of the host. This is attributed to the larger lattice void in which to accommodate the guest being created as n increases[49]. The analyses of crystal structures of inclusion complexes with this host type showed that the inclusion is mediated via hydrogen bond formation. Enhanced inclusion ability is also obtained if the host compound contains bulkier spacer groups (Figure 1.8 b)). If these groups decrease in size, little or no inclusion is obtained[40].

(Figure 1.8 c)) shows a case where the basic Toda's host design has been altered. The hydrogen bonding functionality was eliminated by replacement of hydroxyl groups with phenyl rings. The host-guest complexation was achieved even with the altered molecular backbone length and linearity[43,50].

Other examples of clathrate hosts, whose main mode of action is derived from a combination of the coordination and topological (steric barrier) interactions, was found to be susceptible to inclusion compound formation[51,52]. These hosts have bulky binaphthyl units that display the required topological barrier[53] (Figure 1.9) and suitably positioned substituents that mediate complementary host-guest coordination.

They readily form stoichiometric crystalline inclusion compounds with a variety of uncharged molecules[54-56].

The host compound illustrated in Figure 1.9 readily forms coordinato-clathrates and conventional clathrates with different guest molecules[57], via H-bonding[51].

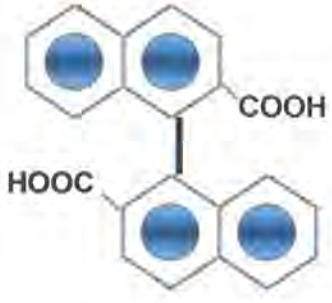

Figure 1.9: The prototype of the scissor-like host.

Further advantages of this host are that it can selectively include a guest from a solvent guest mixture and its chirality may enable the host to include guests enantioselectively[58]. Changing the positions of carboxylic groups influences the inclusion behaviour. Crystal structures of these hosts showed the preference of host-host and guest-guest interactions over host-guest bonding[59]. The extension of the central axis to three to four atoms and attachment of various functionalities and spacer groups led to new lattice-forming hosts. These hosts, synthesised by Weber and co-workers, have a bridged triarylmethane host framework, forming inclusion compounds with various organic molecules. The inclusion process depends on the bridging group, the spacer and functional groups and the substituents[60].

HOST SYSTEMS EMPLOYED IN THIS THESIS

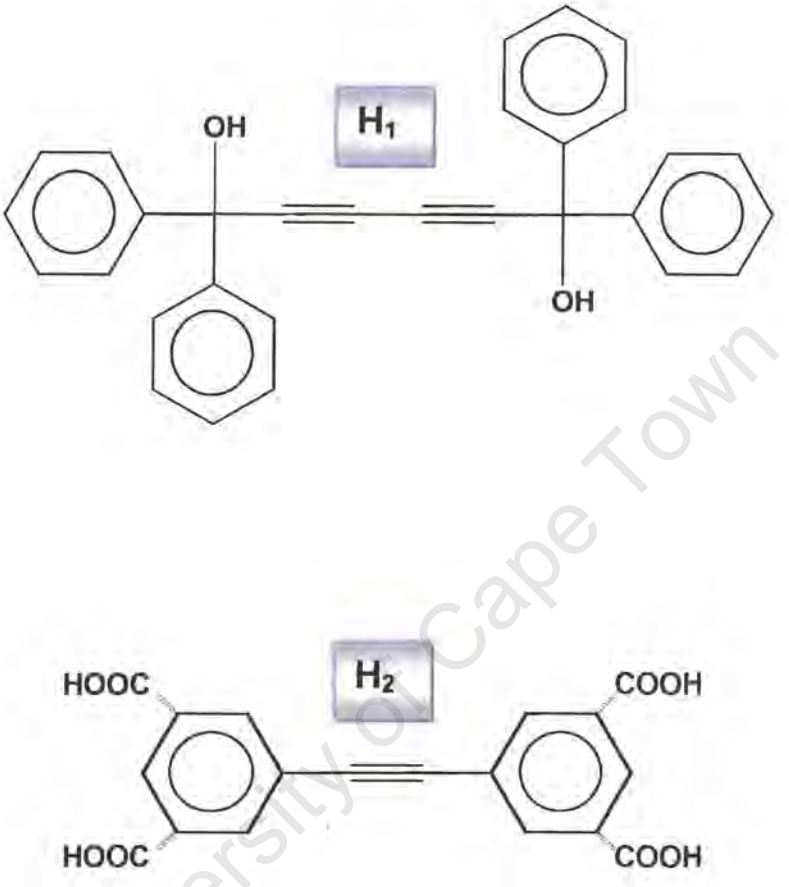

Figure 1.10: Host compounds H_1 and H_2, used in this thesis

The two host compounds, H_1 and H_2, in Figure 1.10 were used in this thesis for structure analysis. They conform to the basic ideas of forming a crystalline host structure, namely molecular bulkiness, rigidity, functional groups in suitable positions and a degree of symmetry[61-63]. They possess one of the typical overall shapes of the host structures, known as a 'dumb-bell' shape equipped with functional groups for hydrogen bonding[64]. Both host compounds are composed of structural elements that favour the efficient lattice inclusion (Figure 1.11). These are described below:

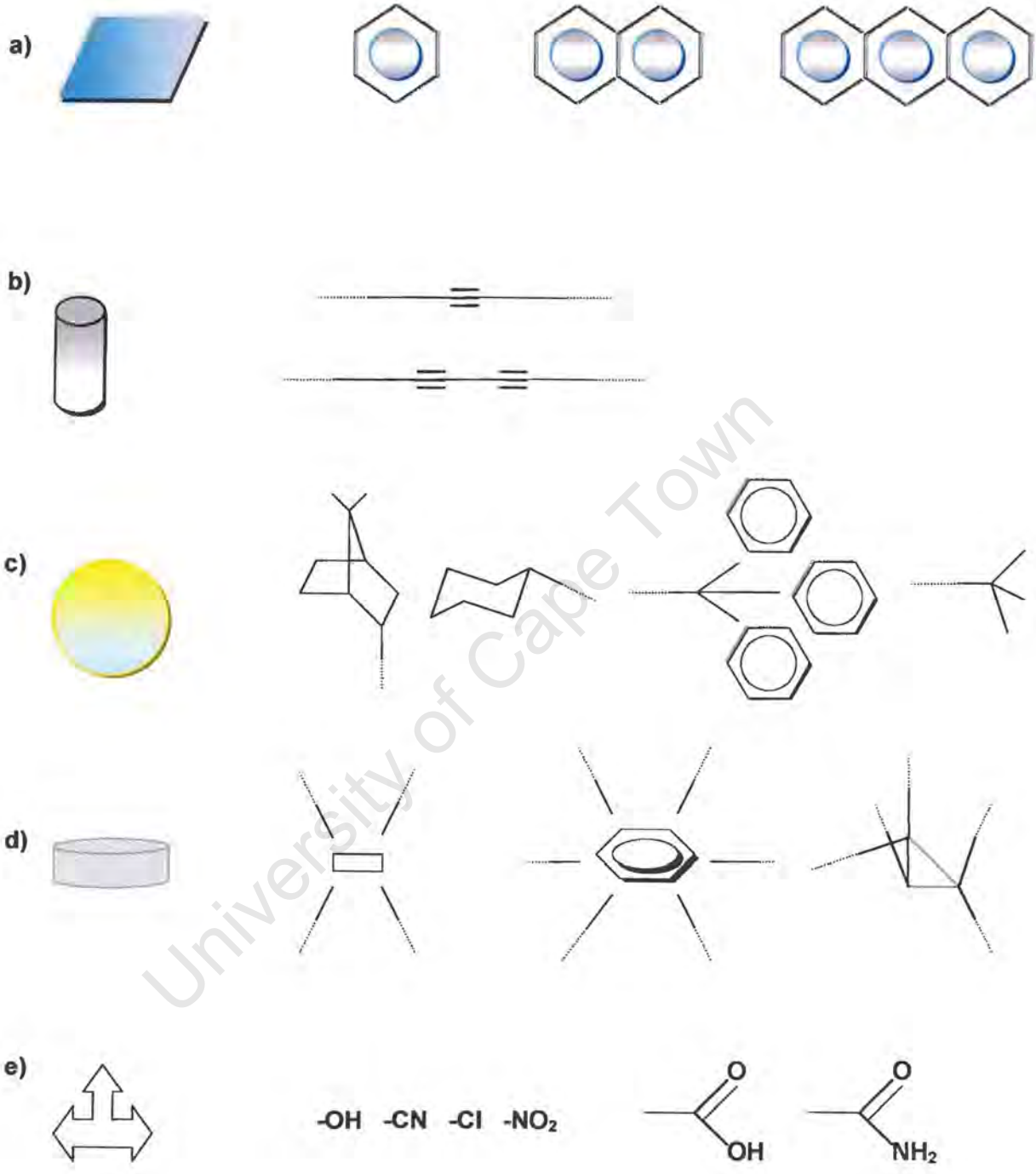

Figure 1.11: Structural building elements: **a)** planes, **b)** rods, **c)** bridged elements and spacer units, **d)** branching core molecules and **e)** anchor groups.

AIM OF THIS WORK

The work of this thesis consisted of synthesising a number of the inclusion compounds and hydrated salt compounds formed between the two hosts, $\mathbf{H_1}$ and $\mathbf{H_2}$, and selected guests. Their crystal structures were analysed in detail and their thermal stabilities investigated. The enthalpies of guest release, as well as the onset temperatures of guest release, were measured and these properties were correlated with their structures.

REFERENCES

1. H. J. Schneider, A. Yatsimirsky, Principles and Methods in Supramolecular Chemistry,Printed by Bookcraft, Great Britain, 1999, Chapter 1.
2. E. Weber, I. Goldberg, *Topics in Current Chemistry*, 1987, 149, 3.
3. R. M. Barrer, *Pure and Appl. Chem.*, 1986, 58, 1317-1322.
4. D. J. Cram, J. M. Cram, Science, 1974, 183, 803.
5. L. F. Lindoy, I. M. Atkinson, Self-Assembly in Supramolecular Systems, Cambridge University Press, Cambridge, UK, 2000, 1-46.
6. J. W. Steed, J. L. Atwood, Supramolecular Chemistry, Printed by Biddles Ltd, Great Britain, 2000, Chapter 1.
7. D. J. Cram, *J. Am. Chem. Soc.*, 1990, 112, 1254.
8. H. M. Powell, *J. Chem. Soc.*, 1948, 61-73.
9. G.R. Newkome, H. C. R. Taylor, F. R. Fronczek, T. J. Delord, D. K. Kohli, F. Vögtle, J. Am. Chem. Soc., 1981, 103, 7376.
10. E. Weber, H. P. Josel, *J. Incl. Phenom.* 1, 1983, 79-85.
11. E. Weber, *Topics in Current Chemistry*, 140, 2.
12. I. Goldberg, *Inclusion Compounds*, Vol 2, 1984, Atwood, Davies, MacNicol, eds., Academic Press, London, Chapter 9.
13. B. Metz, D. Moras, R. Weiss, *J. Chem. Soc., Chem. Commun.*, 217.
14. K. Takemoto, N. Sonoda, Inclusion Compounds, Vol 2, 1984, Atwood, Davies, MacNicol, eds., Academic Press, London, Chapter 2, 47.
15. D. D. MacNicol, Inclusion Compounds, Vol 2, 1984, Atwood, Davies, MacNicol, eds., Academic Press, London, Chapter 1.
16. K. D. M. Harris, Chemistry in Britain, 132, 1992.
17. H. J. Schneider, H. Durr, J. M. Lehn, Frontiers in Supramolecular Organic Chemistry and Photochemistry, Printed by Weinheim, Germany, 1991, 1.
18. J. M. Lehn, Nobel Lecture, Angew. Chem., Int. Ed. Engl., 1988, 112, 90.
19. G. C. Maitland, M. Rigby, E. B. Smith, W. A. Wakeham, Intermolecular Forces: Their Origin and Determination, Oxford University Press, Oxford, 1981.
20. A. D. Buckingham, A. C. Legon, S. M. Roberts, Principles of Molecular Recognition, Blackie Academic & Professional, Glasgow, 1993.
21. N. W. Alcock, Bonding and Structure, Ellis-Horwood, Chichester, 1990.
22. G. A. Jeffrey, An Introduction to Hydrogen Bonding, Oxford University Press, New York, 1997, Chapter 1.

23. C. B. Aakeröy, K. R. Seddon, *Chem. Soc. Rev.*, 1993, 22, 397.

24. M. Mascal, *Chem. Commun.*, 1998, 303.

25. W. C. Hamiton, J. A. Ibers, Hydrogen Bonding in Solids, 1968. W. A. Benjamin New York

26. T. Steiner, *Angew. Chem. Int.* Ed. 2002, Vol 41, 48-76.

27. ~~D. Hadzi, Hydrogen Bonding, Ed.; Pergamon Press, London, 1959.~~ A I Kitaigorodsky, Molecular Crystals & Molecules, Academic Press, New York & London 1973

28. S. N. Vinogravov, R. H. Linnell, Hydrogen Bonding, Eds.; Van Nostrand Reinhold, New York, 1971.

29. L. Leiserowitz, *Acta Crystallogr.*, Sect. B 1976, B32, 775.

30. G. R. Desiraju, *Acc. Chem. Res.*, 1991, 24, 291.

31. G. R. Desiraju, T. Steiner, The Weak Hydrogen Bond in Structural Chemistry and Biology, Vol. 9, Oxford University Press, Oxford, 1999.

32. H. Adams, F. J. Carver, C. A. Hunter, N. J. Osborne, *Chem. Commun.*, 1996, 2529.

33. H. Adams, K. D. M. Harris, G. A. Hembury, C. A. Hunter, D. Livingstone, J. F. McCabe, *Chem. Commun.*, 1996, 2531.

34. E. Weber, Comprehensive Supramolecular Chemistry, Vol. 6, (Solid-state Supramolecular Chemistry—Crystal Engineering), ed. J. L. Atwood, J. E. D. Davies, D. D. MacNicol, F. Vögtle, Elsevier Science, Oxford, 1996, Chapter 1.

35. E. Weber, I. Csöregh, B. Stensland, M. Czugler, *J. Amer. Chem. Soc.*, 106, 1984, 3297-3306.

36. E. Weber, *J. Mol. Graphics*, 7, 1989, 12.

37. E. Weber, I. Csöregh, J. Ahrendt, S. Finge, M. Czugler, *J. Org. Chem.*, 53, 1988, 5831.

38. E. Weber, *Topics in Current Cemistry*, Vol 140, 1987, 7-8.

39. G. R. Desiraju, G. Tsoukaris, Organic Solid State Chemistry, Elsevier, Amsterdam, 1987.

40. F. Toda, K. Akagi, *Tetrahedron Lett.*, 33, 1968, 3695-3698.

41. E. Weber, M. Czugler, *Topics in Current Cemistry*, Vol 149, 1989, op. cit., 47-55.

42. F. Toda, D. L. Ward, H. Hart, *Tetrahedron Lett.*, 22, no 39, 1981, 3865-3968.

43. H. Hart, L. W. Lin, I. Goldberg, Mol. Cryst. Liq. Cryst., 137, 1986, 277-286.

44. I. Goldberg, Inclusion Compounds, Vol. 4, op.cit., 415

45. F. Toda, K. Tanaka, T. C. W. Mak, *J. Incl. Phenom.*, 3, 1985, 225.

46. F. Toda, K. Tanaka, T. C. W. Mak, Bull. *Chem. Soc.* Japan, Vol. 58, no 8,1985, 2221.

47. F. Toda, D. L. Ward, H. Hart, *Tetrahedron Lett.*, 22, 1981, 3865.

48. F. Toda, K. Tanaka, T. C. W. Mak, *Tetrahedron Lett.*, 25, 1984, 1359.

49. F. Toda, *Topics in Current Chemistry*, 140, 43.

50. H. Hart, L. W. Lin, D. L. Ward, *J. Amer. Chem. Soc.*, 106, 1984, 4043-4045.

51. E. Weber, I. Csöregh, B. Stensland, M. Czugler, *J. Amer. Chem. Soc.*, 106, 1984, 3297-3306.

52. M. Czugler, J. J. Stezowski, E. Weber, *J. Amer. Chem. Soc., Chem. Commun.*, 1983, 154.

53. E. P. Kyba, G. W. Gokel, F. de Jong, K. Koga, L. R. Sousa, M. G. Siegel, L. Kaplan, G. D. Y. Sogah, D. J. Cram, *J.Org. Chem.*, 42, 1977, 4173.

54. I. Csöregh, A. Sjögren, M. Czugler, M. Cserzö, E. Weber, *J. Chem. Soc. Perkin Trans* 2, 1986, 507-513.

55. I. Csöregh, M. Czugler, A. Ertan, E. Weber, J. Ahrendt, *J. Incl. Phenom.*, 8, 1990, 275-287.

56. I. Csöregh, M. Czugler, A. Ertan, E. Weber, J. Ahrendt, *J. Incl. Phenom.*, 8, 1990, 309-322.

57. E. Weber, Comprehensive Supramolecular Chemistry, Vol. 6, (Solid-state Supramolecular Chemistry—Crystal Engineering), ed. J. L. Atwood, J. E. D. Davies, D. D. MacNicol, F. Vögtle, Elsevier Science, Oxford, 1996, 535.

58. S. F. Mason, R. H. Seal, D. R. Roberts, *Tetrahedron*, 30, 1974, 1671.

59. I. Csöregh, M. Czugler, A. Ertan, E. Weber, J. Ahrendt, *J. Incl. Phenom.*, 9, 1990, 309-322.

60. E. Weber, N. Dörpinghaus, I. Csöregh, *J. Chem. Soc. Perkin Trans* 2, 1990, 2167-2177.

61. E. Weber, *J. Mol. Graphics*, 7, 1989, 12.

62. E. Weber, Inclusion compounds, Vol. 4, eds. J. L. Atwood, J. E. D. Davies, D. D. MacNicol, Oxford University Press, Oxford, 1991, 188-262.

63. E. Weber, M. Czugler, Molecular Inclusion and Molecular Recognition—Clathrates II', *Topics in Current Cemistry*, Vol 149, ed. E. Weber, Springer, Berlin, 1988, Vol. 149, 45-135.

64. E. Weber, Comprehensive Supramolecular Chemistry, Vol. 6, (Solid-state Supramolecular Chemistry—Crystal Engineering), ed. J. L. Atwood, J. E. D. Davies, D. D. MacNicol, F. Vögtle, Elsevier Science, Oxford, 1996, Chapter 17.

2 EXPERIMENTAL

"What immortal hand or eye

Could frame thy fearful symmetry?"

William Blake (1757-1822), 'The Tyger'

HOSTS

The host compounds below were used in the preparation of inclusion and salt compounds. Their purity has been ensured by the melting points. The melting point of H_1 is 147°C and of H_2 is 417°C.

- **H_1:** 1,1,6,6-Tetraphenyl-hexa-2,4-diyne-1,6-diol. This host has been synthesised by Professor F. Toda, Okayama University of Science, Japan. McGreal has described the preparation of this host[1].

- **H_2:** 5-(3,5-Dicarboxyphenylethynyl)-isophthalic acid was synthesised and supplied by Professor E. Weber, Institute of Organic Chemistry, Freiberg, Germany. This work has not been published yet.

GUESTS

Inclusion and salt compounds were prepared using the following compounds:

- **TED** (Triethylenediamine); solid, m.p = 158°C
- **TBDA** (N,N,N',N'-Tetracyclohexyl-2,2'-biphenyldicarboxamide) was synthesised and supplied by F. Toda; solid, m.p = 213-214°C
- **PA** (1,10-Phenanthroline); solid, m.p = 93-94°C
- **4PP** (4-Phenylpyridine); solid, m.p = 69-73°C
- **RPEA** ((+)-(R)-1-Phenylethylamine); liquid, b.p = 180-181°C
- **RSPEA** ((±)-(R,S)-1-Phenylethylamine); liquid, b.p = 185°C
- **PEA** (2-Phenylethylamine); liquid, b.p = 199°C
- **Na**OH, **Cs**OH, **Rb**OH

Triethylenediamine, 4-Phenylpyridine, (+)-(R)-1-Phenylethylamine, (±)-(R,S)-1-Phenylethylamine, 2-Phenylethylamine and the bases were supplied by the Aldrich Chemical Company. 1,10-Phenanthroline was obtained from Merck (South Africa).

SOLVENTS

Inclusion and salt compounds were prepared using the following solvents:

- Diethyl ether, 1-butanol, methanol, ethanol and distilled water.

CRYSTAL GROWTH

The crystals were prepared by using a simple method of dissolving the host and the guest separately in a chosen solvent, mixing them together and leaving to evaporate at room temperature. In some cases stirring and heating were performed in the dissolution process. A fixed host to guest molar ratio was used in the crystal preparation. The solutions were kept in covered glass vials and allowed to evaporate in a fume hood. The evaporation time varied depending on which solvent was used. Full details of the preparation of the individual host-guest compounds are given in the appropriate chapters.

THERMAL ANALYSIS

Thermal analysis is any method of heating the sample and measuring changes in its physical properties[2]. A thermal analysis curve is obtained describing events such as change in sample mass, melting, sublimation or phase transition (when the sample is in the solid state).

Thermal analysis methods used in this study were TGA-thermogravimetric analysis, DSC-differential scanning calorimetry and HSM-hot stage microscopy.

TGA-thermogravimetric analysis and DSC-differential scanning calorimetry

The TGA method involves a continuous monitoring of sample mass change with temperature, and was used to study the loss of solvent of crystallisation and guests, in host-guest inclusion compounds. From the measured mass loss, the stoichiometry of complexed compound was determined. In host-guest complexes, solvent and guest release must occur before host decomposition in order to determine the guest mass percentage of the sample. TGA and DSC curves are affected by heating rate, particle size distribution, atmosphere, thermal conductivity of the sample and flow velocity of the purging gas.

The DSC method involved monitoring of the enthalpy change of the sample with temperature, and is used to evaluate the enthalpy changes associated with guest release, phase changes and melting.

TG and DSC were performed on a Perkin Elmer PC Series 7 system. The sample mass range was between 1 and 6 mg. A continuous stream of nitrogen gas was passed over the samples at 40ml/min flow rate. In TG experiments the sample was placed in an open platinum pan, whereas for DSC samples, closed, vented aluminium pans were used. An empty aluminium pan was used as the reference for DSC. Each experiment had a starting temperature of 30°C and ending temperatures about 20°C above the

melting point of the compound analysed. The heating rates used here were 20°C/min. and 30°C/min.

The TG analyser was calibrated using built-in procedures for furnace and mass calibration. The furnace was calibrated by measuring the Curie points of alumel (163°C) and nickel (354°C). The DSC analyser was calibrated by measuring the melting points of zinc (419.5°C) and indium (156.6°C) as well as measuring the enthalpy of melting of indium (28.5J/g).

TG and DSC onset temperatures were not always in perfect agreement due to different geometries of the instrumentation.

HSM-hot stage microscopy

This is a thermoanalytical technique in which the loss of solvent of crystallisation, solid-solid transitions or a guest loss in host-guest inclusion compounds can be visually observed. This technique can be used to complement DSC and TG results on desolvation and decomposition processes. It can also be used to inspect whether the host-guest inclusion was formed by measuring the melting points of host, guest and of a complex.

The loss of volatile guests can be detected by covering the crystals in silicone oil. Gas bubbles can be observed emerging from the crystals at temperatures correlating with the decomposition endotherms in DSC. Decomposition of the inclusion compound submitted to increasing temperatures is also evident by the change in crystal shape or colour.

Measurements were carried out by placing the crystals between two glass coverslips with oil on them, and heating them using a hot stage apparatus, Linkam TH600. The release of a guest component from a host-guest compound was observed as the evolution of bubbles from the sample into the surrounding oil. Heating rates of 10°C/min and 20°C/min were used. The temperature was controlled using a Linkam

CO600 controller. Any changes were monitored on a Nikon SMZ-10 microscope equipped with a polarizing transilluminator and an overhead light. Images were captured using a real-time Sony Digital Hyper HAD colour video camera, and analysed using the Soft Imaging program, analySIS[3].

CRYSTAL STRUCTURE ANALYSIS

Each crystal submitted for data collection was selected according to its size (dimensions should not exceed 0.5 mm), shape and the ability to extinguish plane polarised light uniformly. Once the suitable crystal had been selected, it was glued onto the end of a glass fibre held by a brass collar in the standard way. All of the chosen crystals were stable in the air and at room temperature. In the case of data collections at low temperatures the crystals were covered in Paratone N oil[4] and placed onto the glass fibres.

Accurate cell parameters were determined by least-squares analysis of reflections collected and centred on a Nonius Kappa-CCD diffractometer. Intensity data were collected using an ~~Enraf~~ Nonius FR590 generator that emits graphite-monochromated molybdenum K_α radiation (λ = 0.71073Å). COLLECT[5] software was used to evaluate the strategies for data collection and the collected data were reduced using DENZO-SMN[6]. All of the data were corrected for Lorentz-polarization effects during reduction. The intensity data were collected at 173K (-100°C) using an Oxford Cryosystems cryostream cooler. The crystals were cooled by a liquid nitrogen device, blowing a cold jet of dry nitrogen onto the crystal. The cryostream is stable to 0.1 K, creating uniform temperature conditions for the crystal.

The crystal structures of all complexes were solved by direct methods using the SHELX-86[14] program together with the X-Seed interface[7]. Equivalent reflections were merged and those with $I<2\sigma(I)$ were suppressed. The structures were refined using least-squares refinement, minimising the sum of the squares of the differences between the observed and calculated intensities, $\Sigma w(F_o^2 - kF_c^2)^2$, in SHELX-97[15]. The agreement between the observed and calculated structure factors for the refinement against F is expressed by the residual index, R_1. The observed structure factors are obtained from the measured reflection intensities and the calculated structure factors are computed from the model undergoing refinement.

$R_1 = \Sigma(||F_O| - |F_c||) / \Sigma(|F_O|)$

The agreement between intensities for the refinement against F^2 is given by the residual index R_2. The values of the residual indices obtained for refinement against F^2, R_2, are larger than those obtained for refinement against F, R_1.

$wR_2 = [\Sigma(w(F_O^2 - F_c^2)^2) / \Sigma(w(F_o^2)^2)]^{1/2}$,
where $w = 1 / [\sigma^2(F_o)^2 + (aP)^2 + (bP)]$ and $P = [\max(F_o,0) + 2F_c^2] / 3$

The above weighting scheme contains a and b parameters for making the distribution of $(w(F_O^2 - F_c^2)^2)$ with $\sin\theta$ and $(F_o/F_{max})^{1/2}$ functions constant.

Refinement against F^2 tends to magnify the deviation of the Goodness of Fit, S, from unity. Expressed through the values of F^2, the Goodness of Fit, S, is given by

$S = [\Sigma(w(F_O^2 - F_c^2)^2) / (n - p)]^{1/2}$,

where n represents number of reflections and the total number of refined parameters.

R_{int} is a measure of the agreement between all equivalent reflections.
R_σ is the summation of the standard deviation of F_o^2.

$R_{int} = \Sigma | F_0^2 - |F_0^2| | / \Sigma [F_0^2]$

$R_\sigma = \Sigma [\sigma (F_0^2)] / \Sigma [F_0^2]$.

ADDITIONAL RESOURCES

The computer packages used for analysing the crystal structures are:

The Cambridge Structural Database, **CSD**[9] was used to investigate published crystal data, for the comparison with the structures used in this study.

Program called **X-SEED**[7] was used to provide a graphical interface for crystallographic programs such as SHELX-97, SHELX-86, SECTION, POV-RAY.

Molecular and packing diagrams were drawn with the program **POV-RAY**.[8]

From the intensity data and simulated precession photographs of all levels of the reciprocal lattice one could determine the space group symmetry and systematic absences of the crystals using the program called **LAYER**[10].

SECTION[11] is the program that allows the analysis of the geometry of the molecular voids created by the packing of the host molecules and occupied by the guest molecules. The guests were removed leaving the hosts alone forming differently shaped voids. The program then allows one to plot cuts through the unit cell down a selected axis at certain height.

Structural parameters, including bond distances, angles, torsion angles, mean planes and hydrogen bond data, together with standard deviation values were obtained using **PLATON**[12].

WINGX32[13] was used as an interface for running PLATON and generation of Fourier maps.

REFERENCES

1. M. E. McGreal, V. Niederl, J. B. Niederl, *J. Am. Chem. Soc.,* 61, 1939, 345.
2. M.E.Brown, Introduction to Thermal Analysis, Chapman and Hall, London, 1988.
3. Soft Imaging System GmbH: Digital Solutions for Imaging and Microscopy, Version 3.1 for Windows.
4. Paratone N oil (Exxon Chemical Co., TX, USA).
5. Collect, data collection software, Nonius, 1998.
6. Z. Otwinowski, W. Minor, Methods in Enzymology, (eds) C.W. Carter and R.M. Sweet, Academic Press, New York, 276, 307, 1996.
7. L. J. Barbour, X-Seed, A graphical interface to shelx, University of Missouri, Columbia, MO 65211, U.S.A., 1999.
8. Pov-Ray for Windows, Version 3.1e.watcom.win32, The persistence of vision development Team, © 1991-1999.
9. Cambridge Structural Database and Cambridge Structural Database System, Version 5.20 (October 2000), Cambridge Crystallographic Data Centre, University Chemical Laboratory, Cambridge, England.
10. L. J. Barbour, LAYER, A computer program for the graphic display of intensity data as simulated precession photographs, *J. Appl. Cryst.*, 32, 1999, 351.
11. L. J. Barbour, SECTION, A computer program for the graphic display of cross sections through a unit cell, *J. Appl. Cryst.*, 32, 1999, 353.
12. A. L. Spek, PLATON, A multipurpose crystallographic tool, Version 10500, © 1980-2000.
13. L. J. Ferrugia, WinGX, An integrated system of windows programs for the solution, refinement and analysis of single crystal X-ray diffraction data, Version 1.63, *J. Appl. Cryst.*, 32, 1999, 837.
14. G. M. Sheldrick, SHELX-86, ~~Crystallographic Computing 3, G. M. Shedrick, C. Kruger and R. Goddard (Eds), Oxford University Press, 1985, 175.~~ Acta Cryst. A46, 1990, 467.
15. G. M. Sheldrick, SHELX-97, Program for the Refinement of Crystal Structures, University of Göttingen, Germany, 1997.

3 INCLUSION COMPOUNDS WITH H_1

"The Gods are here, too."

-Heraclitus

THERMAL ANALYSIS, MOLECULAR STRUCTURE AND CRYSTAL PACKING OF COMPOUNDS WITH HOST H_1

The abbreviations for the inclusion compounds in this chapter are:

H_1: 1,1,6,6-Tetraphenyl-hexa-2,4-diyne-1,6-diol

H_1 • TED : H_1 and Triethylenediamine
H_1 • TBDA : H_1 and N,N,N',N'-Tetracyclohexyl-2,2'-biphenyldicarboxamide
H_1 • PA : H_1 and 1,10-Phenanthroline
H_1 • 4PP : H_1 and 4-Phenylpyridine

The structures of the inclusion compounds formed between the host and the guest compounds were solved and analysed in this chapter. The thermal investigation of their behaviour was performed using thermal techniques such as TG, DSC and HSM.

Crystal data, experimental and refinement parameters for the four inclusion compounds are provided in Table 3.3.

The guest numbering schemes are given at the beginning of each structure analysis while the host numbering scheme can be found on the bookmark.

COMPLEX PREPARATION

Crystalline complexes of the host **H_1** with **TED**, **TBDA**, **PA** and **4PP** were obtained from the slow evaporation of solutions of host and guest in 1:2 and 1:1 molar ratios. The solutions were prepared according to the concentrations listed in Table 3.1. The crystallisation process lasted between 24 hours and three days in order to obtain single crystals of suitable quality.

Table 3.1: The details of the complex preparation of **H_1 • TED**, **H_1 • TBDA**, **H_1 • PA** and **H_1 • 4PP** complexes

Complex	*H_1 (mmol)*	*Guest (mmol)*	*Molar ratio*	*Solvent used*
H_1 • TED	0.24	0.24	1:1	Diethyl ether
H_1 • TBDA	0.073	0.15	1:2	Diethyl ether
H_1 • PA	0.073	0.17	1:2	1-butanol
H_1 • 4PP	0.12	0.25	1:2	Diethyl ether

THERMAL ANALYSIS

The TGA and DSC results for the **H_1 • TED**, **H_1 • TBDA**, **H_1 • PA** and **H_1 • 4PP** complexes are shown in Figure 3.1. A summary of the observed changes with the increase in temperature in TG and DSC traces is presented in Table 3.2.

H_1 • TED decomposes with a single step 1 in the TG curve with a mass loss of 92.8% (Figure 3.1a)). This corresponds to endotherm A in the DSC trace indicating a melt of the complex. The mass loss is due to the sublimation of the host and guests.

H_1 • TBDA structure decomposes in a single step, shown in the TG trace. The melt of the complex is shown by the endotherm A corresponding to step 1. The mass loss is due to the sublimation of the host and guests. This is shown in Figure 3.1b).

In the TG trace of **H_1 • PA** there is a gradual mass loss with no distinct steps. However, the DSC trace shows a broad endotherm A, which can indicate a gradual breaking of the crystal structure followed by the host melt and decomposition. This is shown in Figure 3.1c).

Figure 3.1d) illustrates TG and DSC traces for the **H_1 • 4PP** inclusion complex. The DSC trace displays a fairly sharp endotherm at 114°C corresponding to a melt of the complex. This peak (labelled A) occurs with an additional peak, B, at 139°C, indicating that the melting of the complex is a multi step process, the crystal structure breaking gradually as the temperature increases. Gradual mass loss is observed in the TG trace after the melting temperature.

The enthalpy is the energy that must be supplied to release the guest component from the crystal or to break the entire host-guest crystal structure at a specific temperature. It is a measure of the strength with which the crystal is held together and it can be positive (the energy is absorbed) or negative (the energy is released). Table 3.2 gives the enthalpy values recorded during the thermal analysis.

Table 3.2: Thermal analysis results for H_1 inclusion compounds

Inclusion compound			H_1 • TED	H_1 • TBDA	H_1 • PA	H_1 • 4PP
TG/	Step 1	T_{on}(°C)	180.2	221.0	-	-
		Exp. (Calc.) % mass loss	92.6(92.8)	96.6(96.0)	-	-
DSC/	Peak A	T_{on}(°C)	179.3	217.6	164.8	114.0
		ΔH (kJ.mol^{-1})	149.1	136.8	56.4	58.9

Figure 3.1: TG and DSC curves for **a) H_1 • TED**, **b) H_1 • TBDA**, **c) H_1 • PA** and **d) H_1 • 4PP**

a)

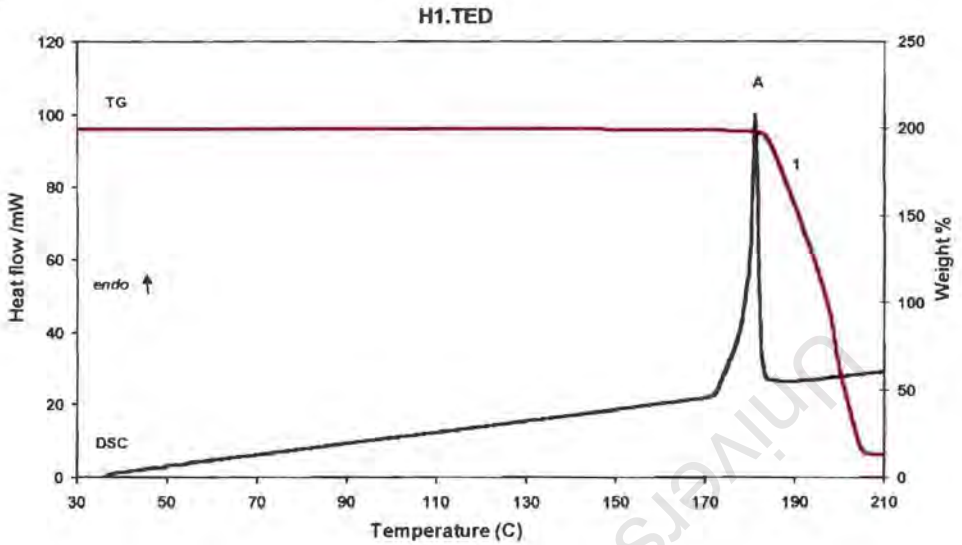

b)

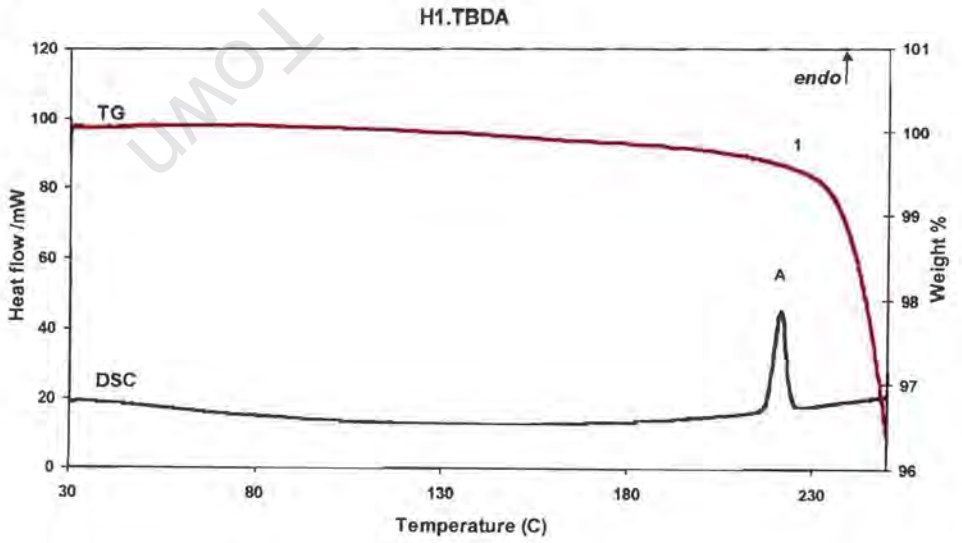

c)

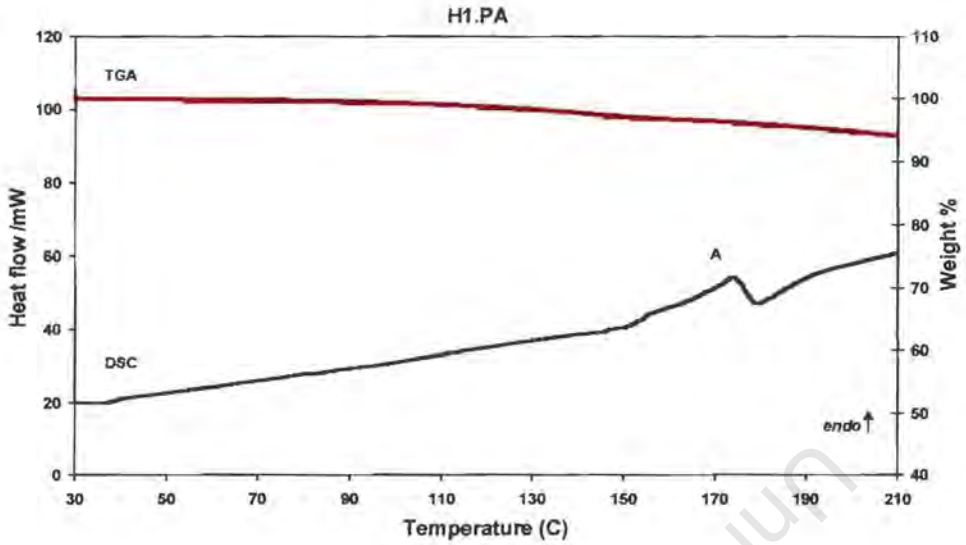

d)

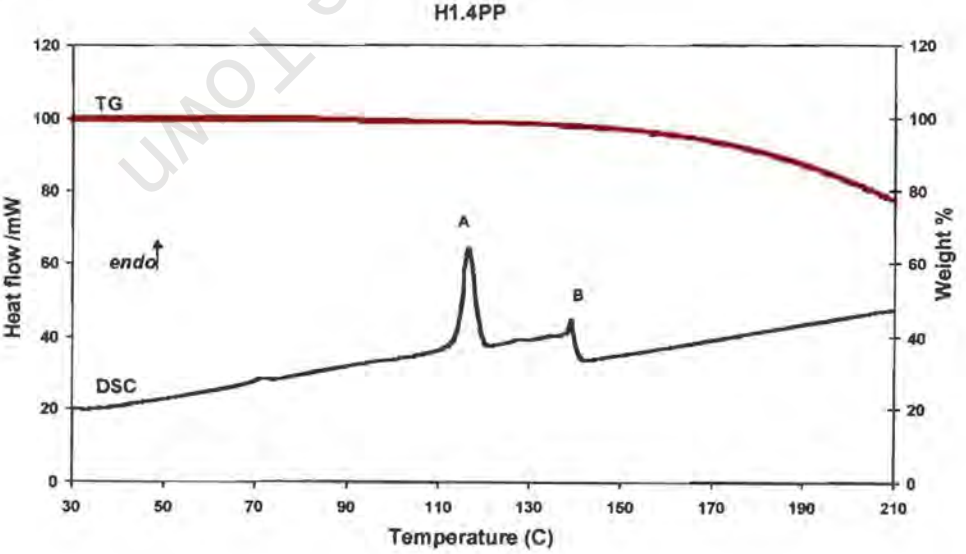

HSM

The HSM results for **H_1 • TED**, **H_1 • TBDA**, **H_1 • PA** and **H_1 • 4PP** are presented in Figures 3.2, 3.3, 3.4, and 3.5 respectively. HSM was used to analyse the thermal behaviour of those complexes upon heating at a constant rate.

H_1 • TED

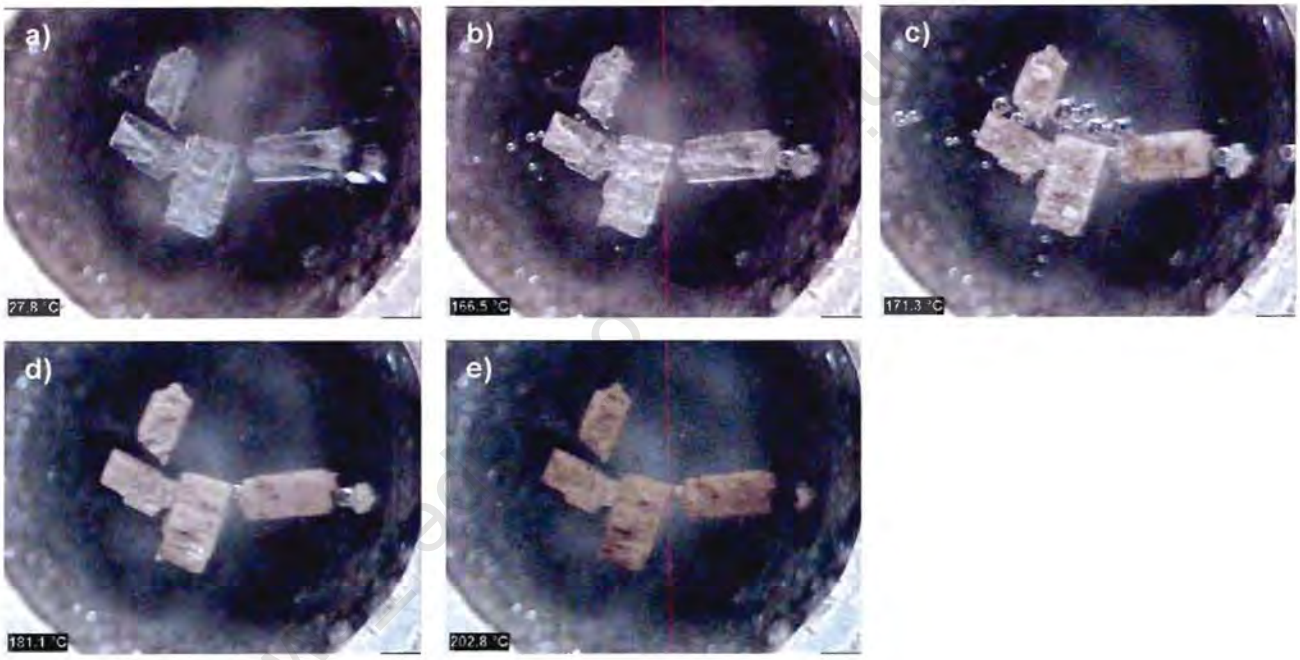

Figure 3.2:

a) Translucent crystals are coated with silicone oil at room temperature.

b) Crystals are going darker in colour and are producing bubbles due to guest loss.

c) At the onset temperature the crystal structure collapses due to the guest loss (bubbles are given off) and the crystals turn opaque.

d) Generation of bubbles ceases.

e) Host decomposition and crystals turn dark yellow.

H_1 • TBDA

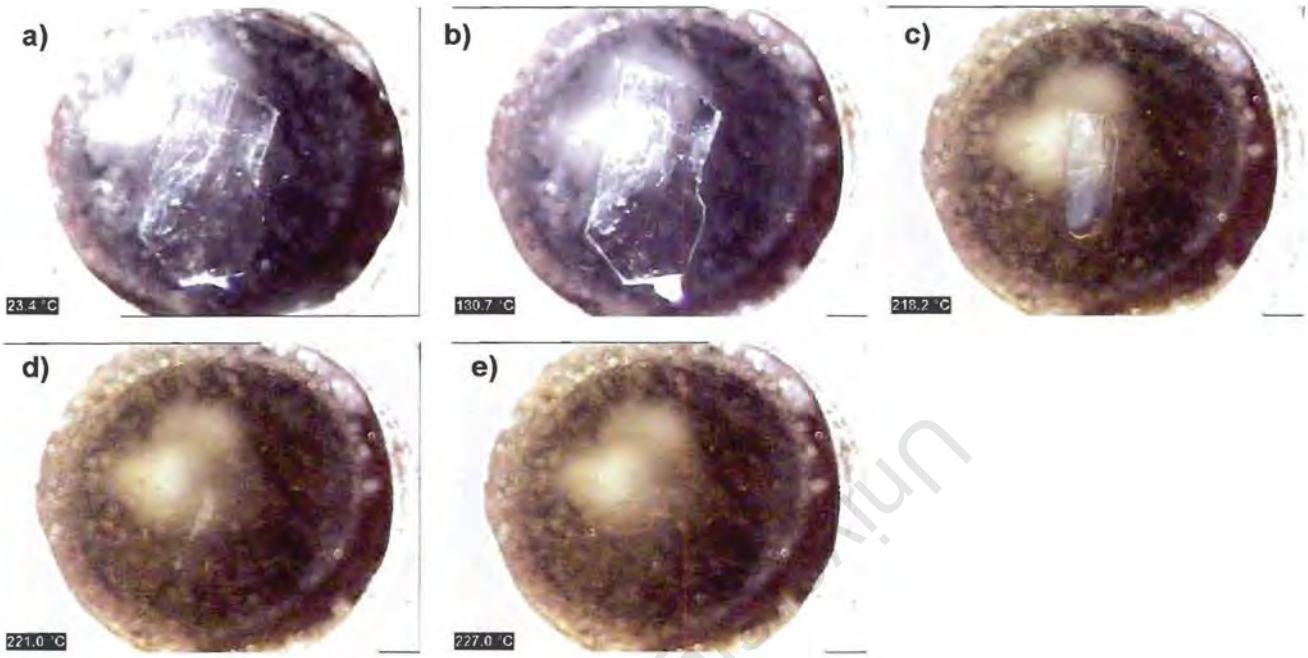

Figure 3.3:

a) At room temperature the translucent crystals of **H_1 • TBDA** are immersed in silicone oil.

b) As the temperature increases no colour change is observed by HSM.

c) and ***d)*** At the onset temperature crystal structure of the complex collapses upon melting.

e) Complex melt.

H_1 • PA

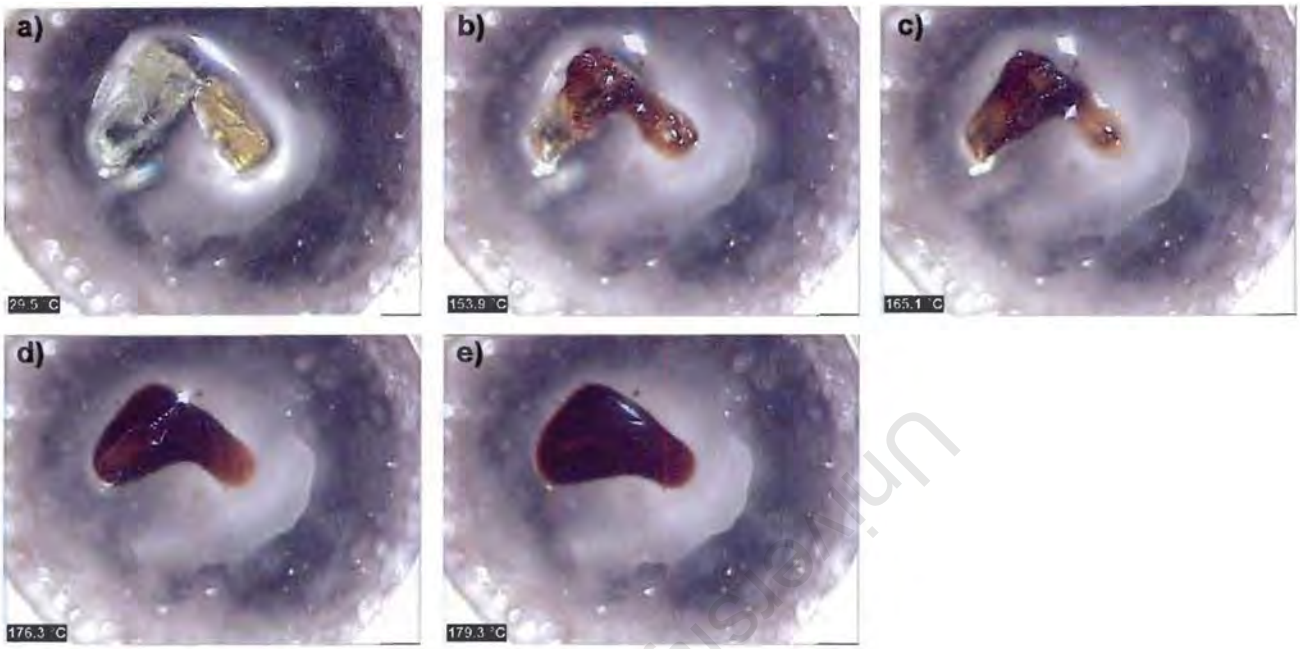

Figure 3.4:

a) The translucent yellow crystals of **H_1 • PA** shown here at room temperature coated with silicone oil.

b) The translucent yellow crystals turn orange in colour, marking the collapse in crystal structure and guest release.

c) At the onset of the ligand release step, the colour of the crystals turns red, before melting to a dark red liquid.

d) Host melt.

H_1 • 4PP

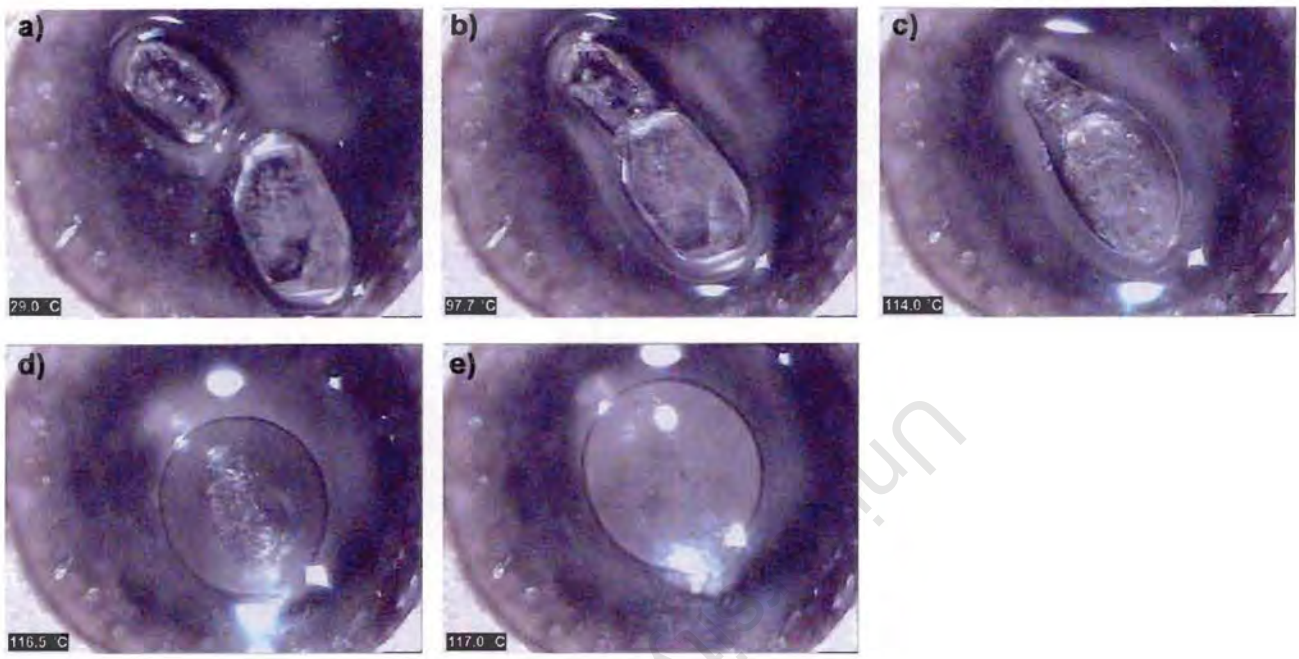

Figure 3.5:

a) The translucent crystals of **H_1 • 4PP** immersed in silicone oil at room temperature.

b) No colour change is observed.

c) and ***d)*** The melting of the complex to a colourless liquid is observed at the onset temperature.

e) Complex melt.

Table 3.3: Crystal data and refinement parameters

Compound	$H_1 \bullet TED$	$H_1 \bullet TBDA$	$H_1 \bullet PA$	$H_1 \bullet 4PP$
Molecular formula	$C_{30}H_{22}O_2 \cdot C_6H_{12}N_2$	$C_{30}H_{22}O_2 \cdot 2C_{38}H_{48}O_2N_2$	$C_{30}H_{22}O_2 \cdot 2C_{12}H_8N_2$	$C_{30}H_{22}O_2 \cdot 2C_{11}H_9N$
Formula weight	526.65	1544.04	774.88	724.86
Crystal system	triclinic	monoclinic	triclinic	triclinic
Space group	P-1	$P2_1/n$	P-1	P-1
Temperature, K	293(2)	293(2)	293(2)	293(2)
a, Å	6.124(1)	9.696(2)	9.644 (2)	8.259(2)
b, Å	14.193(3)	16.569(3)	10.737(2)	10.484(2)
c, Å	18.209(4)	28.144(6)	11.486(2)	12.280(3)
α, °	70.04(1)	90	105.56(3)	73.47(3)
β, °	80.32(1)	97.18(3)	100.85(3)	71.77(3)
γ, °	77.72(2)	90	113.20(3)	76.83(3)
V, $Å^3$	1445.7(5)	4486 (2)	993.4(3)	956.9(3)
Z	2	2	1	1
Absorption coefficient, mm^{-1}	0.075	0.070	0.079	0.076
F(000)	560	1660	406	382
Crystal size, mm	0.35x0.25x0.13	0.51x0.13x0.08	0.50x0.42x0.23	0.48x0.36x0.18
Index ranges	-4<=h<=6, -13<k<=10, -17<l<=17,	-10<=h<=10, -17<=k<=17, -30<=l<=20,	-12<=h<=12, -13<=k<=13, -13 =<l<=14,	-10<=h<=10, -12<=k<=13, -14<=l<=15,
Reflections collected/unique	2464/2095 [R(int) =0.0622]	14082/5965 [R(int) =0.0384]	6948/4523 [R(int) =0.0141]	5390/3868 [R(int) =0.0165]
Refinement method	Full-matrix least-squares on F^2	Full-matrix least-squares on F^2	Full-matrix least-squares on F^2	Full-matrix least-squares on F^2
Data/ restarints/ Parameters	2095/0/361	5965/0/524	4523/0/272	3868/0/254
Goodness-of-fit on F^2	1.032	1.033	1.044	1.094
ρ_{calc}, $g.cm^{-3}$	1.2097	1.1430	1.2951	1.2578
Final R indices [I >2σ(I)]	R_1=0.1087, wR_2=0.2605	R_1=0.0519, wR_2=0.0931	R_1=0.0594, wR_2=0.1520	R_1=0.0396, wR_2=0.1040
R indices (all data)	R_1=0.1535, wR_2=0.3058	R_1=0.1086, wR_2=0.1119	R_1=0.0733, wR_2=0.1628	R_1=0.0571, wR_2=0.1214
Largest diffraction peak and hole, $eÅ^{-3}$	0.43 and –0.22	0.13 and –0.15	1.31 and -0.28	0.22 and -0.19

MOLECULAR STRUCTURE AND CRYSTAL PACKING

H_1 • TED

H_1: 1,1,6,6-Tetraphenyl-hexa-2,4-diyne-1,6-diol

TED: Triethylenediamine

$C_{30}H_{22}O_2 \cdot C_6H_{12}N_2$

Space group: $P\bar{1}$

Unit cell parameters: a = 6.1240(1) b = 14.193(3) c = 18.209(4) /Å

α = 70.04(1) β = 80.32(1) γ = 77.72(2) /°

Unit cell volume: 1445.7(5) Å^3

Z = 2

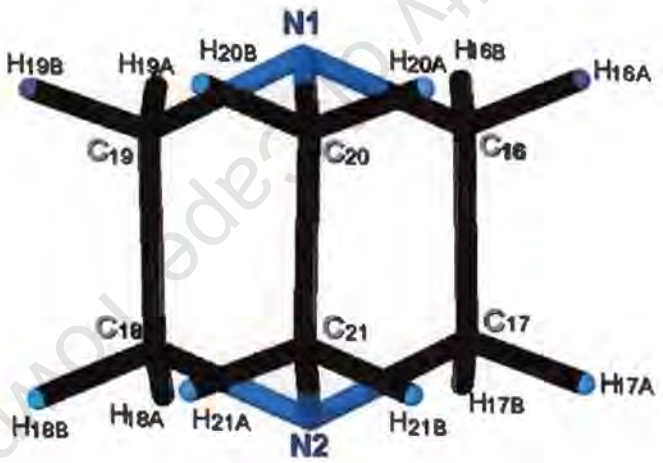

Figure 3.6: TED guest numbering scheme

TED physical properties*: ***m.p*** = 158°C

b.p = 174 °C

* Measured at standard pressure and temperature.

H_1 • TED

H_1 • TED crystallises in the triclinic crystal system and the structure was successfully solved in the space group P $\bar{1}$. There are two half host molecules and one guest molecule present in the asymmetric unit. Two independent halves of the host molecules are labelled with suffixes A and B.

The intensity data collection yielded 2464 reflections, of which 2095 were unique. The data were merged and 1315 reflections were observed with $I_{rel} > 2\sigma I_{rel}$. Positions of all the host and guest non-hydrogen atoms were obtained by direct methods using SHELX-86[1].

Host hydroxyl hydrogens were located in the difference electron density map and were refined with bond length constraints, O-H = 0.820Å, and isotropic temperature factors. The rest of the host and guest hydrogens were included in the model with geometric constraints and refined with isotropic temperature factors of $1.2xU_{eq}$ of their parent atoms. The structure refined to $R_1 = 0.1087$.

One half of the host molecule was located on the centre of inversion, Wyckoff special position e (1/2,1/2,0), while the other independent half of the host molecule was located on the centre of inversion, Wyckoff special position f (1/2,0,1/2). The guest molecules are located in general positions.

The packing of **H_1 • TED** is such that the host molecules pack to form layers that run parallel to each other, are perpendicular to the [100] direction and are related by the centres of inversion (Figure 3.7 and 3.8). The layers of host molecules pack to form square-shaped channels that run in the [100] direction. The guest molecules that occupy these channels are hydrogen bonded to host hydroxyl oxygens. A space-filling projection of the channels in **H_1 • TED**, with the guest molecules omitted, is shown in Figure 3.7a).

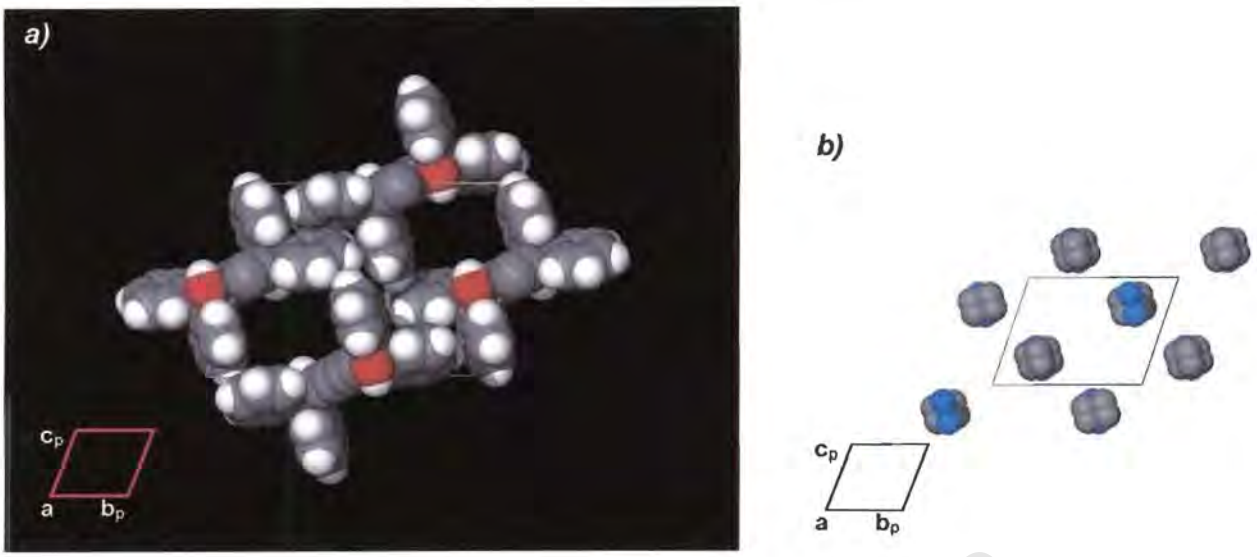

Figure 3.7: a) Space-filling projection of H_1 • **TED** along [100], with guest molecules omitted, showing square-shaped channels. **b)** The packing arrangement of guests omitted in a) in the [100] direction. The guest molecules pack in layers parallel to each other (hydrogens were omitted for simplicity). ***c)*** Host molecules represented in grey with guest molecules omitted in H_1 • **TED**, viewed down [100]. The unit cell is sectioned at section height x_q=0Å.

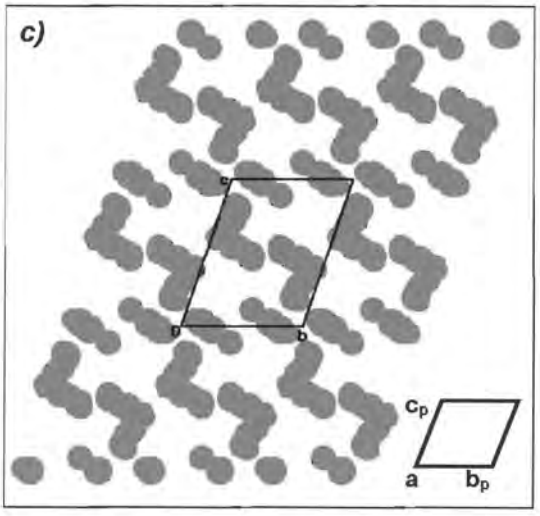

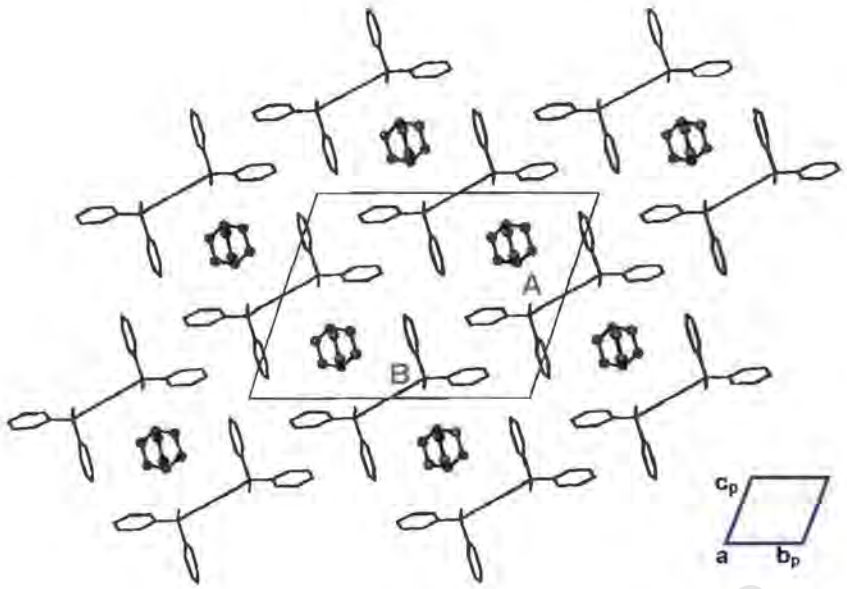

Figure 3.8: Packing diagram of H_1 • **TED** viewed along [100] direction showing the channels with guest molecules in them. Host molecules are shown in stick form while guest molecules are shown in stick-and-ball form.

Hydrogen bonding interactions: This crystal structure is stabilised by hydrogen bonding where the nitrogens of the guest and oxygens of hydroxyl groups belonging to the host molecule form intramolecular and intermolecular hydrogen bonds.

Tables 3.4 and 3.5, list a summary of the appropriate contacts for inter-layer and intra-layer host-guest interactions respectively, showing hydrogen bonding. Inter-layer, O-H···N hydrogen bonds were identified between each guest molecule and one of the host hydroxyl sites.

Table 3.4: Inter-layer hydrogen bonding details for the H_1 • **TED** structure

O-H···N	O-H/Å	H···N/Å	O···N/Å	Angle/°
O1B-H1B···N2	0.820	1.915(1)	2.729(1)	171.24(4)
O1A-H1A···N1$^{\#1}$	0.820	1.941(1)	2.754(1)	170.84(4)

Symmetry code: #1= x, y-1, z

Table 3.5: Intra-layer hydrogen bonding details for the **H_1 • TED** structure

C-H···O	C-H/Å	H···O/Å	C···O/Å	Angle/°
C11B-H10B···O1B	0.930	2.314(1)	2.679(1)	102.89(3)
C5A-H5A···O1A	0.930	2.253(1)	2.635(1)	103.83(3)

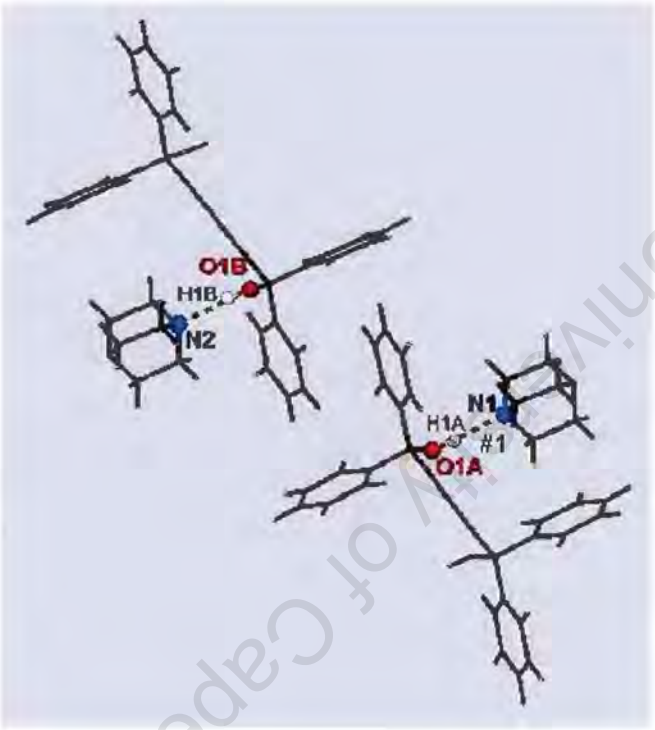

Figure 3.9: Hydrogen bonding interactions in **H_1 • TED**

MOLECULAR STRUCTURE AND CRYSTAL PACKING

H_1 • TBDA

H_1: 1,1,6,6-Tetraphenyl-hexa-2,4-diyne-1,6-diol

TBDA: (N, N, N', N'-Tetracyclohexyl-2,2'-biphenyldicarboxamide)

$C_{30}H_{22}O_2 \cdot 2C_{38}H_{48}O_2N_2$

Space group: $P2_1/n$

Unit cell parameters: a = 9.696(2) b = 16.569(3) c = 28.144(6) /Å

β = 97.18(3) /°

Unit cell volume: 4486(2) Å^3

Z = 2

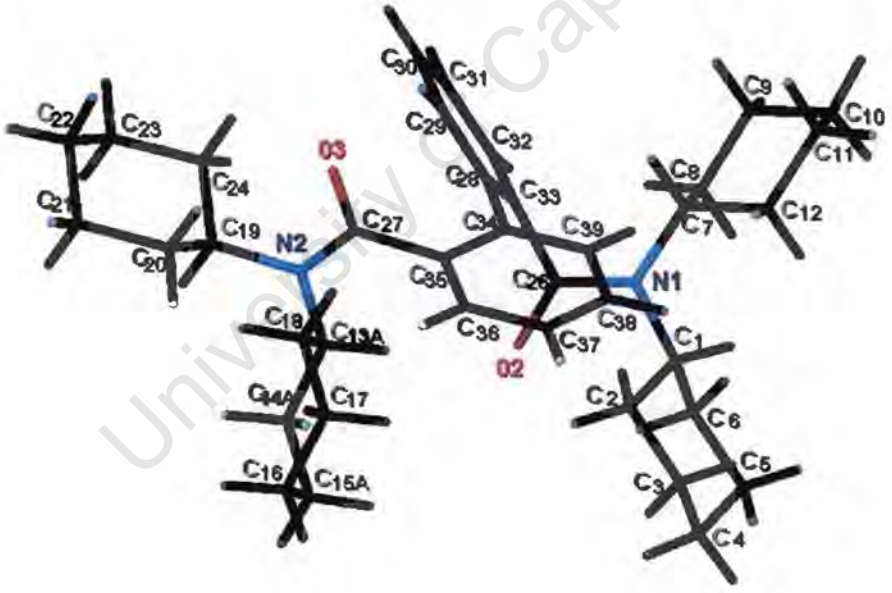

Figure 3.10: TBDA guest numbering scheme

TBDA physical properties*: ***m.p*** = 213-214°C

* Measured at standard pressure and temperature.

H_1 • TBDA

The space group was identified as $P2_1/n$. The space group $P2_1/n$ is equivalent to $P2_1/c$. However due to a different cell choice, the c-glide plane is converted into an n-glide plane. The reflection conditions observed here, after the X-ray data collection of 14082 reflections in the range of $1° \leq 2\theta \leq 45°$, were:

hkl : none

h0l : h + l = 2n

0k0 : k = 2n

After 15 systematically absent reflections had been rejected and equivalent reflections merged, 5965 unique reflections remained of which 3743 were observed with $I_{rel} > 2\sigma(I_{rel})$. The structure was then solved by direct methods using SHELX-86. Values for $R_{int} = 0.0384$ and $R_\sigma = 0.0621$ show a relatively good quality data set. This structure refined to $R_1 = 0.0519$ successfully.

The **H_1 • TBDA** structure solution revealed an asymmetric unit with half of the host molecule and a single guest molecule. Since the host molecule is centered on the Wyckoff special position d (1/2, 0, 0) which has a site symmetry of inversion, with guests located in general positions, it indicates Z = 2 and host to guest ratio of 1:2. Such a small Z value is due to a considerable size of the guest. The molecular packing diagram is shown in Figure 3.11d).

Non-hydrogen atoms of the host and a guest were refined anisotropically and aromatic hydrogen atoms were geometrically constrained to their parent atoms at C-H bond distance of 0.930Å. Host hydroxyl hydrogen was located in the difference electron density map and was refined with bond length constraints and isotropic temperature factors. The rest of the host hydrogens were included in the model with geometric constraints and refined with isotropic temperature factors of $1.2xU_{eq}$ of their parent atoms. Hydroxyl hydrogen was located on the half-host molecule and O···O distances indicated the presence of intermolecular hydrogen bonding.

The packing diagram of **H_1 • TBDA** in Figure 3.11a) showing only the host molecules, suggests that the guest molecules occupy channels parallel to [100]. Host molecules form open s-shaped channels filled by guest molecules, creating a closely packed crystal structure.

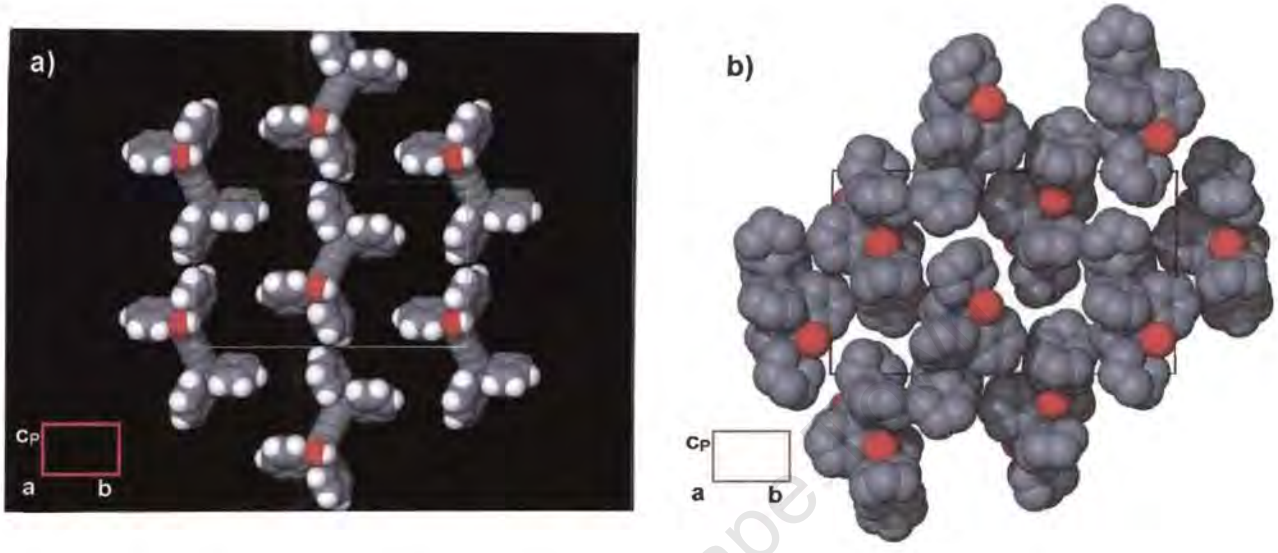

Figure 3.11: a) Space-filling representation of host molecules forming open channels along [100]. Guest molecules are omitted for clear vision. **b)** Packing arrangement of guest molecules viewed along the [100] direction. **c)** SECTION diagram of **H_1 • TBDA** (unit cell sectioned at section height of a=0Å), showing channels parallel to the b-axis. Guest molecules are omitted for clarity.

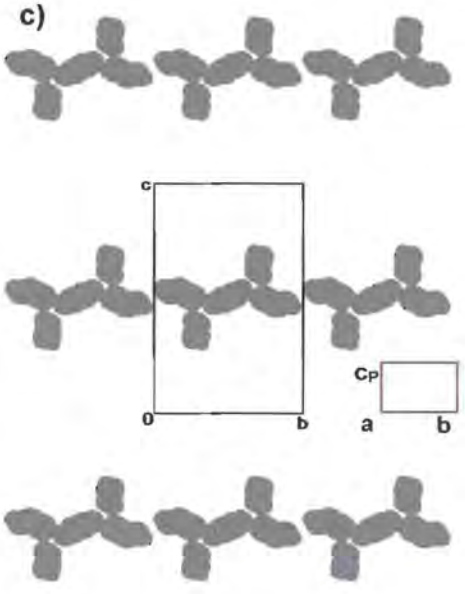

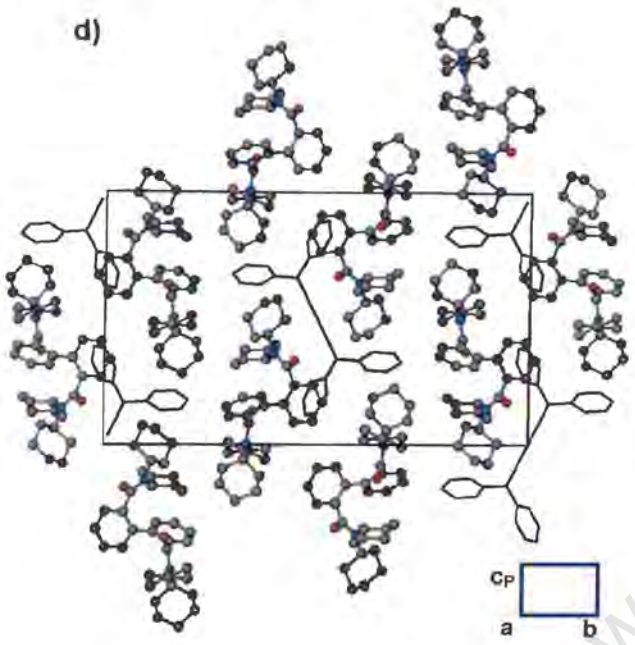

Figure 3.11: d) The molecular packing of **H_1 • TBDA** viewed along [100] direction. Guest molecules are shown in ball-and-stick form and host molecules in stick form. Hydrogen atoms are omitted for clarity.

Hydrogen bonding: In the **H_1 • TBDA** structure each guest carbonyl oxygen atom is hydrogen bonded to the host hydroxyl oxygen atom (shown by the dotted lines in Figure 3.12). The hydrogen bond length and bond angle values are listed in Tables 3.6 and 3.7. The host-guest interactions are shorter than the sum of the van der Waals radii between the two heavy atoms (O···O = 3.04Å)[3]. This strong hydrogen bonding stabilises the crystal structure.

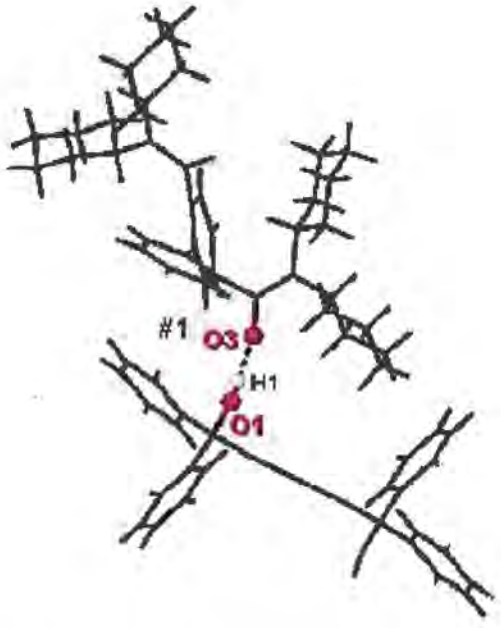

Figure 3.12: Schematic representation of hydrogen bonding between host and guest molecules.

Table 3.6: Inter-layer hydrogen bonding details for the **H_1 • TBDA** structure

O-H···O	O-H/Å	H···O/Å	O···O/Å	Angle/°
O1-H1···O3$^{\#1}$	0.819(2)	1.927(1)	2.742(2)	173.5(2)

Symmetry code: #1= 2-x, 1-y, -z

Table 3.7 shows intramolecular distances that are in a close agreement with the sum of the van der Waals radii between the two heavy atoms (C···O = 3.22Å)[4].

Table 3.7: Intra-layer hydrogen bonding details for the **H_1 • TBDA** structure

C-H···O	C-H/Å	H···O/Å	C···O/Å	Angle/°
C(2A) -H(2A)···O(2)	0.9700	2.446(1)	3.005(1)	116.4(2)
C(6A) -H(6A)···O(2)	0.9700	2.468(2)	3.021(1)	115.9(3)
C(15)-H(15)···O(1)	0.9301	2.308(1)	2.660(2)	101.9(2)
C(17)-H(17B) O(2)	0.9699	2.550(1)	3.365(2)	141.6(3)
C(20)-H(20A)···O(3)	0.9699	2.324(2)	2.914(1)	118.5(2)
C(24)-H(24A)···O(3)	0.9700	2.476(1)	3.030(1)	116.0(2)
C(29)-H(29)···O(3)	0.9300	2.573(2)	3.228(2)	127.9(2)

MOLECULAR STRUCTURE AND CRYSTAL PACKING

H_1 • PA

H_1: 1,1,6,6-Tetraphenyl-hexa-2,4-diyne-1,6-diol

PA: 1,10-Phenanthroline

$C_{30}H_{22}O_2 \cdot 2C_{12}H_8N_2$

Space group: $P\bar{1}$

Unit cell parameters: a = 9.644(2) b = 10.737(2) c = 11.486(2) /Å

α = 105.56(3) β = 100.85(3) γ = 113.20(3) /°

Unit cell volume: 993.5(3) Å^3

Z = 1

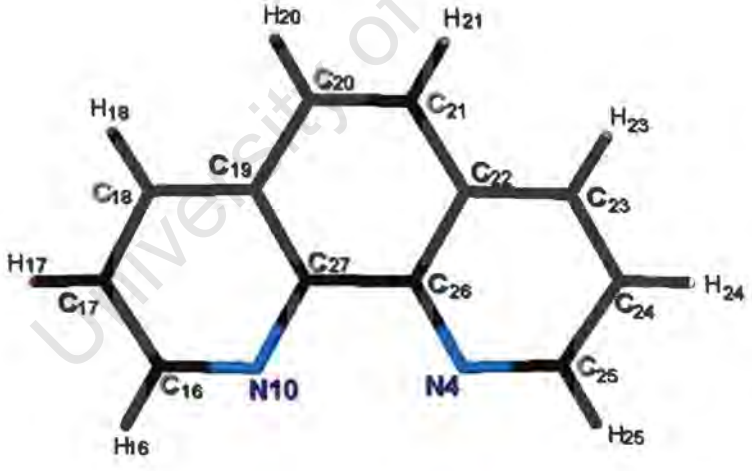

Figure 3.13: PA guest numbering scheme

PA physical properties*: ***m.p*** = 93-94°C

* Measured at standard pressure and temperature.

$H_1 \bullet PA$

H_1 • PA crystallises in the triclinic crystal system, space group $P\bar{1}$. The data collection yielded a total of 6948 reflections, of which 4523 were unique. The data were merged and 3675 reflections were observed with $I_{rel} > 2\sigma(I_{rel})$. The structure was then solved by direct methods using SHELX-86.

Positions of all non-hydrogen atoms of the one guest molecule and half of the host molecule in the asymmetric unit were located by direct methods using the SHELX-86 program. The two nitrogen atoms of the guest molecule, N_4 and N_{10}, were placed with certainty, since their electron density peaks were greatest in magnitude compared to other peaks attributed to carbon atoms in guest aromatic rings. Also, their location was confirmed by the hydrogen bonding distance between their peaks and those of hydroxyl oxygen of the host. All of the non-hydrogen atoms of the half-host and guest were refined with anisotropic temperature factors, while all of the hydrogen atoms were refined isotropically. The hydroxyl hydrogen atom of the half-host was located in the difference electron density map and refined with a length constraint. Aromatic hydrogens of the half-host and the guest, however, were geometrically placed in idealised positions with bond length constraint and refined with linked thermal parameters. The final $R_1 = 0.0594$.

The host molecule is placed on the inversion centre corresponding to the Wyckoff special position d, multiplicity of one, while the guest is in the general position. There is one guest and half the host molecule in the asymmetric unit with the H:G ratio of 1:2 , and Z = 1.

The intermolecular distances indicate the presence of a hydrogen bond network, where each guest is hydrogen bonded to the host molecule through an O···H–N bond. This kind of bonding stabilises the entire crystal structure.

The packing diagram of **H_1 • PA** structure depicted in Figure 3.14a) suggests that the host molecules pack to form hive-like channels. The channels were analysed, using program SECTION[2] (Figure 3.15c)) and it was found that the channels run in the [100]

direction with hosts being arranged in such a way as to form closed circles large enough for the guest molecules to occupy them (Figure 3.14b)).

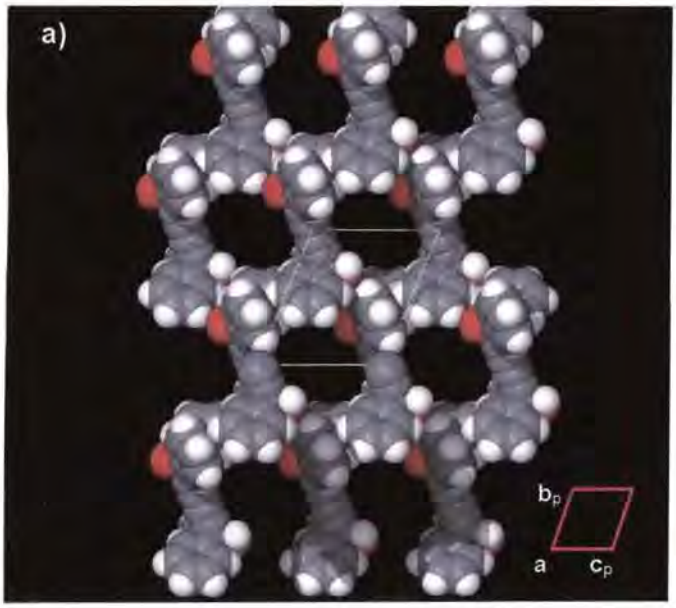

Figure 3.14: a) Space-filling representation of the H_1 • **PA** structure, showing host molecules forming circular, closed channels viewed in the [100] direction (guests are omitted for clarity).

Figure 3.14: b) Packing diagram showing guest molecules stacked together along the a-axis. Hydrogen atoms are omitted for clarity.

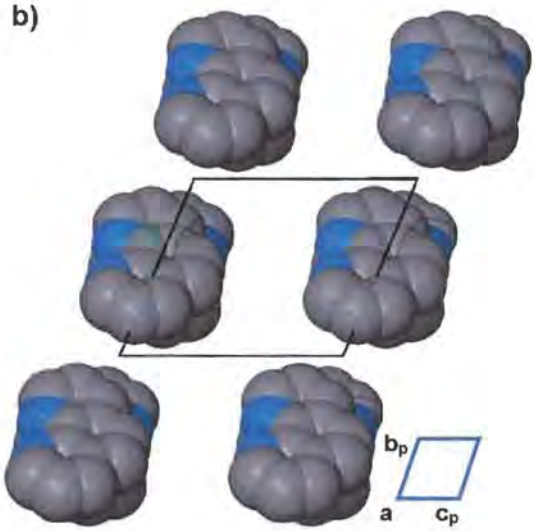

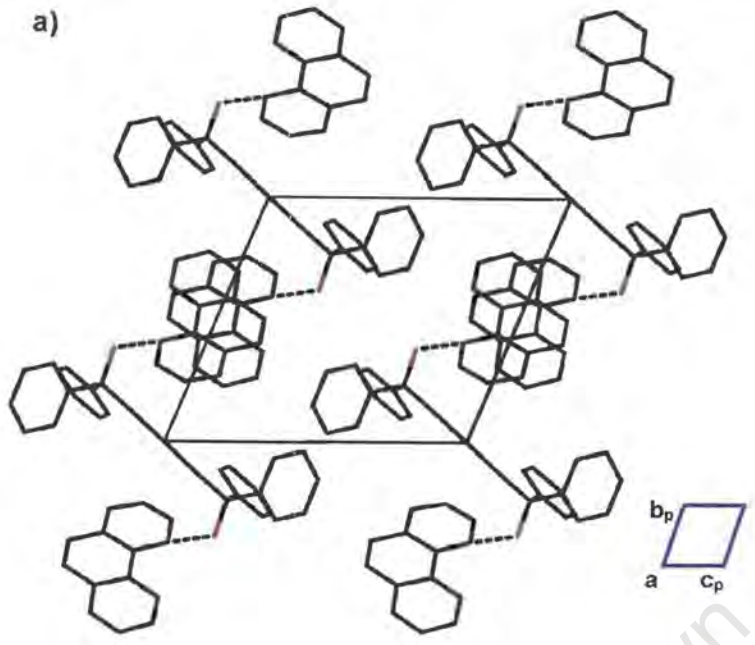

Figure 3.15: a) Packing diagram of $\mathbf{H_1}$ • **PA** down [100] showing hydrogen bonding between host and guest molecules. **b)** The channel structure viewed along [001] direction. Ball-and-stick representation of guest molecules and stick form representation of host molecules, with hydrogens omitted.

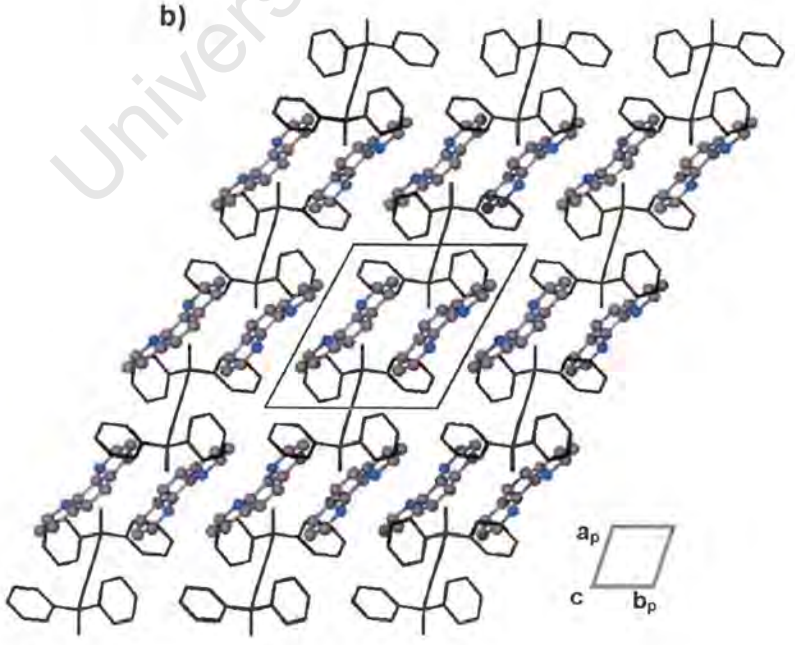

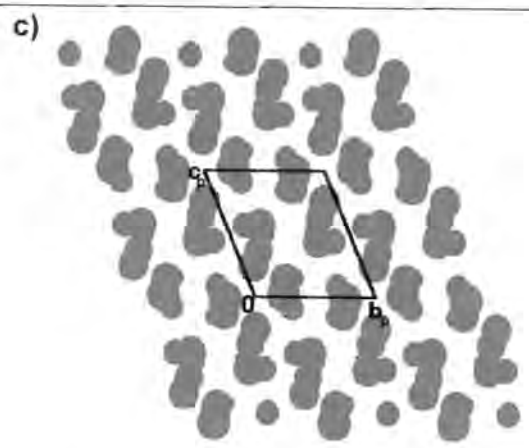

Figure 3.15: c) The unit cell of **H_1 • PA** was sectioned and analysed using program SECTION, here viewed down [100]. Host molecules are represented in gray and guests are omitted.

Hydrogen bonding is found between each host hydroxyl oxygen atom and guest nitrogen atom. These hydrogen bonds shown in Figures 3.16 and 3.17 are represented by dotted lines. The hydrogen bond length and bond angle values are listed in Tables 3.8 and 3.9.

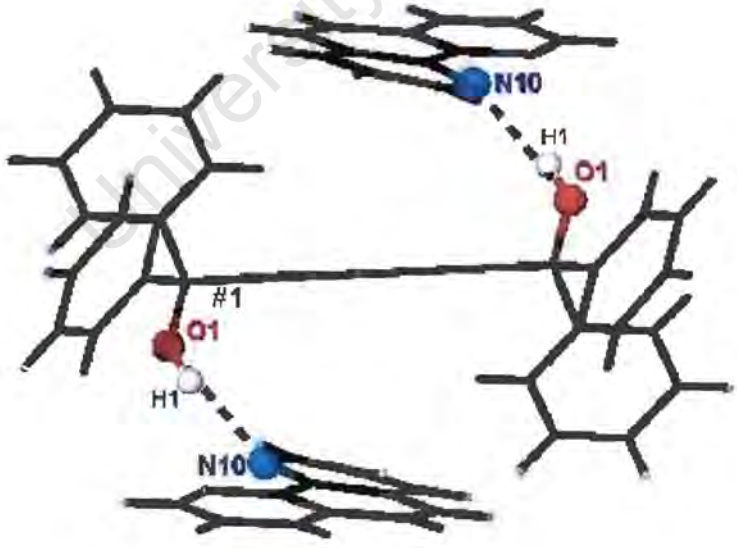

Figure 3.16: Host-guest hydrogen bonding in the **H_1 • PA** structure. (#1= 1-x, -y, -z)

Table 3.8: Inter-layer hydrogen bonding details for the **H_1 • PA** structure

O-H···N	O-H/Å	H···N/Å	O···N/Å	Angle/°
O1-H1···N10	0.8201	2.081(2)	2.887(1)	168(3)

Table 3.9: Intra-layer hydrogen bonding details for the **H_1 • PA** structure

C-H···O	C-H/Å	H···O/Å	C···O/Å	Angle/°
C18-H18···O1	0.9299	2.449(3)	2.804(1)	103(2)

The structure is stabilised by host-guest O-H···N and guest-guest π-π interactions (Figures 3.16, 3.17 and 3.18). Orientation of the guest molecules involved in π-π interactions is presented in Figure 3.18. The guest molecules are stacked together in layers, parallel to each other with ring centroid distances listed in Table 3.10.

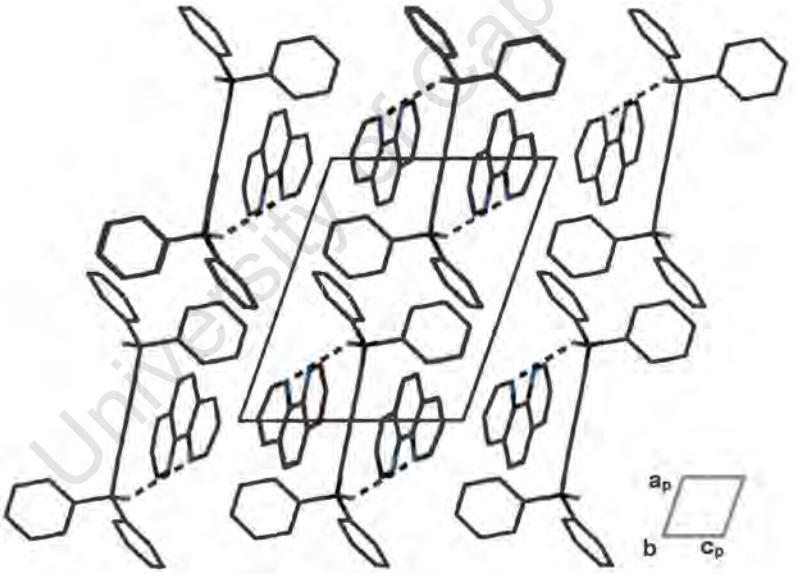

Figure 3.17: Packing diagram of **H_1 • PA** along the [010] direction, showing hydrogen bonding between host and guest molecules; O-H···N interactions.

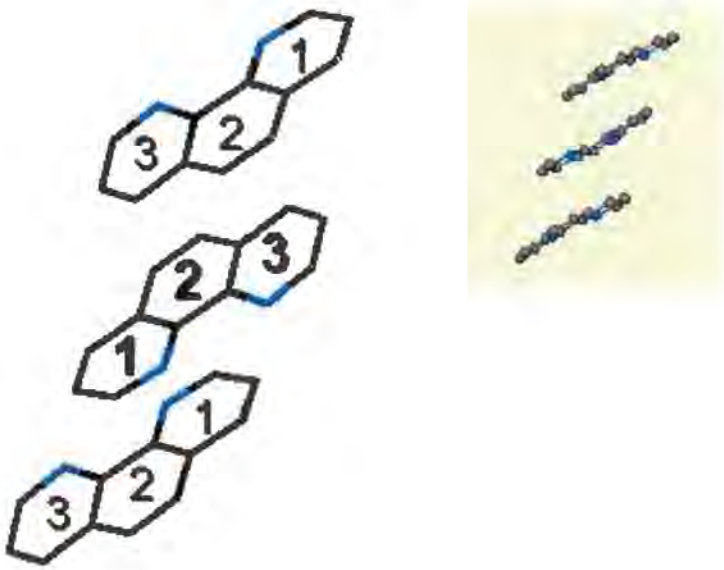

Figure 3.18: π-π stacking of guest molecules in the **H_1 • PA** structure (the insert shows parallel layers of guest molecules). 1, 2 and 3 represent the centroids of aromatic rings.

Table 3.10: π-π interaction details between guest molecules in the **H_1 • PA** structure

Ring centroid	*Distance/Å*
2···1$^{\#1}$	3.758
2···3$^{\#1}$	3.755
2···2$^{\#2}$	3.840
2···3$^{\#2}$	3.360
2···2$^{\#2}$	3.360

Symmetry codes: #1= 1-x, 1-y, -z, #2= 2-x, 1-y, -z

Van der Waals radii of carbon atoms are reported to be 1.7Å, hence the distance for π-π interaction between two aromatic rings is expected to have a value around 3.4Å[3]. The values describing the distances between aromatic ring centroids show that the π-π interactions are weak.

MOLECULAR STRUCTURE AND CRYSTAL PACKING

H_1 • 4PP

H_1: 1,1,6,6-Tetraphenyl-hexa-2,4-diyne-1,6-diol

4PP: 4-Phenylpyridine

$C_{30}H_{22}O_2 \cdot 2C_{11}H_9N$

Space group: $P\bar{1}$

Unit cell parameters: a = 8.259(2) b = 10.484(2) c = 12.280(3) /Å

α = 73.47(3) β = 71.77(3) γ = 76.83 /°

Unit cell volume = 956.9(3) Å^3

Z = 1

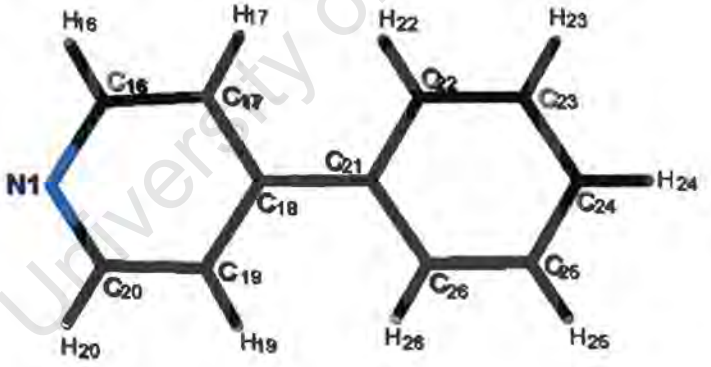

Figure 3.19: 4PP guest numbering scheme

4PP physical properties*: ***m.p*** = 69-73°C

* Measured at standard pressure and temperature

$H_1 \bullet 4PP$

The crystal structure of **H_1 • 4PP** was solved by direct methods that gave the positions of all host and guest non-hydrogen atoms. The total number of 5390 reflections measured yielded 3868 unique reflections. The $R_{(\sigma)}$ and $R_{(int)}$ – internal consistency of reflection intensities for merged pairs, having values of 0.0433 and 0.0165 respectively indicate the data to be of good quality.

All heavy atoms i.e. C, N, O, of the host and guest were refined with anisotropic temperature factors. This reduced the R-factor and also allowed the identification of all hydrogen atoms other than the hydroxyl hydrogens in the difference Fourier synthesis. These hydrogen atoms were placed with geometrically idealised positions, all being constrained to a distance of 0.930Å from their parent atom, and refined with isotropic thermal parameters $1.2xU_{eq}$ of their parent atoms. The hydroxyl hydrogen of the host was located in the difference electron density maps. Refinement led to a final O(1)-H(1) distance of 0.820Å and this represented a satisfactory location of the hydroxyl hydrogen H(1). Analysis of the interatomic distances revealed that the distance between the host oxygen O(1) and the guest nitrogen N(1) is 2.835(1)Å, indicating the presence of a hydrogen bond. The structure refined to $R_1 = 0.0396$.

The space group is $P\bar{1}$ with Z = 1 and H:G ratio 1:2. Therefore the host molecule is situated on the Wyckoff special position c (0,1/2,0), which has a site symmetry of inversion, and a multiplicity of 1, while the guest molecules are on the general positions.

The packing of **H_1 • 4PP** shows closed, square-shaped channels formed by the host molecules. The molecular packing, as shown in Figure 3.20, reveals the guest molecules to be placed in channels running in the [100] direction.

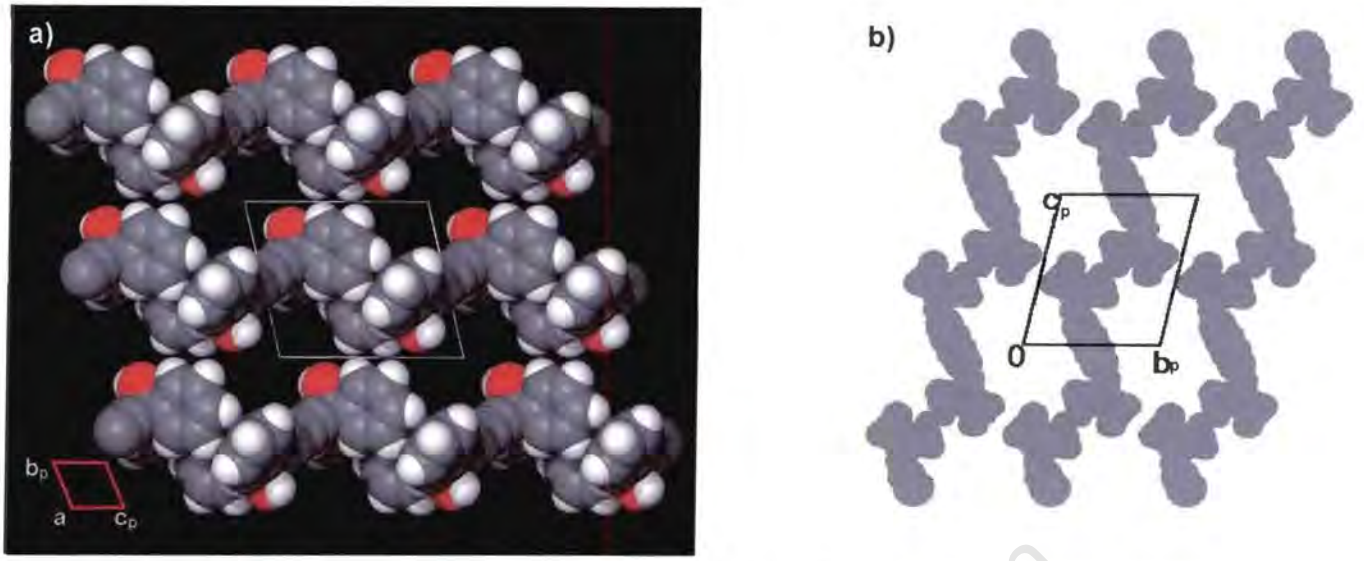

Figure 3.20: ***a)*** Space-filling representation of host molecules showing channels viewed along the [100] direction. Guest molecules are omitted. ***b)*** SECTION diagram of $\mathbf{H_1 \bullet 4PP}$, viewed down the a-axis, showing packing of host molecules with no guests present in the formed channels. ***c)*** Packing diagram of $\mathbf{H_1 \bullet 4PP}$ down [100] with guest molecules in ball-and-stick form and host molecules in stick form. Hydrogen atoms are not shown for clarity.

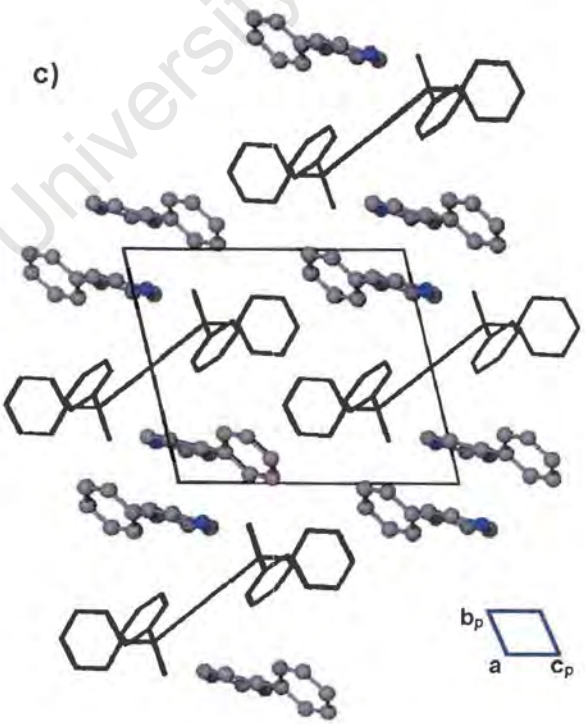

Hydrogen bonding The **H_1 • 4PP** structure is stabilised by host-guest (O-H···N) hydrogen bonding. These interactions shown in Figure 3.21 are represented by dotted lines. The bond length and bond angle values are listed in Tables 3.11 and 3.12.

The requirement of hydrogen bonding is that the distance between atoms is less than the sum of the van der Waals radii[3]. The distance between host hydroxyl oxygen and guest nitrogen is in close agreement with the required value for hydrogen bonding.

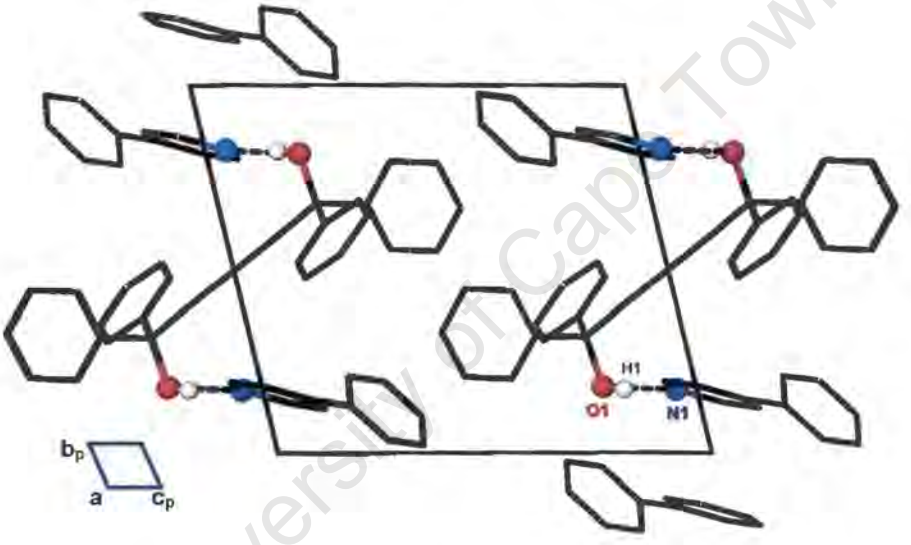

Figure 3.21: Packing diagram in **H_1 • 4PP** viewed down the [100] direction, showing O-H···N hydrogen bonding.

Table 3.11: Inter-layer hydrogen bonding details for the **H_1 • 4PP** structure

O-H···N	O-H/Å	H···N/Å	O···N/Å	Angle/°
O1-H1···N1	0.8200	2.016(3)	2.835(1)	176(2)

Symmetry codes: #1= 1-x, 1-y, -z

Table 3.12: Intra-layer hydrogen bonding details for the H_1 • **4PP** structure

C-H···O	C-H/Å	H···O/Å	C···O/Å	Angle/°
C15-H15···O1	0.9300	2.381(3)	2.732(1)	102(1)

DISCUSSION

In this work four structures with the 1,1,6,6-Tetraphenyl-hexa-2,4-diyne-1,6-diol host have been analysed, **H_1 • TED**, **H_1 • TBDA**, **H_1 • PA** and **H_1 • 4PP**, reporting the crystal structures of their final products. In all four structures the conformation of the diol-host shows the two hydroxyl groups to be *trans* and hydrogen bonding present between host and guest molecules, as is usually the case in inclusion compounds with this host.

In all four structures the host molecules pack to form single layers, which in turn stack together resulting in channels that run in the [100] direction. The structures are stabilised by host···guest hydrogen bonding interactions. The guest molecules are located in channels parallel to the a-axis. **H_1 • TED** and **H_1 • PA** inclusion compounds can be classified as thermodynamically unstable, as the guest molecules are being released before the onset temperature for the host decomposition. The **TED** guests are released at much higher temperature than **PA** guest molecules.

H_1 • 4PP and **H_1 • PA** crystallise in triclinic system, space group $P\bar{1}$, with Z value equal to 1. Guest molecules of both compounds are found in general positions, while host molecules are located on the center of inversion, at Wyckoff positions, c and d respectively. The cell dimensions as well as the cell volumes observed are comparable in size. In both cases the hydroxyl oxygen of the host is hydrogen bonded to the guest nitrogen. The O···N hydrogen bond distances are 2.835(1) Å and 2.887(1) Å respectively, which can be characterised as medium strength hydrogen bonds when compared to some reported values[5]. The packing arrangement in the **H_1 • PA** structure is such that the guest-guest, π-π interactions are observed.

H_1 • TED crystallises in the space group $P\bar{1}$, with Z = 2 and the unit cell volume one half as large as that observed in the two structures mentioned above. The host molecule is located on the center of inversion, at Wyckoff position e, while the guest molecules occupy general positions. The O···N hydrogen bond distance is 2.729(1) Å, which indicates a strong hydrogen bond[5].

The **H_1 • TBDA** structure crystallises in the monoclinic system, space group $P2_1/n$, with Z = 2. The host single layers pack in an open channel manner, due to bulky guest molecules. The host and guest molecules pack efficiently and are stabilised by O-H···O hydrogen bonds that are moderately strong, the distance being 2.742(2) Å. The carbonyl group of each guest is hydrogen bonded to the hydroxyl group of each host, creating a hydrogen-bonding network that stabilises the structure. Due to the size of the guest molecules the unit cell volume is four times larger than that observed in the **H_1 • 4PP** and **H_1 • PA** structures.

4 INCLUSION COMPOUNDS WITH H_2

"Things should be made as simple as possible, but not simpler."

-Albert Einstein

"Nothing can be found in nature that is not a part of science."

-Leonardo da Vinci

THERMAL ANALYSIS, MOLECULAR STRUCTURE AND CRYSTAL PACKING OF COMPOUNDS WITH HOST H_2

The abbreviations for the salt compounds in this chapter are:

H_2: 5-(3,5-Dicarboxyphenylethynyl)-isophthalic acid

H_2 • RPEA *:* H_2 and (+)-(R)-1-Phenylethylamine
H_2 • RSPEA *:* H_2 and (±)-(R,S)-1-Phenylethylamine
H_2 • PEA *:* H_2 and 2-Phenylethylamine
H_2 • Na *:* H_2 and sodium
H_2 • Rb *:* H_2 and rubidium
H_2 • Cs *:* H_2 and caesium

Six salt structures formed between the host anions and the guest cations were solved and analysed in this chapter. The thermal investigation of their behaviour was performed using thermal techniques such as TG, DSC and HSM.

Crystal data, experimental and refinement parameters for the six salt compounds are provided in table 4.3.

The guest numbering schemes are given at the beginning of each structure analysis while the host numbering scheme can be found on the bookmark.

COMPLEX PREPARATION

Crystalline complexes, **H_2 • RPEA**, **H_2 • RSPEA** and **H_2 • PEA**, were obtained from the slow evaporation of solutions of host and guest in 1:4 molar ratios. The solutions were prepared according to the concentrations listed in Table 4.1. The crystallisation process lasted up to 5 days in order to obtain single crystals of suitable quality.

Table 4.1: Preparation details for H_2-complexes with guests, **RPEA**, **RSPEA** and **PEA**

Complex	*H_2 (mmol)*	*Guest (mmol)*	*Molar ratio*	*Solvent used*
H_2 • RPEA	0.14	0.69	1:4	methanol
H_2 • RSPEA	0.14	0.69	1:4	methanol
H_2 • PEA	0.14	0.69	1:4	methanol

Hydrated metal salts, **H_2 • Na**, **H_2 • Rb** and **H_2 • Cs**, were obtained by dissolving 0.030g (0.085mmol) of the host in NaOH, CsOH and a solution of $RbCO_3$ in methanol of 0.1mol/L strength. Crystals of suitable quality were obtained in a period up to 25 days with a host to guest ratio of 1:1.

THERMAL ANALYSIS

Traces obtained from DSC and TG analyses of **H_2 • RPEA**, **H_2 • RSPEA**, **H_2 • PEA**, **H_2 • Na**, **H_2 • Rb** and **H_2 • Cs** are shown in Figures 4.1a), b), c), d), e) and f). The decomposition of the **H_2 • RPEA**, **H_2 • RSPEA** and **H_2 • PEA** structures is complex. For the DSC traces all complexes show endothermic events corresponding to water loss in the range 30 to 150°C, labelled A.

For **H_2 • RPEA** the Differential Scanning Calorimetry (DSC) showed the loss of six water molecules by a characteristic broad endotherm A (Figure 4.1a). The TG trace corresponds to this result showing the percentage weight loss of 11.6% (calc.11.4%). After the water molecules have been lost the DSC shows three distinct steps of guest loss. The TG trace shows three overlapping steps of guest loss with three individual mass losses of 25.3%, 13.1% and 12.2%, the values of which suggest that two ligands are lost in a single step, followed by successive loss of two remaining ligands. The weight percentage loss of 50.6% for the four guests corresponds well to the calculated value of 51.6%. The two-ligand mass loss in a single step in the TG trace corresponds to endotherm B in the DSC. This is followed by two individual endotherms C and D representing the successive losses of the two remaining ligands. At this stage only host has remained and an exotherm F indicating its decomposition at a slightly higher temperature than the standard melting point of the host alone (417°C) appears. Endotherm E can be explained as endothermic crystal transition preceding the decomposition of the host alone.

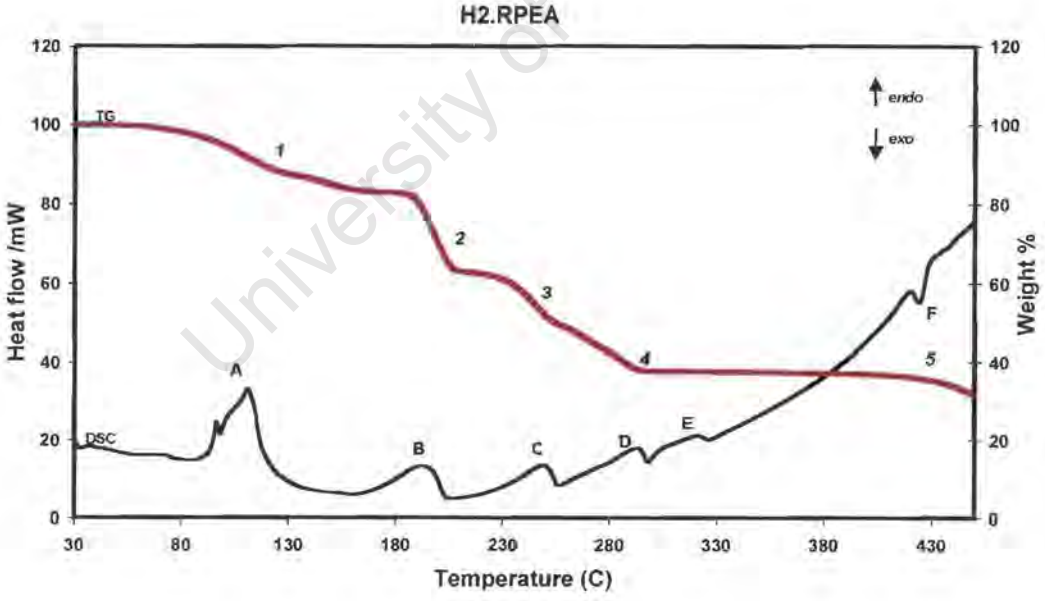

Figure 4.1a: TG and DSC traces for **H_2 • RPEA**

The **H_2 • RSPEA** and **H_2 • RPEA** structures contain the same guest component (+)-(R)-1-Phenylethylamine with **H_2 • RSPEA** having its enantiomer as well and therefore their DSC and TG traces appear to have similarities (Figure 4.1b). Therefore, mass loss percentage upon decomposition of **H_2 • RPEA** corresponds to the mass loss percentage of **H_2 • RSPEA**. **H_2 • RSPEA** decomposes in five distinct steps with the mass loss values of 11.1%, 23.3%, 12.5%, 12.5% and 7.8% respectively as the temperature increases. This corresponds to a loss of six water molecules (calc.11.4%), four guests (two in a single step and two in two distinct steps) and decomposition of the host alone. The first four decomposition steps have a corresponding endotherm in the DSC trace viz. A, B, C, D, while the fifth step has a corresponding exotherm due to the host decomposition. There is an additional endotherm E due to a host phase transition.

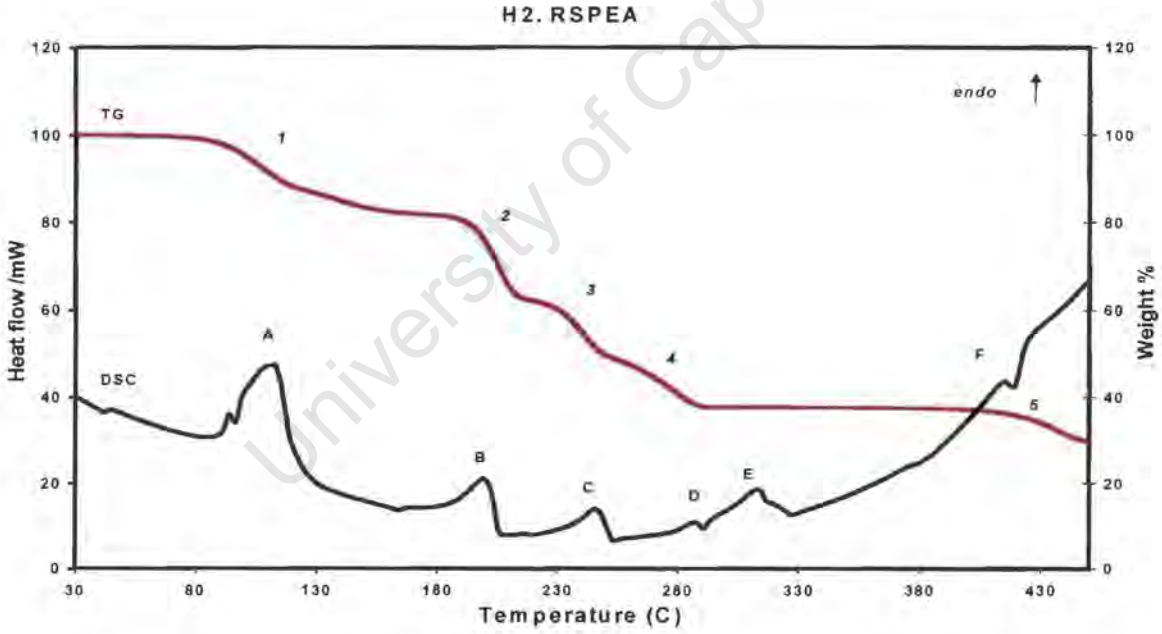

Figure 4.1b: TG and DSC traces for **H_2 • RSPEA**

The DSC experiment for **H_2 • PEA** yielded five endotherms labelled A, B, C, D and E and an exotherm F (Figure 4.1c). The endotherm A, at the lowest temperature, shows loss of five water molecules. Endotherm B is due to loss of two guests while two remaining guest losses correspond to endotherms C and D. The host alone melts and subsequently decomposes. This is shown by an endotherm E followed by an exotherm F. In the TG trace there are four distinct decomposition steps, each corresponding to the DSC trace endotherm.

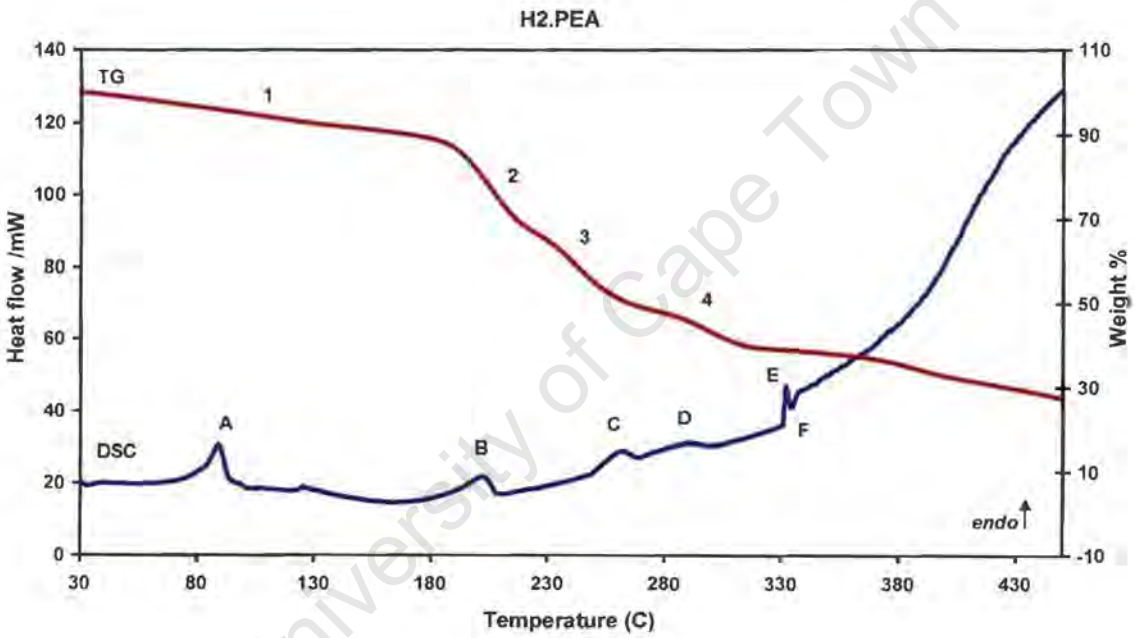

Figure 4.1c: TG and DSC traces for **H_2 • PEA**

The TG for metal salt structure **H_2 • Na** (Figure 4.1d) shows a two-step mass loss corresponding to endotherms A and B in the DSC trace. Steps 1 and 2 mass losses of 9.7% and 16.8% correspond to the loss of ten water molecules found in the structure, bonded to metal ions, being released at two different temperatures. The reason for this is that some waters of crystallisation are more strongly bonded to sodium ions compared to the others therefore requiring more energy for their release. The sum of the experimental values for percentage weight loss is 26.5%(calc. 28.9%). The DSC trace shows two distinct endotherms A and B corresponding to water loss.

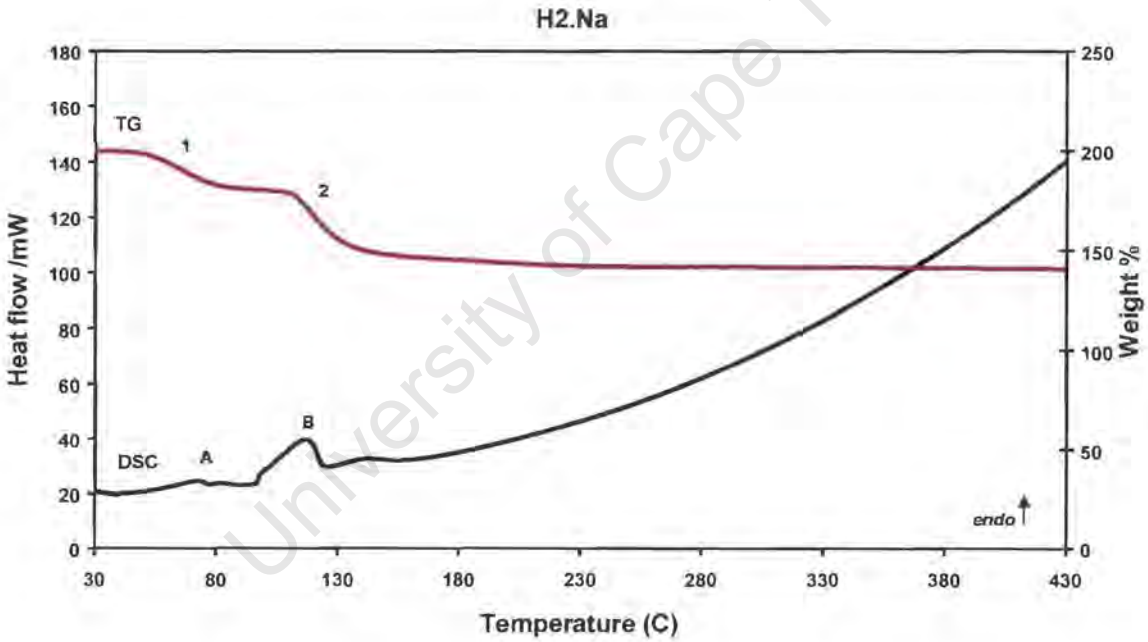

Figure 4.1d: TG and DSC traces for **H_2 • Na**

TG and DSC traces for **H_2 • Rb** show no distinct peaks or steps in the recorded temperature range (Figure 4.1e). A DSC peak marked A and a corresponding step 1, show a multistep process that can be attributed to water loss.

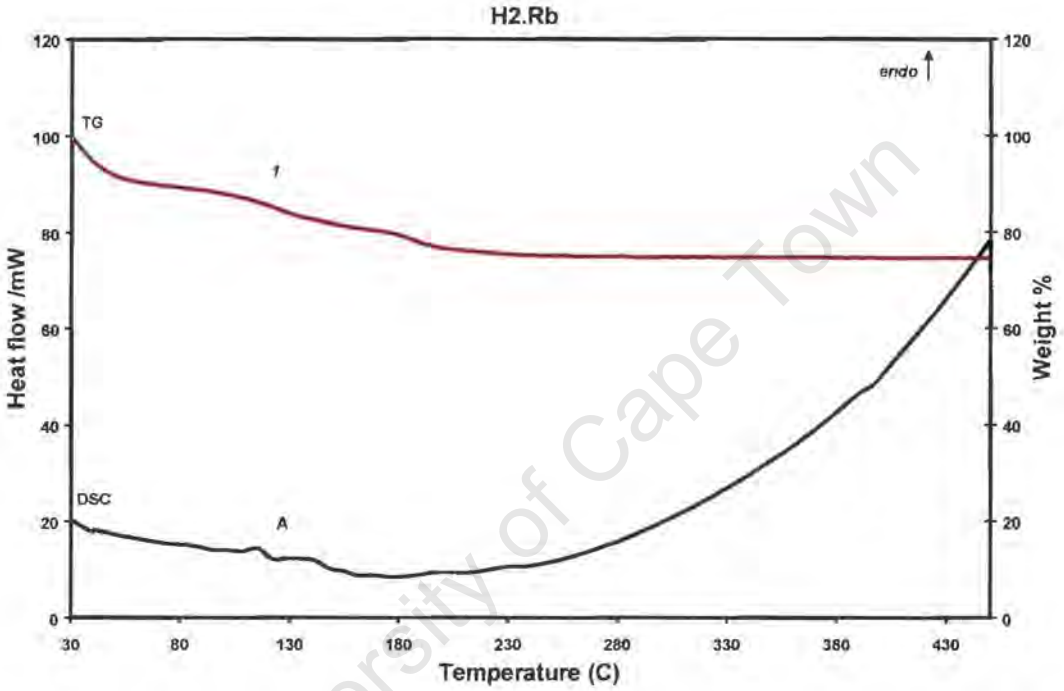

Figure 4.1e: TG and DSC traces for **H_2 • Rb**

Thermal analysis results for **H_2 • Cs** are given in Figure 4.1f. The TG shows three distinct mass loss processes. At low temperatures the mass loss due to water molecules coordinated to caesium ions and being lost upon temperature increase is shown by step 1. This corresponds to a weak endotherm A in the DSC trace, but recorded at a higher temperature. Step 2, at 195°C, is a mass loss due to water molecules that are coordinated to caesium ions, with no correspondence in the DSC trace. We surmise that this is because the enthalpy change is very small. Above 180°C the TG curve shows mass loss indicating salt decomposition. This is shown by step 3 in the TG trace.

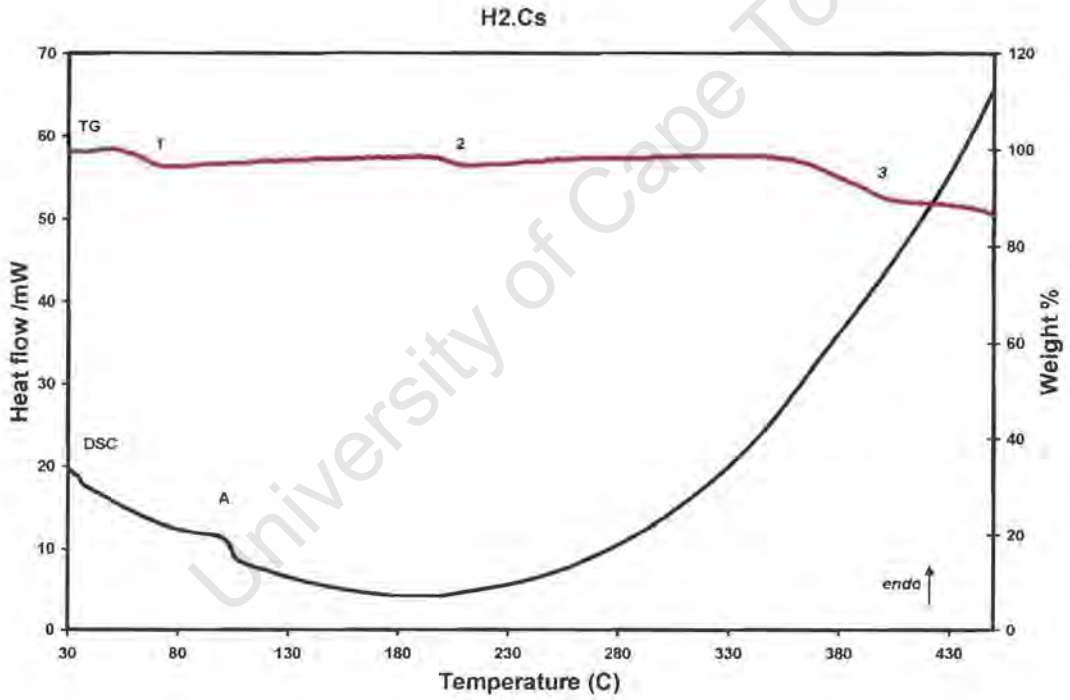

Figure 4.1f: TG and DSC traces for **H_2 • Cs**

Thermal analysis results for all six structures are summarised in Tables 4.2a and 4.2b.

Table 4.2a: TG thermal analysis results for **H_2 • RPEA**, **H_2 • RSPEA** and **H_2 • PEA**

Inclusion compound		H_2 • RPEA	H_2 • RSPEA	H_2 • PEA
Step 1	**Range(°C)**	46.4 – 179.6	68.0 – 174.97	46.4 – 168.4
	Exp.(Calc)%	11.6(11.4)	11.1(11.4)	8.9(9.69)
Step 2	**Range (°C)**	178.9 – 210.4	176.3 – 215.6	168.4 – 228.1
	Exp.(Calc.)%	25.3(25.6)	23.3(25.6)	24.6(26.1)
Step 3	**Range (°C)**	209.7 – 255.0	215.6 – 248.4	228.1 – 260.9
	Exp.(Calc.)%	13.1(12.8)	12.5(12.8)	14.2(13.0)
Step 4	**Range (°C)**	255.0 – 298.3	248.4 – 295.7	260.9 – 335.0
	Exp. %	12.2(12.8)	12.5(12.8)	12.1(13.0)

The enthalpy represents the energy that must be supplied to release the guest component from the crystal or to break the entire host-guest crystal structure at a specific temperature. It is a measure of the strength with which the crystal is held together and it can be positive (the energy is absorbed) or negative (the energy is released). Tables 4.2a and 4.2b give the enthalpy values recorded during the thermal analysis.

Table 4.2a (continued): DSC thermal analysis results for **H_2 • RPEA**, **H_2 • RSPEA** and **H_2 • PEA**

Inclusion compound		H_2 • RPEA	H_2 • RSPEA	H_2 • PEA
Peak A	**T_{on}(°C)**	92.9	94.6	82.4
	ΔH (kJ.mol^{-1})	206.7	262.2	45.2
Peak B	**T_{on}(°C)**	168.6	181.3	188.7
	ΔH (kJ.mol^{-1})	102.0	102.8	31.5
Peak C	**T_{on}(°C)**	228.6	232.0	249.0
	ΔH (kJ.mol^{-1})	44.0	50.8	21.7
Peak D	**T_{on}(°C)**	272.6	288.6	276.2
	ΔH (kJ.mol^{-1})	25.8	5.1	11.0
Peak E	**T_{on}(°C)**	301.5	299.4	330.8
	ΔH (kJ.mol^{-1})	11.0	38.3	8.6
Peak F	**T_{on}(°C)**	420.0	413.7	332.9
	ΔH (kJ.mol^{-1})	-13.2	-11.5	-3.5

Table 4.2b: Thermal analysis results for **H_2 • Na**, **H_2 • Rb** and **H_2 • Cs**

Inclusion compound		**H_2 • Na**	**H_2 • Rb**	**H_2 • Cs**
TG/				
Step 1	**Range(°C)**	42.5 – 99.5	164.4 – 252.35	45.3 – 86.1
	Exp.(Calc.)%	9.7(*)	13.4(13.5)	5.4(*)
Step 2	**Range(°C)**	104.1 – 228.7	-	182.1 – 232.2
	Exp.(Calc.)%	16.8(*)	-	4.5(*)
DSC/				
Peak A	**T_{on}(°C)**	56.2	-	80.4
	ΔH (kJ.mol^{-1})	21.0	-	94.7
Peak B	**T_{on}(°C)**	96.7	-	-
	ΔH (kJ.mol^{-1})	193.6	-	-

* Calculated values for percentage weight loss correspond to the sum of experimental values for percentage weight loss of step 1 and 2 in TG. For **H_2 • Na** and **H_2 • Cs** the Exp.(Calc.)% values are 26.5(28.9) and 9.9(10.91) respectively.

HSM

The thermal behaviour of the complexes was analysed using HSM at a constant heating rate. The HSM results and their descriptions for **H_2 • RPEA**, **H_2 • RSPEA**, **H_2 • PEA**, **H_2 • Na**, **H_2 • Rb** and **H_2 • Cs** are given in Figures 4.2-4.7.

H_2 • RPEA

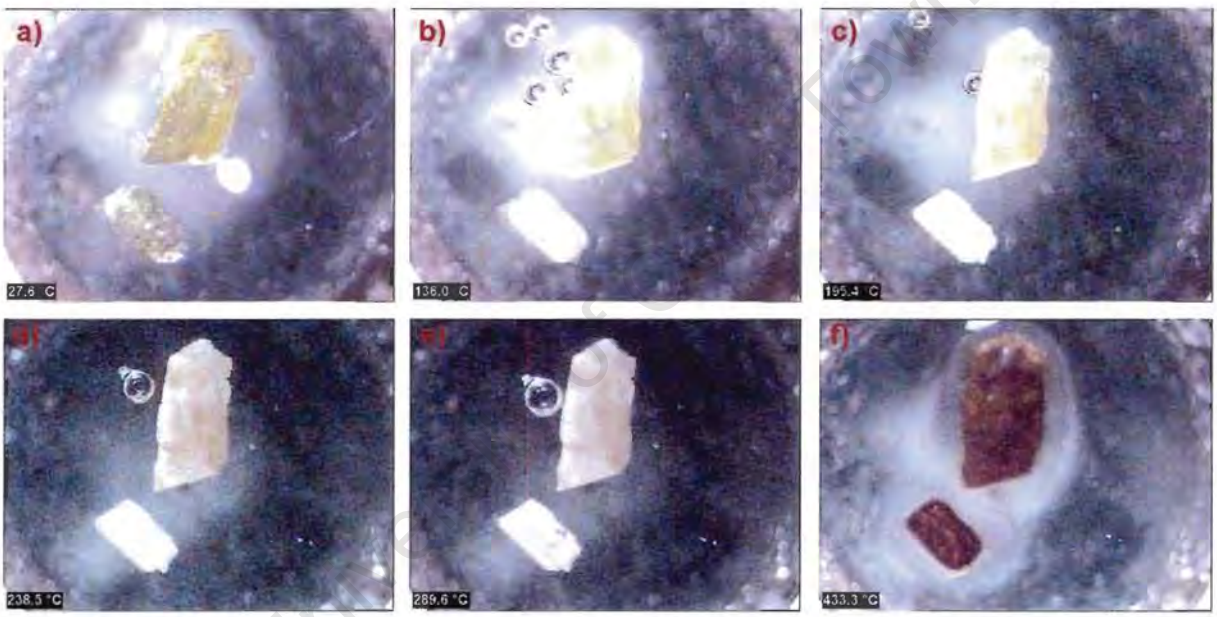

Figure 4.2:

a) The translucent yellow crystals of **H_2 • RPEA** complex are immersed in silicone oil at room temperature.

b) Water molecules escape the structure at low temperatures causing bubbles.

c), ***d)*** and ***e)*** Crystals turn opaque and bubbling is present due to a guest desorption.

f) All bubbling ceases after the ligand release. Crystals change colour from dark yellow to brown as the host decomposes.

H_2 • RSPEA

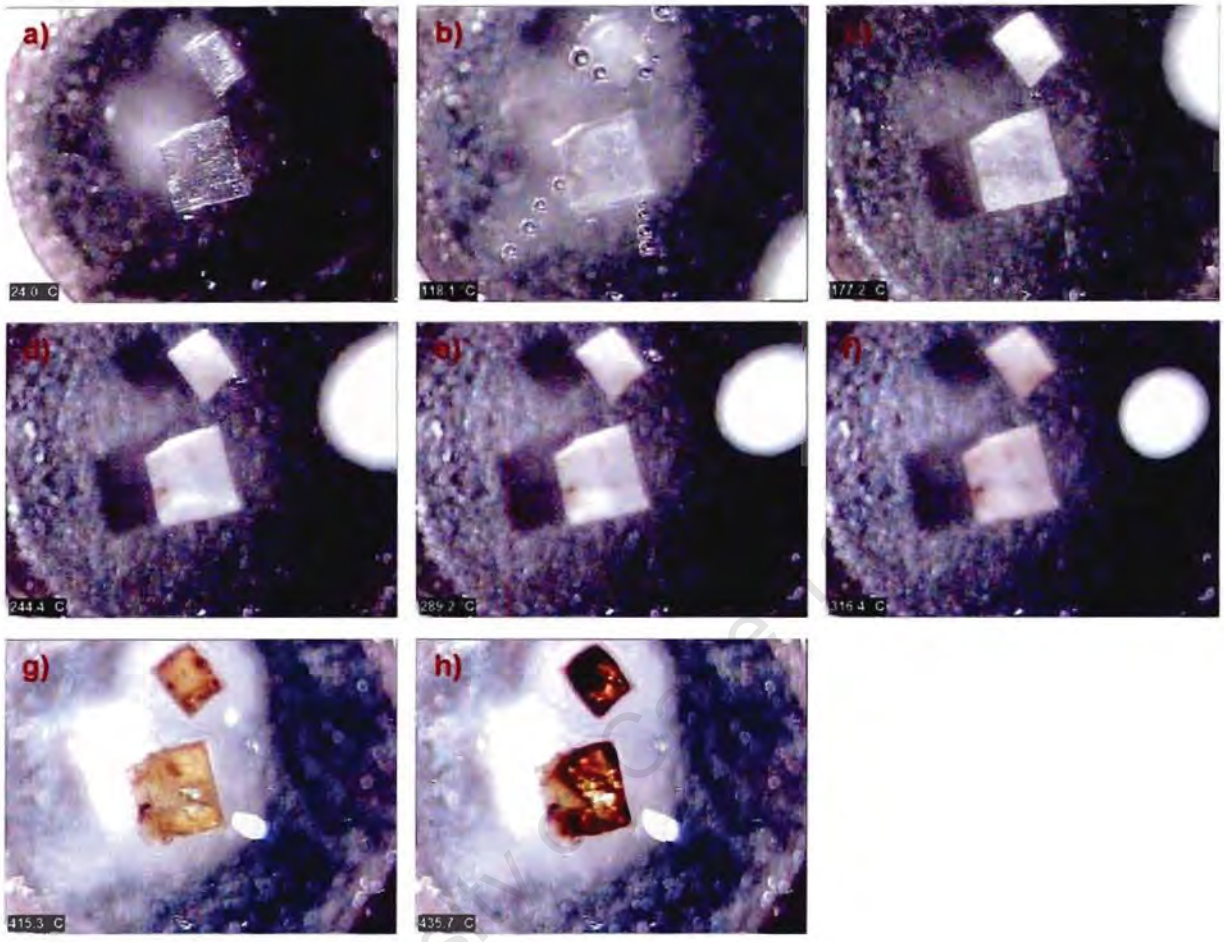

Figure 4.3:

a) **H_2 • RSPEA** complex has translucent crystals, here immersed in silicone oil at room temperature.

b) At the onset temperature of water release the crystals start bubbling.

c), ***d)*** and ***e)*** these onset temperatures correspond to guest release and collapse of the crystal structure. The translucent crystals bubble and turn opaque.

f) and ***g)*** The bubbling is resumed, and the crystals turn from white to light yellow.

h) The crystals turn yellow-red upon host decomposition.

H_2 • PEA

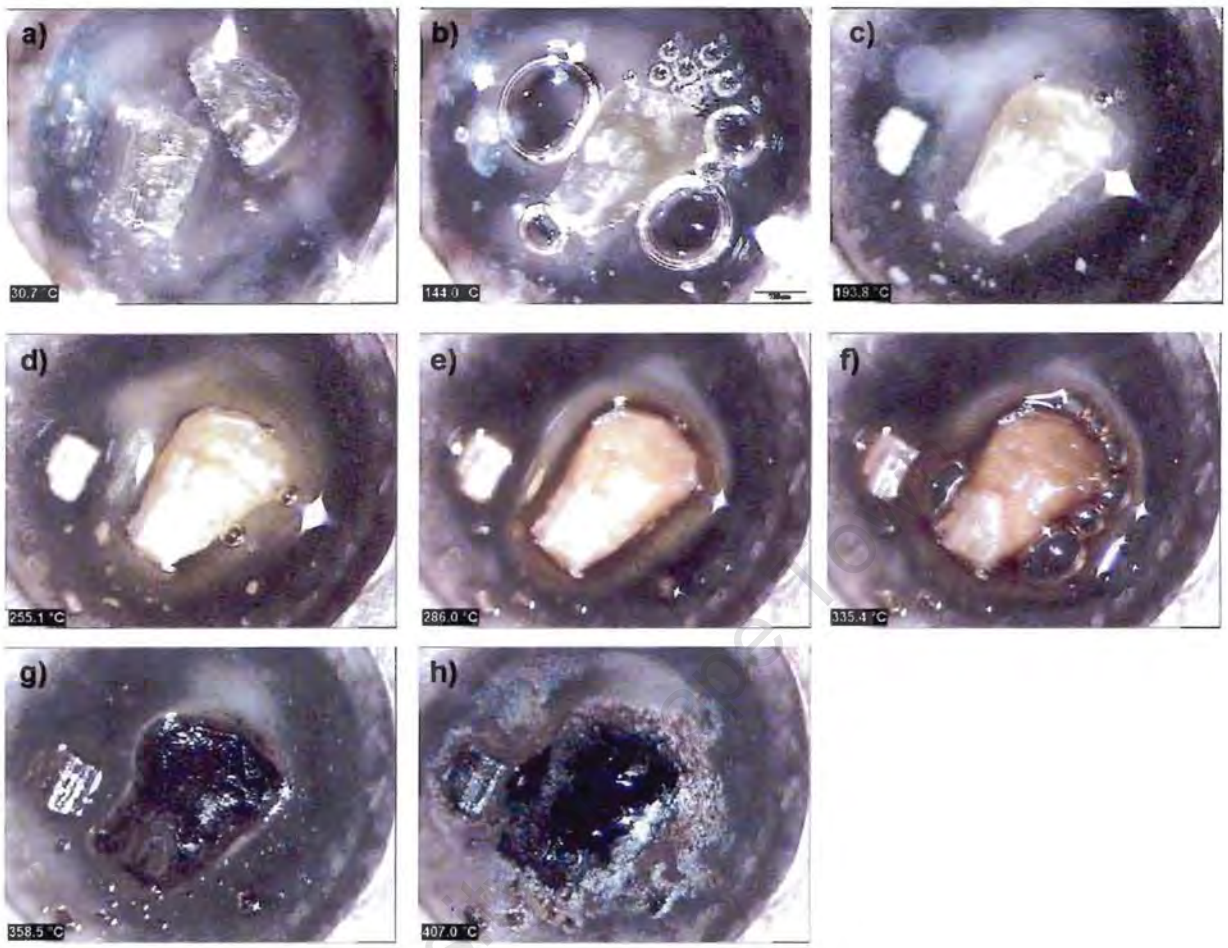

Figure 4.4:

a) The **H_2 • PEA** translucent crystals are immersed in silicone oil at room temperature.

b) The translucent crystals bubble, as a consequence of ligand release and beginning of breaking up of the crystal structure, and turn yellow in colour.

c) and ***d)*** Further bubbling continues due to a ligand release and is accompanied by the colour getting darker.

e) and ***f)*** At the onset of the last ligand being released, the colour of the crystal turns darker in colour and continues bubbling.

g) and ***h)*** Above 335°C the crystal resumes bubbling and a dark brown residue is formed upon host decomposition.

H_2 • Na

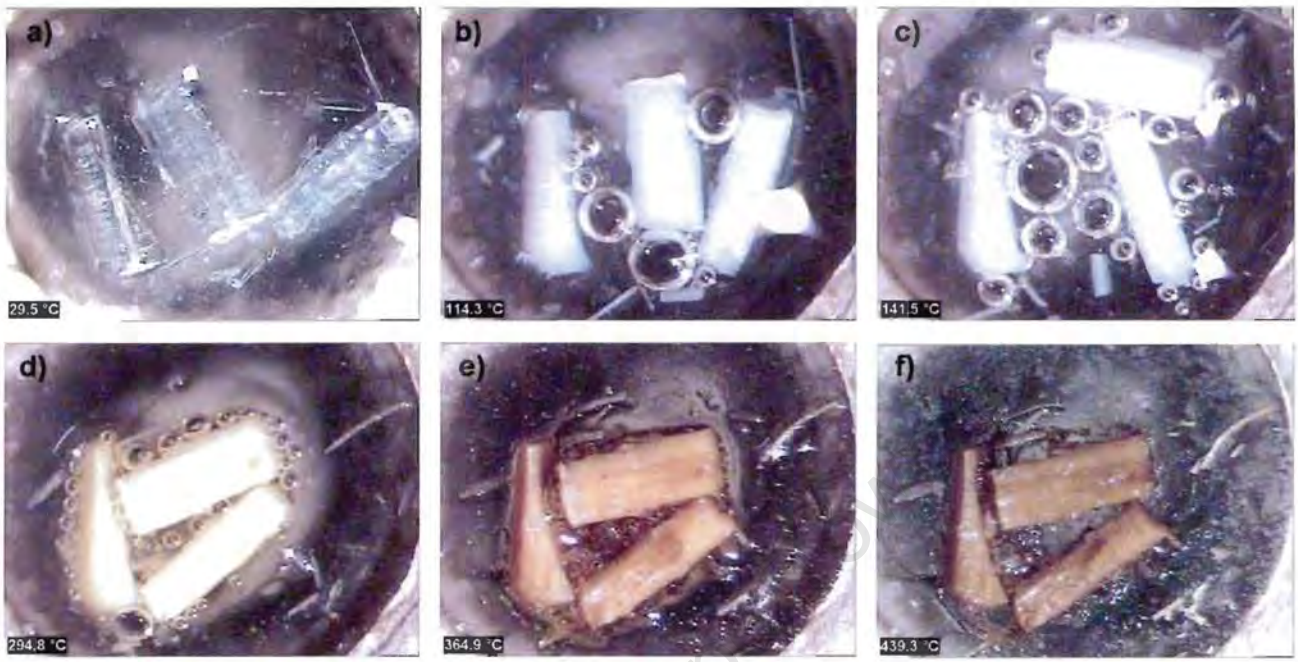

Figure 4.5:

a) The crystals of **H_2 • Na** metal salt complex coated with silicone oil are photographed here at room temperature.

b) and ***c)*** At the onset temperature the translucent crystals bubble and turn opaque due to the loss of water molecules from the crystal structure.

d) Bubbling continues as a result of a desolvation process and the crystals turn yellow.

e) The decomposition of the crystal structure begins as the crystals turn yellow-red.

f) All the bubbling has ceased as the metal salt decomposes.

H_2 • Rb

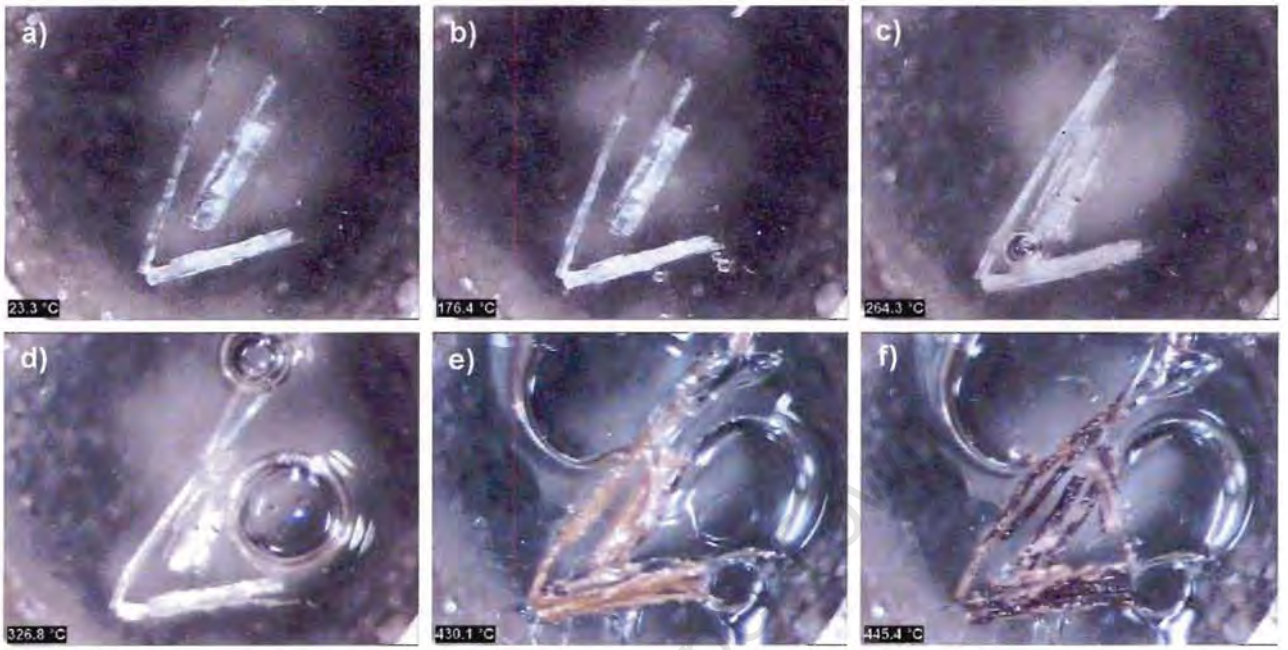

Figure 4.6:

a) The translucent crystals of **H_2 • Rb** complex are immersed in silicone oil at room temperature.

b) Bubbles appear due to the loss of water molecules.

c) Crystals are turning opaque due to the collapse of the crystal structure and release of water molecules.

d) Bubbling persists due to the decomposition of the metal salt with crystals turning yellow.

e) and ***f)*** Bubbles continue to evolve as crystals turn from orange to dark red upon decomposition.

H_2 • Cs

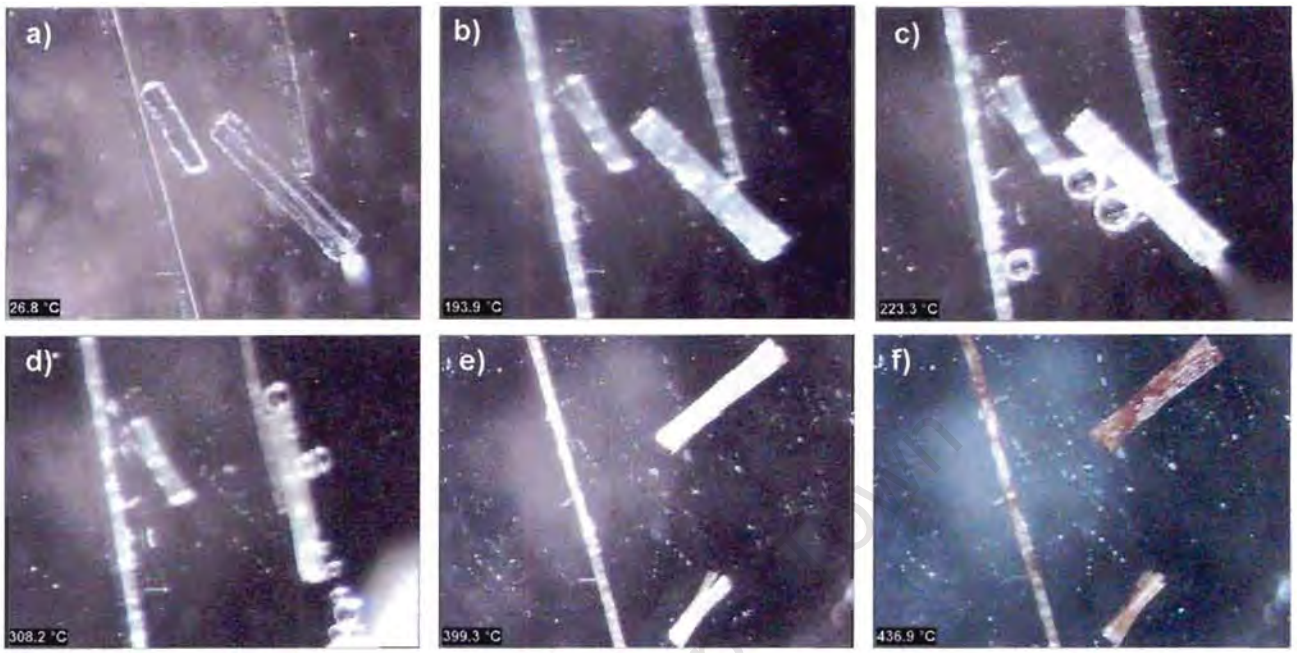

Figure 4.7:

a) The translucent crystals of the **H_2 • Cs** complex are immersed in silicone oil at room temperature.

b) Crystals are turning opaque due to the collapse of the crystal structure and release of water molecules.

c) and ***d)*** Bubbling appears due to decomposition of the metal salt with crystals turning yellow.

e) and ***f)*** Bubbles stop evolving and crystals turn dark red upon decomposition.

Table 4.3: Crystal data and refinement parameters

Compound	H_2 • RPEA	H_2 • RSPEA	H_2 • PEA	H_2 • Na	H_2 • Cs	H_2 • Rb
Molecular formula	$[C_{18}H_6O_8]^{-4}$ · $4[C_8H_{12}N]^+ \cdot 6H_2O$	$[C_{18}H_6O_8]^{-4}$ · $4[C_8H_{12}N]^+ \cdot 6H_2O$	$[C_{18}H_6O_8]^{-4}$ · $4[C_8H_{12}N]^+ \cdot 5H_2O$	$[C_{18}H_6O_8]^{-4}$ · $4Na^+ \cdot 10H_2O$	$[C_{18}H_6O_8]^{-4}$ · $4Cs^+ \cdot 6H_2O$	$[C_{18}H_6O_8]^{-4}$ · $4Rb^+ \cdot 6H_2O$
Formula weight	947.07	947.07	929.05	622.35	989.96	800.20
Crystal system	monoclinic	monoclinic	orthorhombic	monoclinic	monoclinic	monoclinic
Space group	$P2_1$	C2/c	Pbca	$P2_1/c$	$P2_1/n$	$P2_1/n$
Temperature, K	173	173	173	173	173	173
a, Å	7.2739(2)	32.550(7)	16.8061(2)	3.6288(7)	4.2667(9)	4.0435(8)
b, Å	11.3936(2)	11.402(2)	22.5832(2)	21.299(4)	18.4341(3)	18.991(4)
c, Å	31.272(1)	14.549(3)	26.5572(3)	16.022(3)	16.8981(1)	16.411(3)
α, °	90	90	90	90	90	90
β, °	93.247(1)	106.412(3)	90	95.574(2)	94.742(2)	95.894(2)
γ, °	90	90	90	90	90	90
V, Å^3	2587.5(9)	5179.6(18)	10079.4(2)	1232.5(4)	1324.5(5)	1253.5(4)
Z	2	4	8	2	2	2
Absorption coefficient, mm^{-1}	0.089	0.089	0.089	0.206	5.525	7.830
F(000)	1012	2024	3968	644	916	772
Crystal size, mm	0.32x0.35x0.40	0.28x0.45x0.21	0.30x0.40x0.25	0.10x0.26x0.20	0.15x0.10x0.07	0.25x0.1x0.09
Index ranges	-6<=h<=9, -14<=k<=13, -29<=l<=38,	-37<=h<=40, -14<=k<=13, -18<=l<=17,	-14<=h<=20, -27<=k<=25, -32<=l<=29,	-4<=h<=3, -23<=k<=25, -13<=l<=18,	-5<=h<=5, -22<=k<=23, -20<=l<=21,	0<=h<=5, 0<=k<=24, -21<=l<=21,
Reflections collected/unique	8835/7643 [R(int) =0.0289]	12416/5250[R(int) =0.0384]	42756/9754[R(int) =0.0582]	5032/2156[R(int) =0.0346]	7608/2923[R(int) =0.0285]	2505/2505[R(int) =0.0000]
Refinement method	Full-matrix least-squares on F^2	Full-matrix least-squares on F^2	Full-matrix least-squares on F^2	Full-matrix least-squares on F^2	Full-matrix least-squares on F^2	Full-matrix least-squares on F^2
Data/restraints/Parameters	7643/1/665	5250/10/345	9754/0/648	2156/0/213	2923/0/179	2505/0/183
Goodness-of-fit on F^2	1.043	1.020	1.050	1.103	1.079	1.033
ρ_{calc}, g.cm^{-3}	1.2154	1.2143	1.2243	1.6768	2.4818	2.1197
Final R indices [I > 2σ(I)]	R_1=0.0602, wR_2=0.1533	R_1=0.0750, wR_2=0.1714	R_1=0.0503, wR_2=0.1175	R_1=0.0483, wR_2=0.1064	R_1=0.0293, wR_2=0.0651	R_1=0.0582, wR_2=0.1247
R indices (all data)	R_1=0.1050, wR_2=0.1769	R_1=0.1308, wR_2=0.2015	R_1=0.1054 wR_2=0.1426	R_1=0.0882, wR_2=0.1250	R_1=0.0388, wR_2=0.0698	R_1=0.0966, wR_2=0.1468
Largest diffraction peak and hole, eÅ^{-3}	0.43 and –0.23	0.51 and –0.27	0.58 and –0.36	0.57 and –0.50	1.43 and –1.68	1.09 and –1.21

MOLECULAR STRUCTURE AND CRYSTAL PACKING

H_2 • RPEA

H_2: 5-(3,5-Dicarboxyphenylethynyl)-isophthalic acid

RPEA: (+)-R-1-Phenylethylamine

$[C_{18}H_6O_8]^{-4} \cdot 4[C_8H_{12}N]^{+} \cdot 6H_2O$

Space group: $P2_1$

Unit cell parameters: a = 7.2739(2) b = 11.3936(2) c = 31.272(1) /Å

β = 93.247(1) /°

Unit cell volume = 2587.5(1) $Å^3$

Z = 2

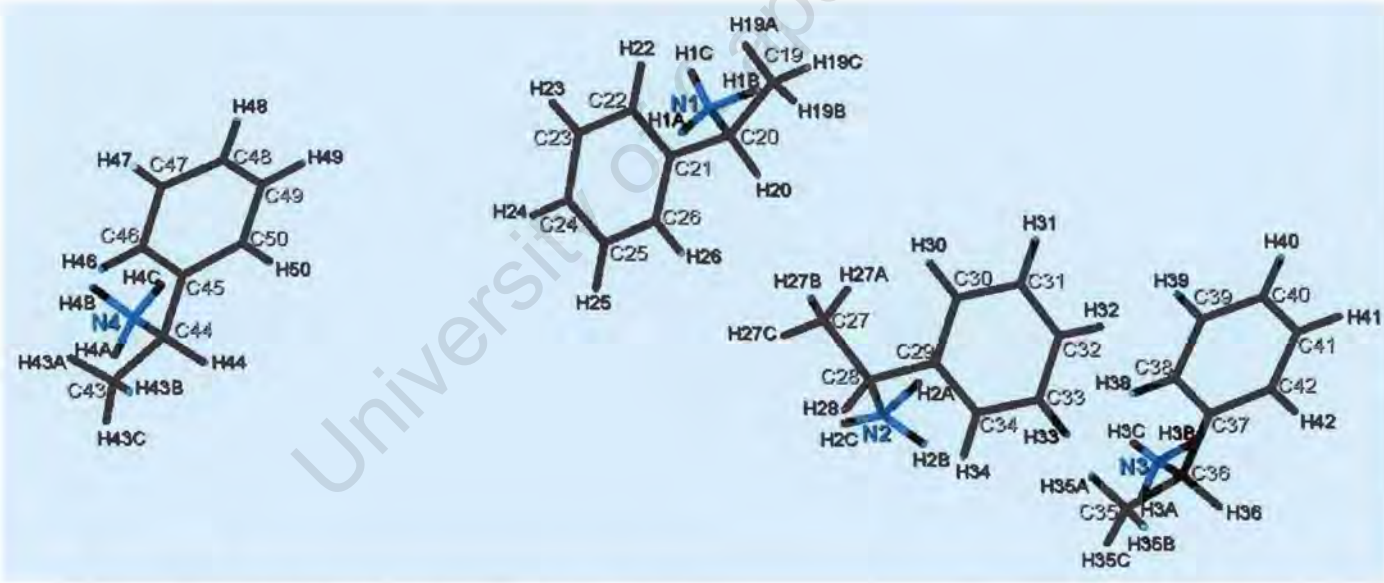

Figure 4.8: RPEA guest numbering scheme

RPEA physical properties*: ***m.p*** = -65°C

b.p = 180-181 °C

* Measured at standard pressure and temperature.

H_2 • RPEA

Space group $P2_1$ was chosen based on the $|E^2-1|$ statistics obtained by direct methods and the fact that the guest component is chiral. The following conditions for systematic absences were observed on inspection of X-ray intensity data:

hkl: none
h0l: none
0k0: k = 2n + 1

confirming the space group $P2_1$. The space group choice was validated by the successful refinement of the structure.

The structure was solved using program SHELX-86 and refined using program SHELX-97. A total of 8835 measured reflections yielded 7643 unique data. A further 1776 were suppressed as unobserved ($4\sigma(F) > F$) leaving 3381 observed reflections. With $R_{int} = 0.0289$ and $R_\sigma = 0.0773$ the data were considered to be of good quality.

Direct methods yielded all non-hydrogen atoms in the asymmetric unit, divided into one host anion, four guest cations and six water molecules. Anisotropic thermal parameters were assigned to all non-hydrogen atoms. Hydrogen atoms of the guest cation and the host anion were geometrically constrained to their parent carbon atoms at C-H distances of 0.930Å for aromatic hydrogens, 0.960Å for the $-CH_3$ group hydrogens and 0.980Å for the guest cation -CH group, after which they were refined with linked temperature factors. The hydrogen atoms belonging to the $-NH_3^+$ group and water were allowed to refine without constraints. The refinement proceeded successfully with the final $R_1 = 0.0602$.

The asymmetric unit contains one host anion, four guest cations and six waters of crystallisation with $H:G_1:G_2$ ratio of 1:4:6 and Z = 2. All of the molecules are located on the general positions.

The **H_2 • RPEA** crystal structure showed the host carboxylate groups and guest NH_3^+ groups hydrogen bonded to each other. The hydrogen bond network includes O-H···O and N-H···O hydrogen bonding. N···O and O···O distances between host

anions, guest cations and water molecules indicated the presence of intra- and intermolecular hydrogen bonding. Each guest cation is hydrogen bonded to two neighbouring host anions and a water molecule, and each host carboxylate group is bonded to two guest cations and a water molecule, thus creating a hydrogen bond network that stabilises the structure.

The packing arrangement of the **H_2 • RPEA** structure shows host anions stacked together in rows making just enough space for the guest cations to fill it. These spaces form channels that run parallel to each other in the [100] direction. The packing diagram is shown in Figure 4.9 (water molecules are omitted for clarity).

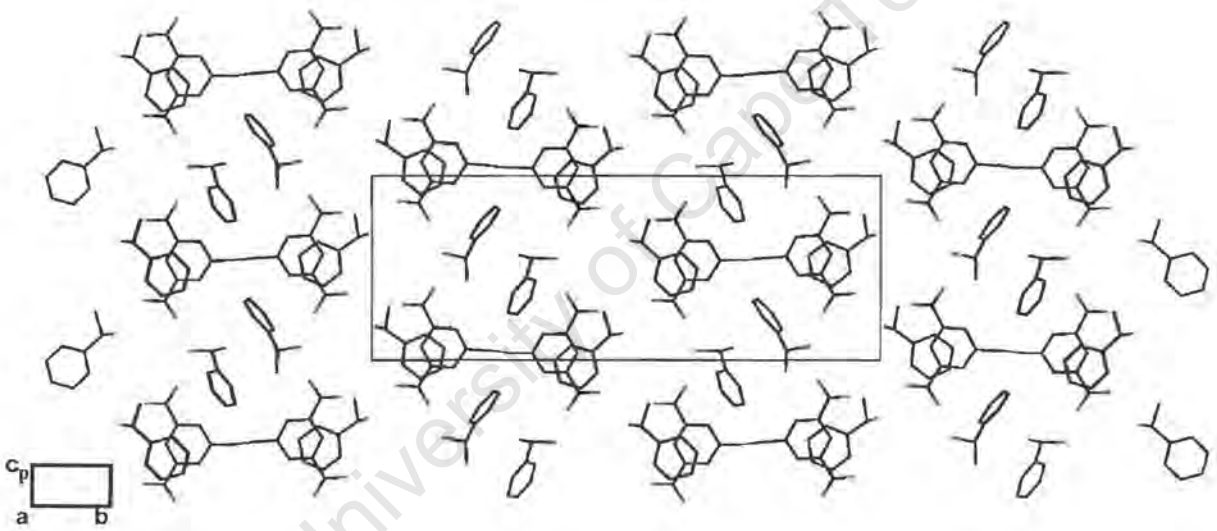

Figure 4.9: Packing diagram of the **H_2 • RPEA** structure viewed along the [100] direction. Hydrogen atoms are omitted for clarity.

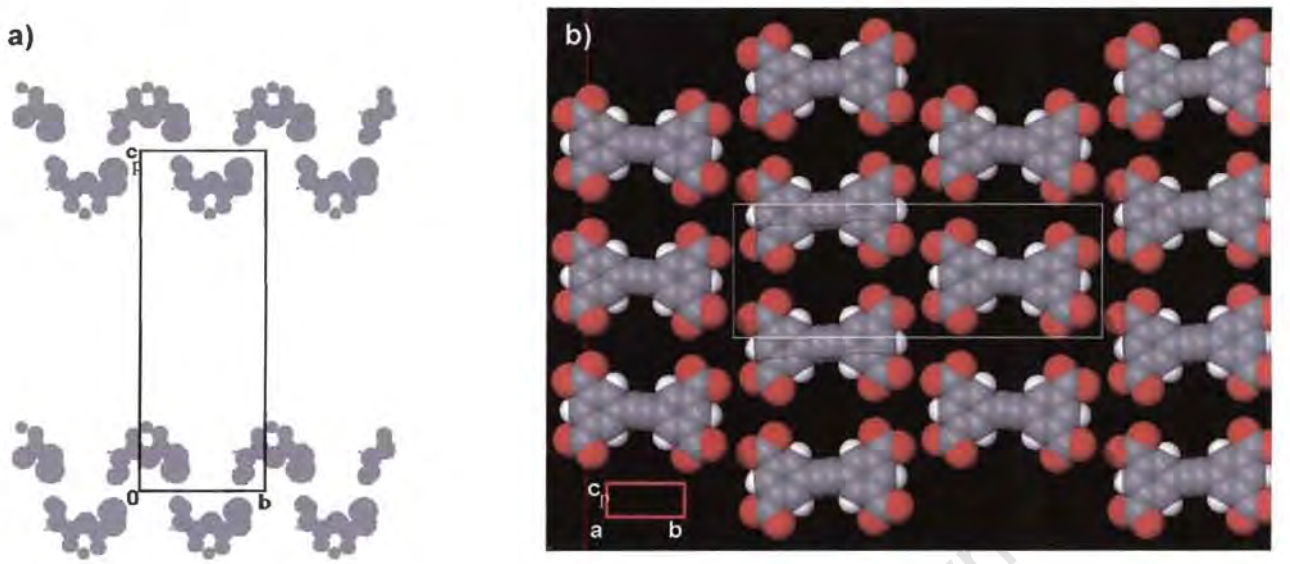

Figure 4.10: a) SECTION diagram viewed down [100] at a=0, with guest cations omitted and host anions showing the channels. **b)** Space-filling representation of host anions forming channels that run in the [100] direction (guests are omitted for clarity). **c)** Space-filling representation viewed along the [100] direction, showing guest cations and their packing in **H_2 • RPEA**.

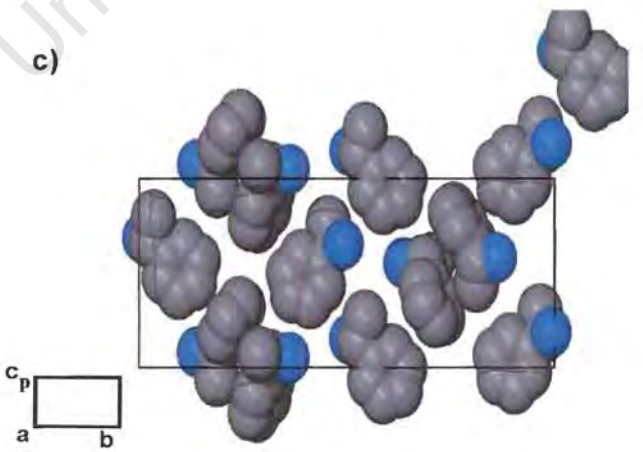

Hydrogen bonding: The structure is stabilised by extensive N-H···O hydrogen bonding interactions that exist between host anions and guest cations (Figure 4.11), The guest cation acts as a hydrogen bonding donor and host anion as a hydrogen bonding acceptor. Table 4.4 contains the details of N-H···O hydrogen bonding geometry. All intermolecular and intramolecular contacts, are shorter than the sum of the van der Waals radii, N···O (2.9Å)[4] and C···O(3.22)[4], associating them with moderately strong hydrogen bonds (Table 4.4 and 4.5).

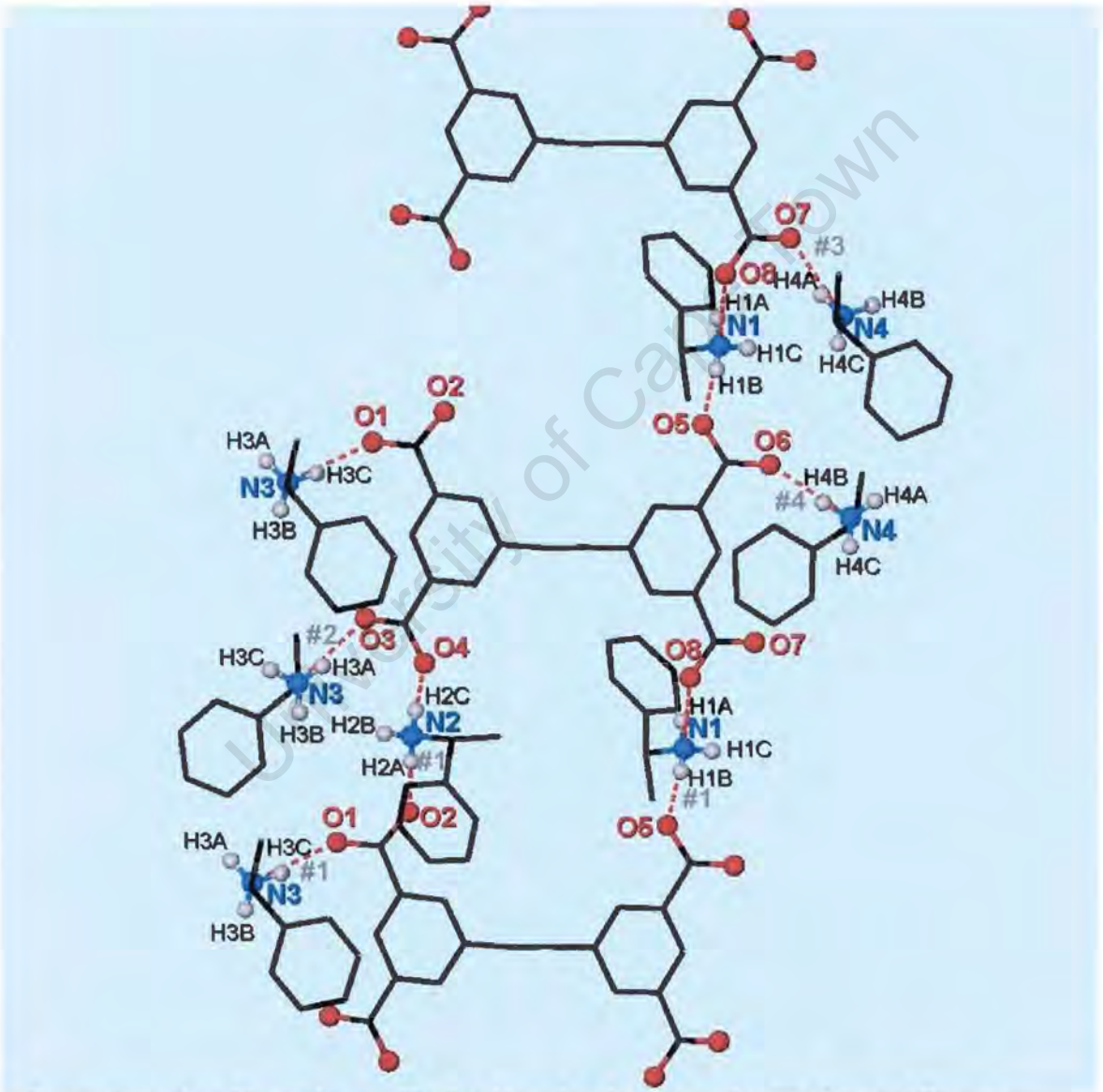

Symmetry codes: #1= x, -1+y, z, #2= 1-x, ½+y, 1-z, 1-z, #3= x, 1+y, z, #4= -x, -1/2+y, -z

Figure 4.11: Hydrogen bonding in **H_2 • RPEA**

Table 4.4: Inter-layer host-guest hydrogen bonding details for the **H_2 • RPEA** structure

D-H···A	D-H/Å	H···A/Å	D···A/Å	Angle/°
N1-H1A···O8	0.94(7)	1.83(6)	2.756(6)	168(6)
N1-H1A···O5$^{\#1}$	1.12(7)	1.67(6)	2.767(6)	164(6)
N2-H2A···O2$^{\#1}$	1.13(5)	1.65(5)	2.754(5)	164(4)
N2-H2C···O4	0.88(4)	1.90(4)	2.769(5)	169(4)
N3-H3A···O3$^{\#2}$	0.95(5)	1.85(5)	2.771(5)	163(4)
N3-H3C···O1$^{\#1}$	0.62(6)	2.16(6)	2.780(5)	170(6)
N4-H4A···O7$^{\#3}$	1.02(5)	1.76(5)	2.745(5)	163(4)
N4-H4B···O6$^{\#4}$	1.01(5)	1.84(7)	2.735(5)	172(5)

Symmetry codes: #1= x, -1+y, z, #2= 1-x, ½+y, 1-z, 1-z, #3= x, 1+y, z,
#4= -x, -1/2+y, -z

Table 4.5: Intra-layer host-guest hydrogen bonding details for the **H_2 • RPEA** structure

D-H···A	D-H/Å	H···A/Å	D···A/Å	Angle/°
C9-H9···O8	0.9300	2.41(5)	2.743(6)	101(3)

MOLECULAR STRUCTURE AND CRYSTAL PACKING

H_2 • RSPEA

H_2: 5-(3,5-Dicarboxyphenylethynyl)-isophthalic acid

RSPEA: (±) - (R, S) - 1 - Phenylethylamine

$[C_{18}H_6O_8]^{-4} \cdot 4[C_8H_{12}N]^{+} \cdot 6H_2O$

Space group: C2/c

Unit cell parameters: a = 32.550(7) b = 11.402(2) c = 14.549(3) /Å

β = 106.412(3) /°

Unit cell volume = 5179.7(18) $Å^3$

Z = 4

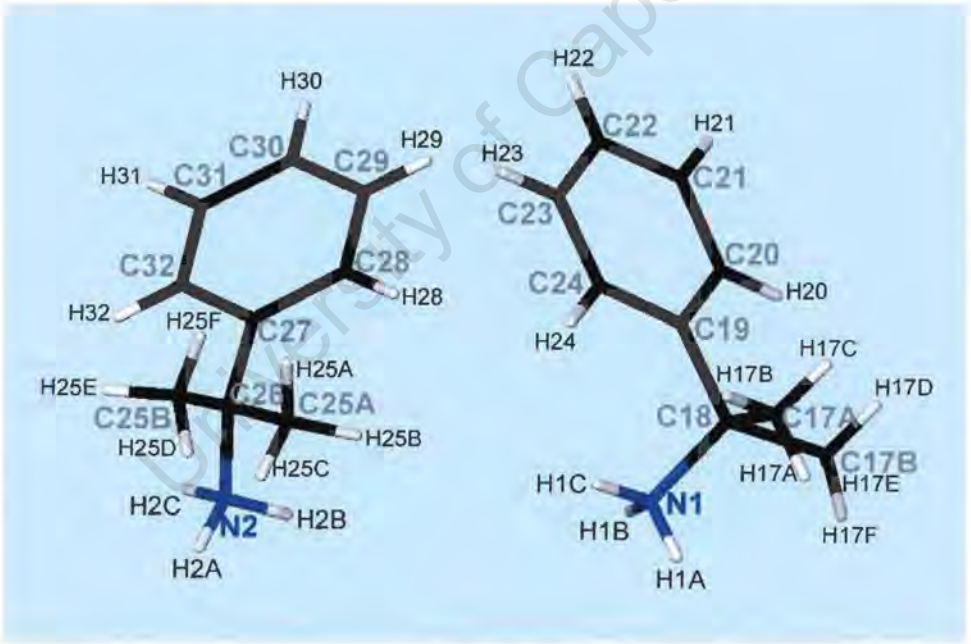

Figure 4.12: RSPEA guest numbering scheme, showing guest cations with disorder in β-carbons, C17A, C17B, C25A and C25B

RSPEA physical properties*: b.p = 185 °C

* Measured at standard pressure and temperature

H_2 • RSPEA

The mean reflection $|E^2-1|$ values in **H_2 • RSPEA** together with systematic absences obtained from the diffraction data indicated the monoclinic centrosymmetric space group C2/c. The refinement in this space group was successful.

The positions of host and guest non-hydrogen atoms were found by direct methods. All non-hydrogen atoms were refined anisotropically. The guest carbon atoms, C17 and C25, were found to be disordered over two positions, C17A and C17B, in one guest cation and C25A and C25B in the other guest cation, with refined site occupancy factors of 44%, 56%, 70% and 30% respectively (Figure 4.13a)). This disorder in the β-carbon defeats

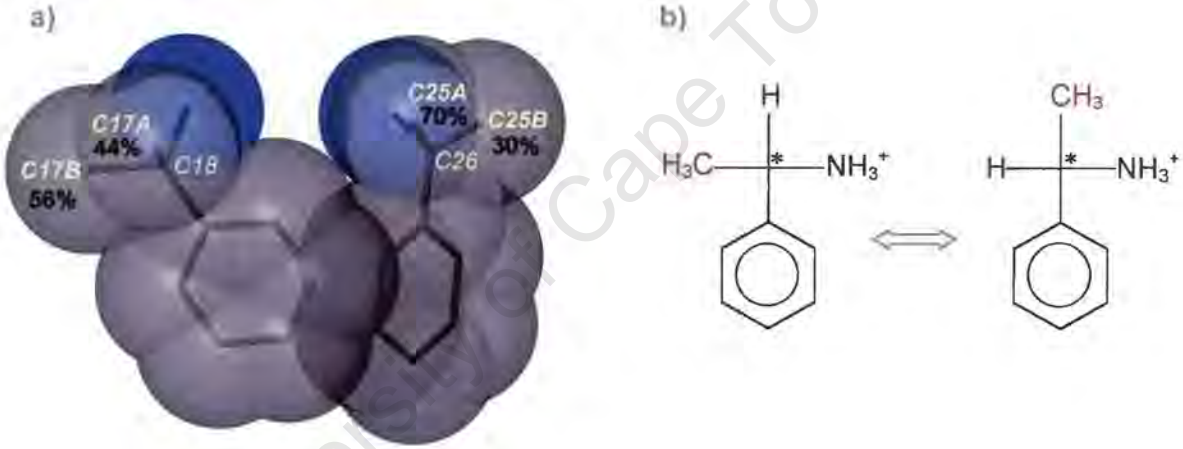

Figure 4.13: a) Space-filling projection of the guest disorder in **H_2 • RSPEA** with site occupancy factors for disordered atoms and **b)** schematic representation of non-disordered chiral guest cations showing β-carbon groups interchanging.

the chirality of the guest cations and this is represented by the equilibrium of the two non-disordered guest enantiomers (Figure 4.13b)).

The guest nitrogen atoms, N_1 and N_2, were easily identified due to their hydrogen bonding distance from the host carboxylate oxygen and their bond lengths (around 1.5Å) to the asymmetric carbon atoms. Hydrogen atoms of the host anion were geometrically constrained to their parent atoms and refined with linked temperature

factors. Aromatic and $-NH_3^+$ hydrogens of the guest cations were geometrically constrained to their parent atoms at C-H = 0.930Å and N-H = 0.890Å and refined with linked temperature factors. Hydrogens on the disordered carbon atoms of the guest cations were also geometrically constrained to their parent carbon atoms at C-H = 0.960Å and refined with linked temperature factors. Hydrogens were not modelled on the asymmetric carbon atoms. The final R-value was 0.0750. The structure crystallises in the centrosymmetric space group C2/c with Z = 4. The asymmetric unit contains half of the host anion and two guest cations. The host anion is placed on the centre of inversion, Wyckoff position b, while the guest cations and the water molecules are occupying the general positions. The structure is stabilised by a hydrogen-bonding network. Interatomic distances indicated the presence of a hydrogen bond network between the host anions, guest cations and water molecules.

The packing revealed the presence of channels in the crystal structure. The host anions pack to form layers that run parallel to the b axis in the [010] direction (Figure 4.14). The layers of host anions pack to form channels, approximately circular in cross section, that run in the [001] direction. The guest cations are located in these channels (Figure 4.15).

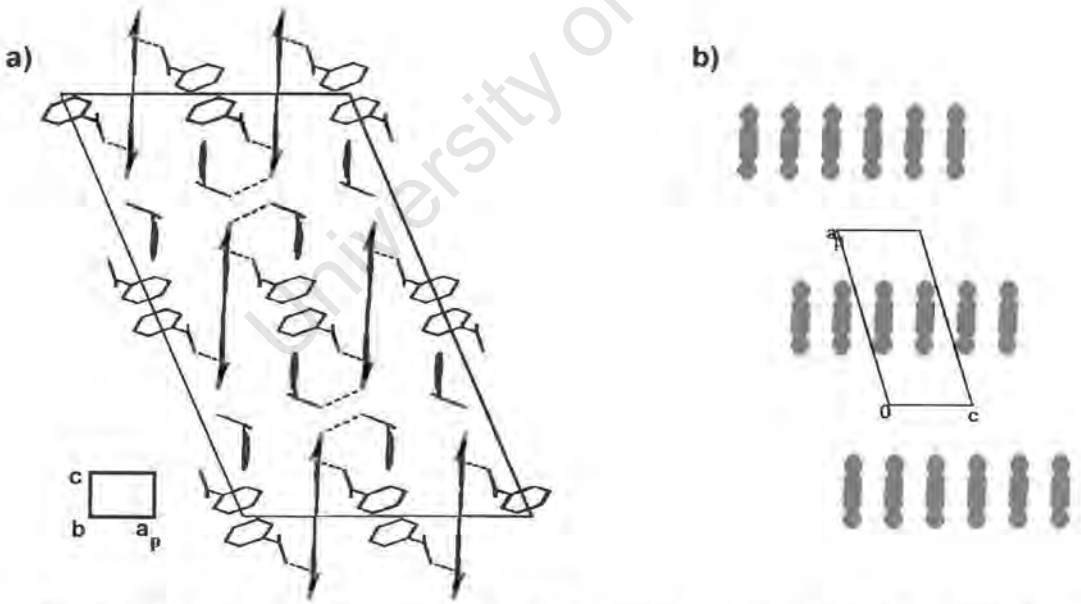

Figure 4.14: a) Packing of H_2 • **RSPEA**, viewed along the [010] direction. Dotted lines represent hydrogen bonds between the host and guest ions, **b)** host anions layered along [010] direction, showing channels (guest cations are omitted for clarity).

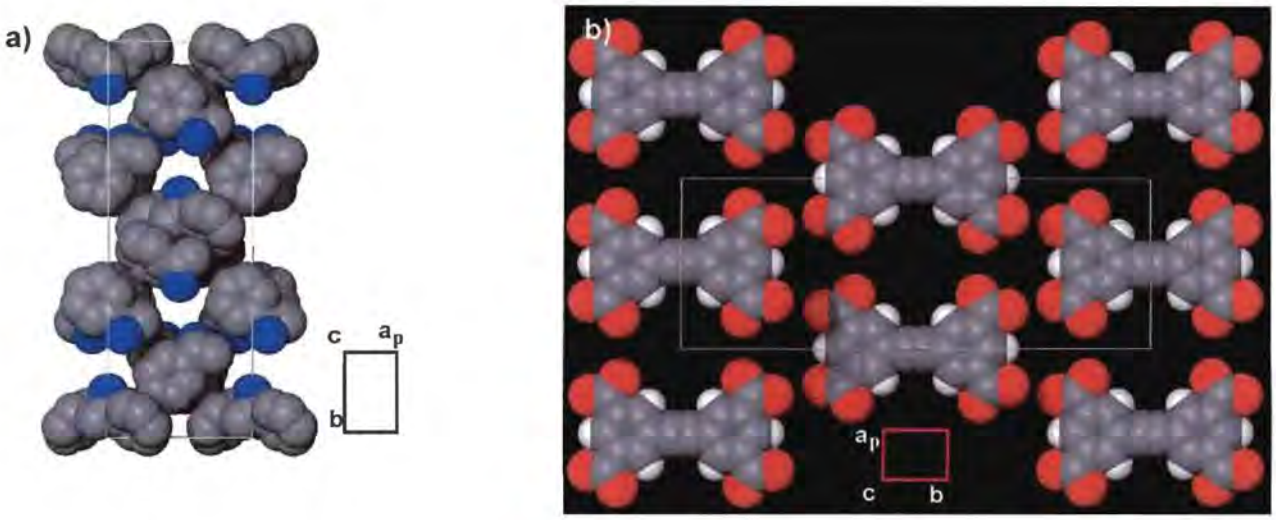

Figure 4.15: Space-filling representation in H_2 • **RSPEA** of **a)** packing arrangement of the guest cations showing the centrosymmetric property of the structure, viewed along the [001] direction, **b)** a single layer of host anions forming channels in the [001] direction.

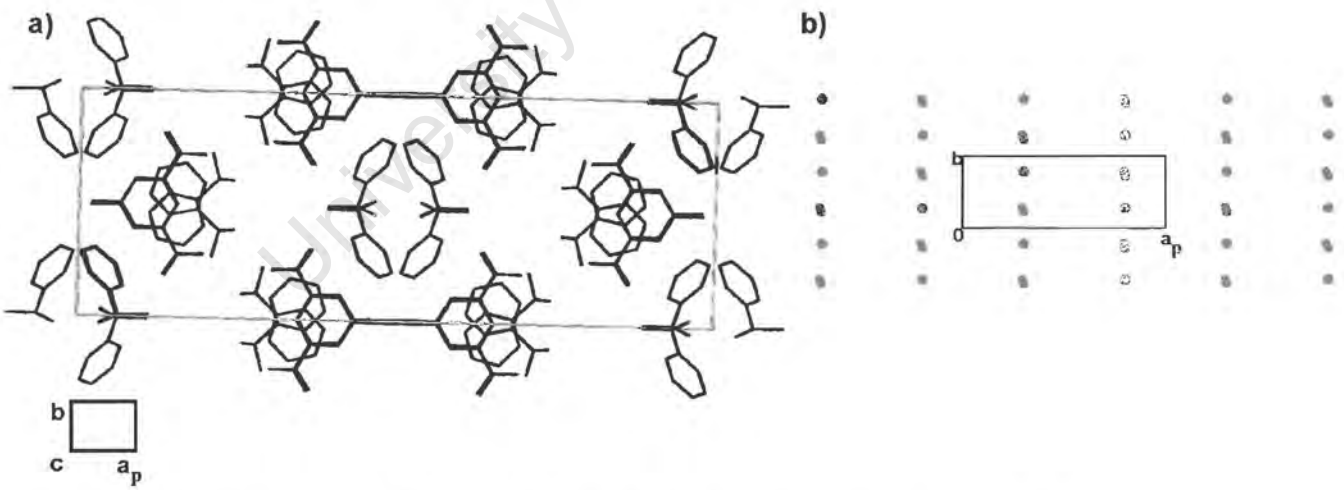

Figure 4.16: a) Stick form packing diagram of the H_2 • **RSPEA** structure, showing centrosymmetric property viewed down the c-axis; SECTION plot of H_2 • **RSPEA** in the [001] direction, showing host anions only (unit cell sectioned at c=20Å).

A hydrogen bonding network is formed between host anions, guest cations and water molecules in the **H_2 • RSPEA** structure. Each guest nitrogen atom is hydrogen bonded to the host anion carboxylate oxygen (shown by the dotted lines in Figure 4.17). Other hydrogen bonds are found to exist between trapped water molecules and host and guest ions. Table 4.6 shows hydrogen bond details for this compound (hydrogen bonds including water molecules are not included). All of the listed bond lengths meet the hydrogen-bonding requirement and classify as hydrogen bonds of moderate strength.

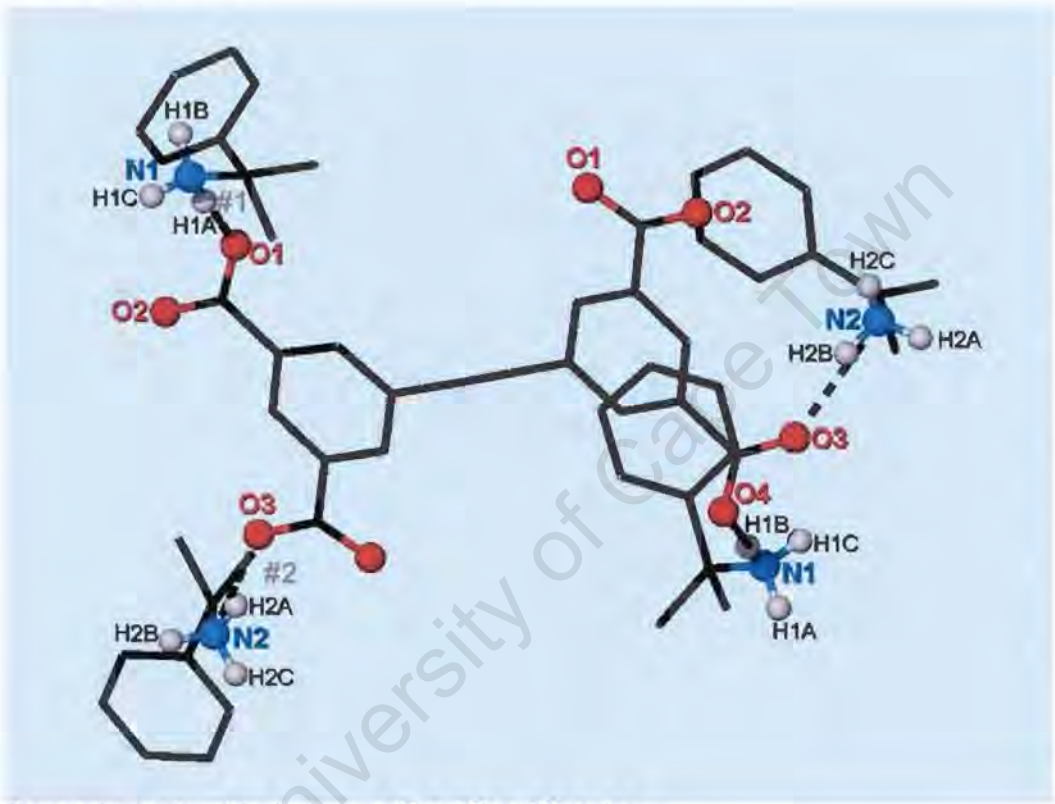

Symmetry codes: #1= x, 1+y, z, #2 = 1/2-x, 3/2-y, 1-z

Figure 4.17: Hydrogen bonding in the **H_2 • RSPEA** structure

Table 4.6: Inter-layer hydrogen bonding details for the **H_2 • RSPEA** structure

D-H···A	D-H/Å	H···A/Å	D···A/Å	Angle/°
N1-H1A···O1$^{\#1}$	0.8900	1.85(4)	2.742(3)	175(4)
N1-H1B···O4	0.89(4)	1.88(4)	2.759(3)	171(3)
N2-H2A···O3$^{\#2}$	0.89(4)	1.88(5)	2.748(3)	164(5)
N2-H2B···O3	0.89(4)	1.93(3)	2.805(3)	168(5)

Symmetry codes: #1= x, 1+y, z, #2 = 1/2-x, 3/2-y, 1-z

MOLECULAR STRUCTURE AND CRYSTAL PACKING

H_2 • PEA

H_2: 5-(3,5-Dicarboxyphenylethynyl)-isophthalic acid

PEA: 2-Phenylethylamine

$[C_{18}H_6O_8]^{-4} \cdot 4[C_8H_{12}N]^{+} \cdot 5H_2O$

Space group: Pbca

Unit cell parameters: a = 16.8061(2) b = 22.5832(2) c = 26.5572(3) /Å

Unit cell volume = 10079.4(2) $Å^3$

Z = 8

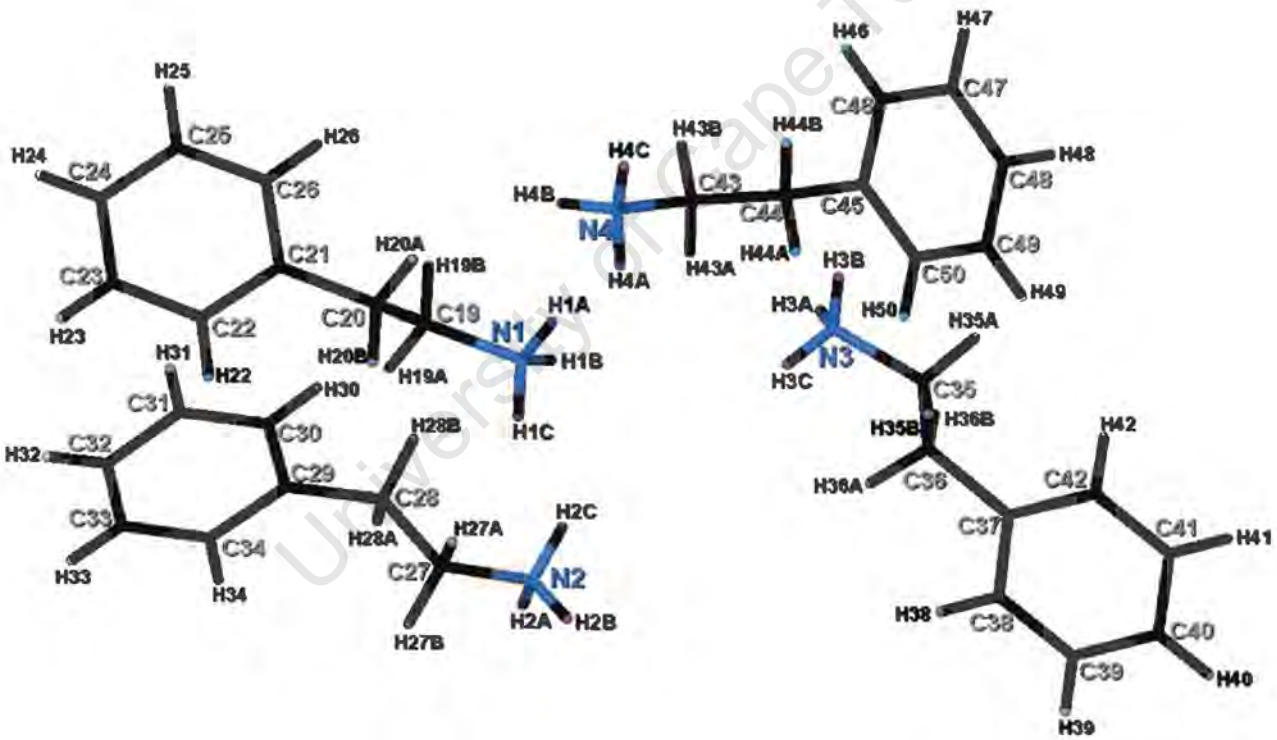

Figure 4.18: PEA guest numbering scheme

PEA physical properties*: ***b.p*** = 199 °C

* Measured at standard pressure and temperature.

H_2 • PEA

The crystal reflection data showed that the **H_2 • PEA** structure crystallises in the space group Pbca. The crystal structure was solved by direct methods using program SHELX-86. The total number of reflections collected was 42756. Equivalent reflections were merged to obtain 9754 unique reflections, of which 6578 reflections were observed, $|F_0| \geq 4\sigma (F_0)$, and the rest were suppressed. $R_\sigma = 0.0627$ and $R_{int} = 0.0582$ values indicate good quality data.

All heavy atoms (C, O and N) were refined anisotropically, after which all hydrogen atoms were identified in the difference Fourier synthesis. Aromatic hydrogen atoms were located in geometrically idealised positions, all being constrained to a C-H distance of 0.930Å and allowed to ride on their parent atom, after which they were refined with linked temperature factors. Hydrogens on the $-CH_3$ group were located in the same way as aromatic hydrogen atoms and constrained to a C-H distance of 0.970Å. Further refinement of the model was achieved by the incorporation of the NH_3^+ hydrogen atoms. The $-NH_3^+$ and water hydrogen atoms were allowed to refine without constraints. The refinement proceeded successfully with the final $R_1 = 0.0503$.

The **H_2 • PEA** structure is a salt formed between the host anions and the guest cations. There is one host anion, four guest cations and five waters of crystallisation in the asymmetric unit (Figure 4.18), with host to guest ratio of 1:4:5 and Z = 8. The independent host anion, guest cations and water molecules are located on general positions.

Analysis of the interatomic distances between the host carboxylate oxygens, guest nitrogens and water oxygens, revealed the presence of the hydrogen bonding.

The packing of the **H_2 • PEA** structure shows host anions, guest cations and water molecules packed closely together. Guest cations are placed in the channels formed by the host anions. The channels are tubular in shape and run along the c-axis (Figures 4.19 and 4.20).

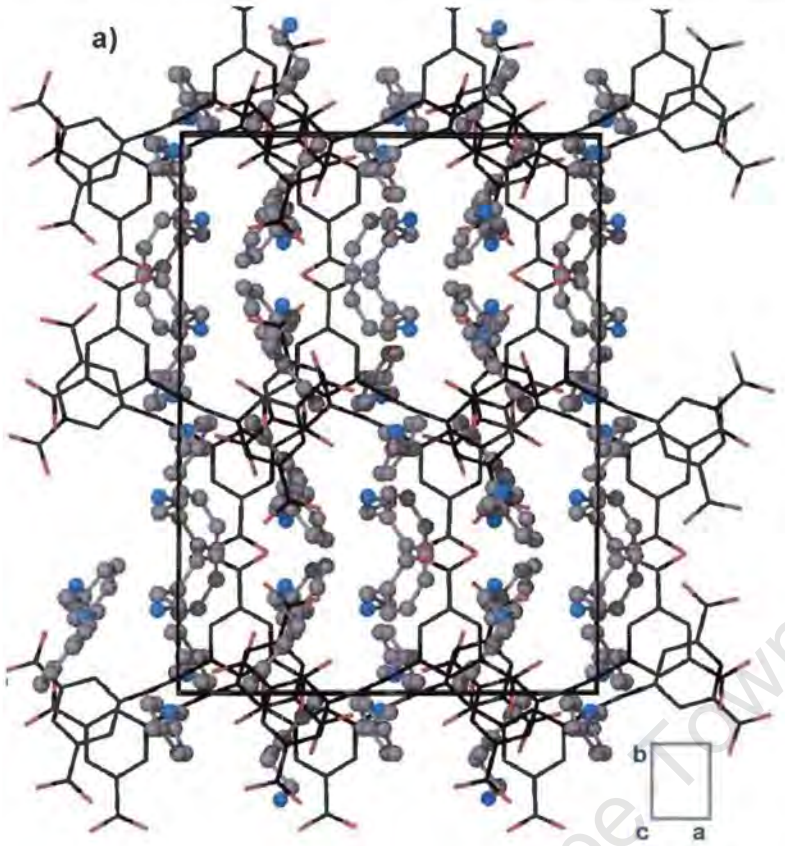

Figure 4.19: Packing diagrams of H_2 • **PEA**, showing host anions and guest cations with high packing efficiency: **a)** stick representation of host anions and stick-and-ball representation of the guest cations, viewed along the [001] direction. Hydrogen atoms and water molecules are omitted for clarity **b)** viewed along the [100] direction

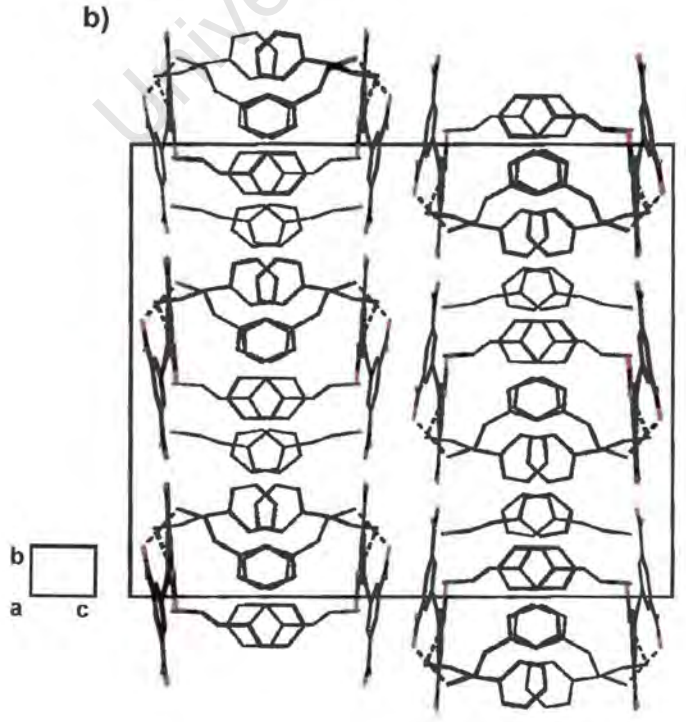

(hydrogen bonds are represented by dotted lines). The host anions are viewed almost along the -C≡C- axis and thus appear greatly foreshortened in this projection.

Host molecules stack together to form layers that are at an angle to each other and are positioned in a zig-zag manner (Figure 4.19b)).

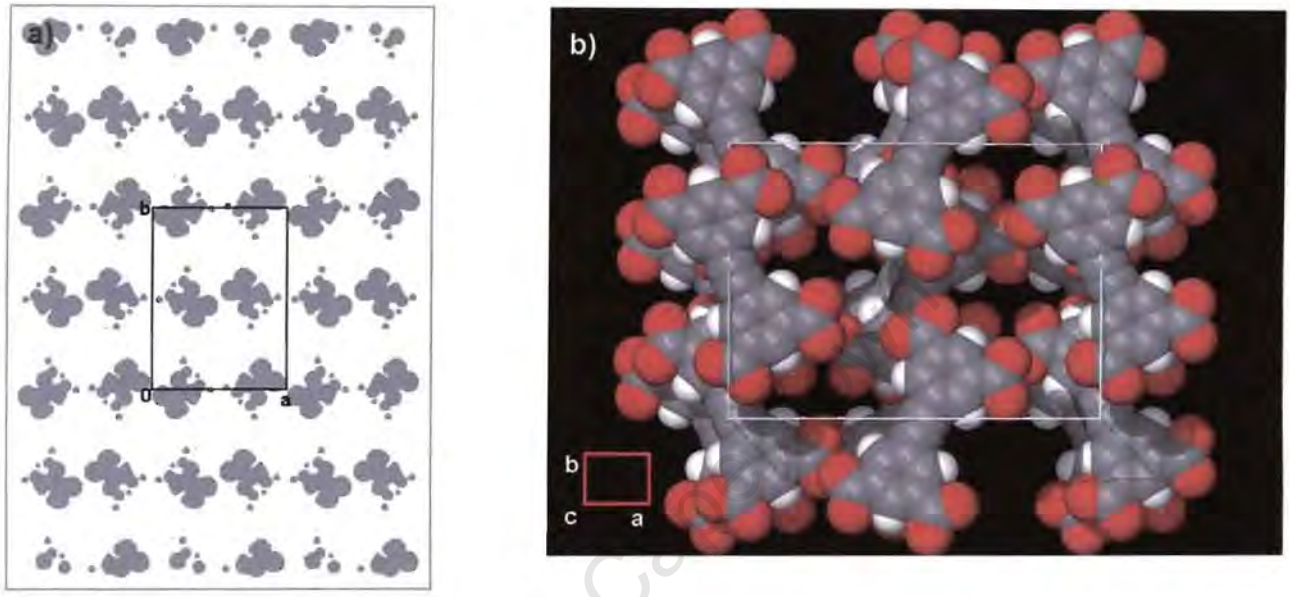

Figure 4.20: a) SECTION plot of H_2 • **PEA**, viewed along the c axis with the unit cell sectioned at a=0Å. Grey areas represent host anions, while guest cations have been omitted. **b)** Space-filling representation of the stacking of the host layers generating cavities that run in the [001] direction (guest cations are omitted for clarity), **c)** the layers of 2-phenylethylamine guest cations alone, viewed along the [001] direction (hydrogen atoms are omitted for clarity).

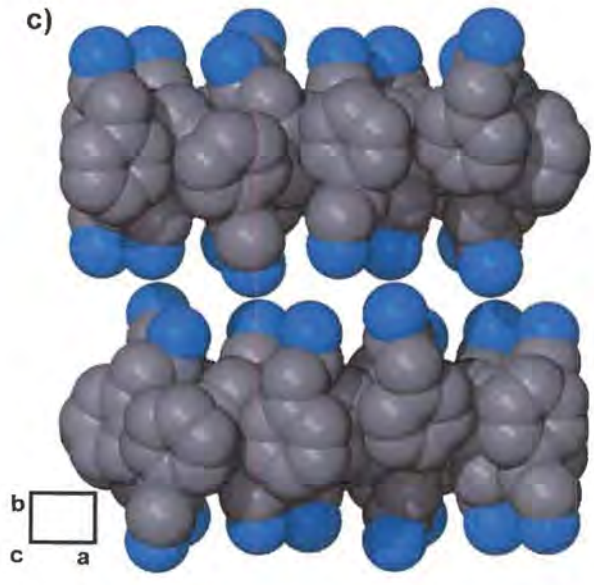

Figure 4.21: (below) Space-filling representation of the host anions in H_2 • **PEA**, viewed along the [010] direction **a)** showing cross-section of the channels, **b)** at b=0Å, showing layer arrangement (guests are omitted for clarity).

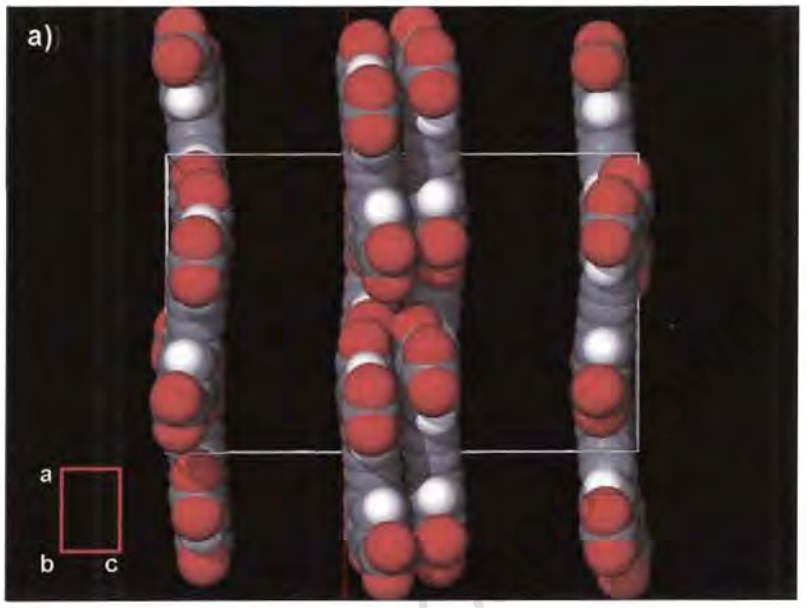

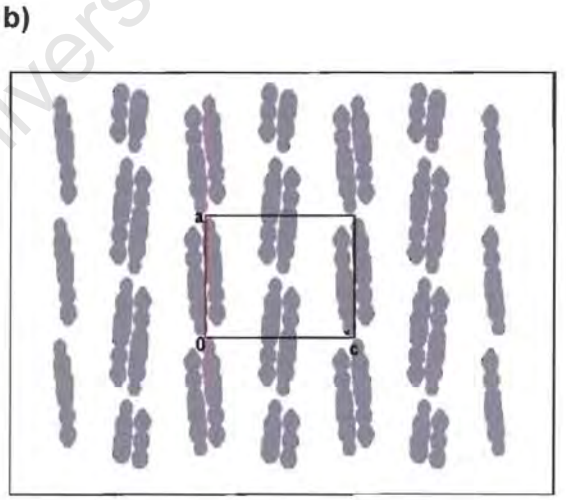

Hydrogen bonding in the **H_2 • PEA** structure is formed between the host carboxylate oxygen and the guest nitrogen. N-H···O hydrogen bond lengths fall in the range associated with moderately strong hydrogen bonds (Table 4.7). The hydrogen bonding requirement that the inter-atomic distance should not exceed the sum of the van der Waals radii is fulfilled. Table 4.8 lists intramolecular hydrogen bond distances.

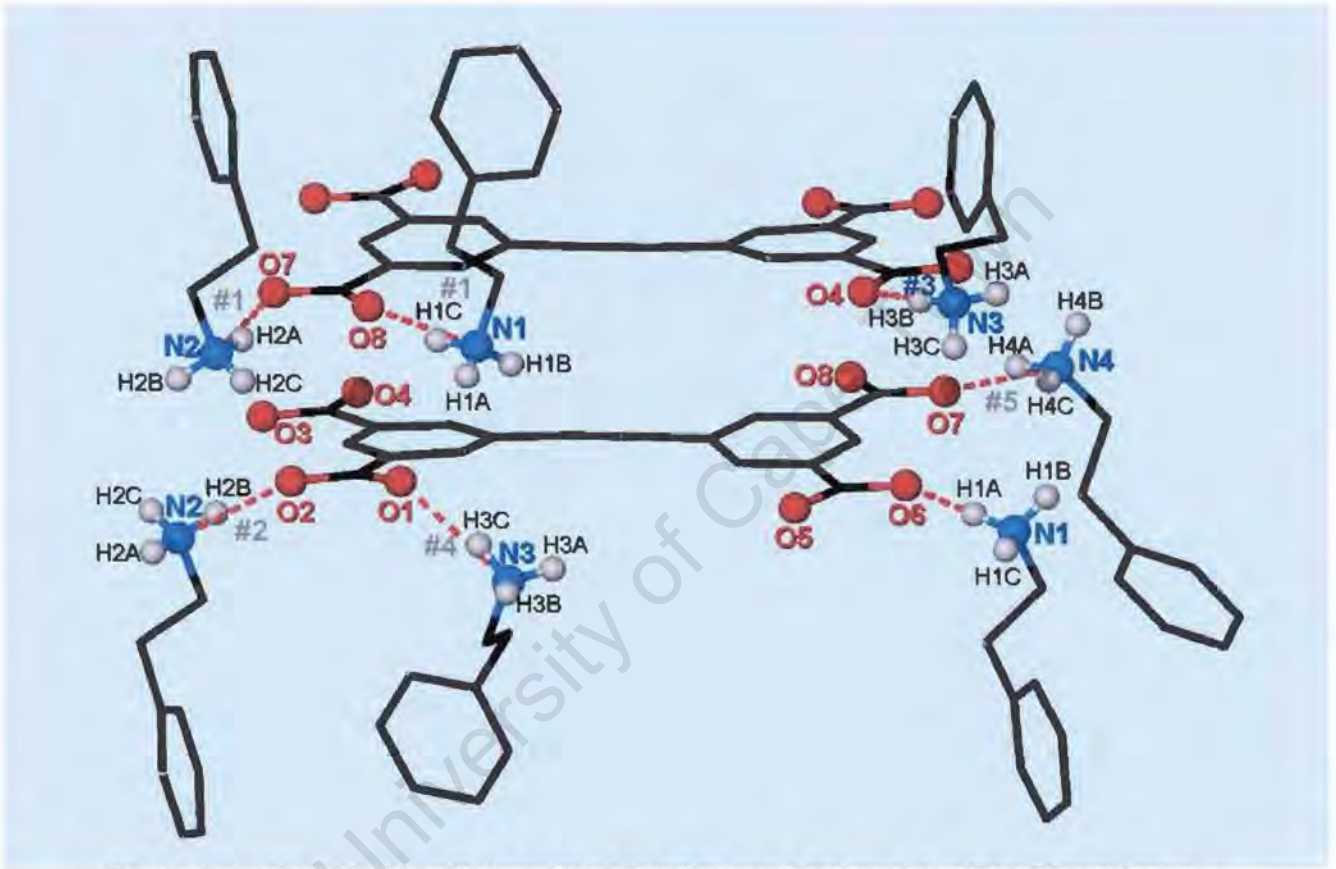

Symmetry codes: #1= ½-x, ½+y, z, #2= 3/2-x, ½+y, z, #3= 1-x, ½+y, 1/2-z, #4= -1/2+x, y, -1/2-z, #5= 1/2+x, y, 1/2-z

Figure 4.22: Hydrogen bonding in **H_2 • PEA**

The host anions form layers, which run perpendicular to the [001] direction. The layers are stabilised by host-guest hydrogen bonding network, as shown in Figure 4.22 above. The layers stack to form spaces that accommodate guest molecules, as shown in Figure 4.23.

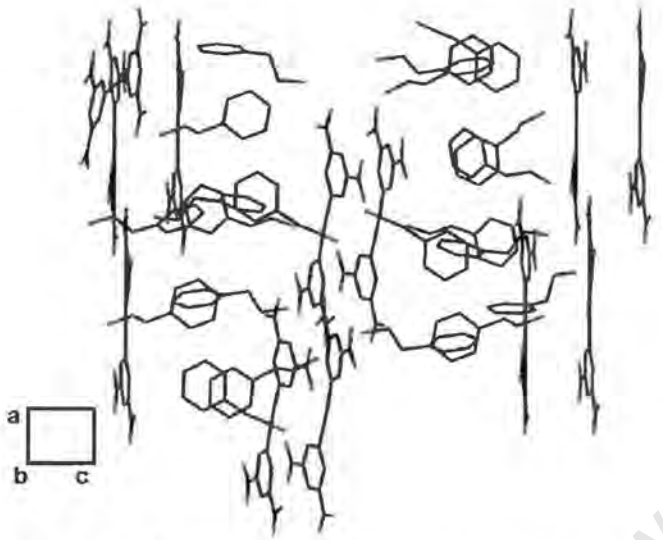

Figure 4.23: The stacking of host layers to accommodate guest cations in the **H_2 • PEA** structure

Table 4.7: Inter-layer hydrogen bonding details for the **H_2 • PEA** structure

D-H···A	D-H/Å	H···A/Å	D···A/Å	Angle/°
N1-H1A···O6	0.8900	1.98(3)	2.817(3)	157(2)
N1-H1C···O8 $^{\#1}$	0.8900	1.87(2)	2.738(3)	165(2)
N2-H2A···O7$^{\#1}$	0.8900	1.96(3)	2.823(3)	164(3)
N2-H2B···O2$^{\#2}$	0.8900	1.87(2)	2.729(3)	161(2)
N3- H3B··· O4$^{\#3}$	0.89(3)	1.86(3)	2.738(3)	171(3)
N3- H3C··· O1$^{\#4}$	0.89(3)	1.95(3)	2.822(3)	168(3)
N4- H4A··· O7$^{\#5}$	0.8900	1.88(3)	2.740(3)	161(3)

Symmetry codes: #1= ½-x, ½+y, z, #2= 3/2-x, ½+y, z, #3= 1-x, ½+y, 1/2-z, #4= -1/2+x, y, -1/2-z, #5= 1/2+x, y, 1/2-z

Table 4.8: Intra-layer hydrogen bonding details for the **H_2 • PEA** structure

D-H···A	D-H/Å	H···A/Å	D···A/Å	Angle/°
C28-H28A···O8$^{\#1}$*	0.9700	2.55(3)	3.319(3)	100(2)
C5-H5···O5*	0.9301	2.44(3)	3.777(3)	100(2)
C14-H14···O1*	0.9300	2.46(3)	3.760(3)	137(2)

*sum of the van der Waals radii of C and O is 3.22Å[4].

MOLECULAR STRUCTURE AND CRYSTAL PACKING

H_2 • Na

H_2: 5-(3,5-Dicarboxyphenylethynyl)-isophthalic acid

Na: sodium

$[C_{18}H_6O_8]^{-4} \cdot 4Na^+ \cdot 10H_2O$

Space group: $P2_1/c$

Unit cell parameters: a = 3.6288(7) b = 21.299(4) c = 16.022(3) /Å

β = 95.574(2) /°

Unit cell volume = 1232.5(4) $Å^3$

Z = 2

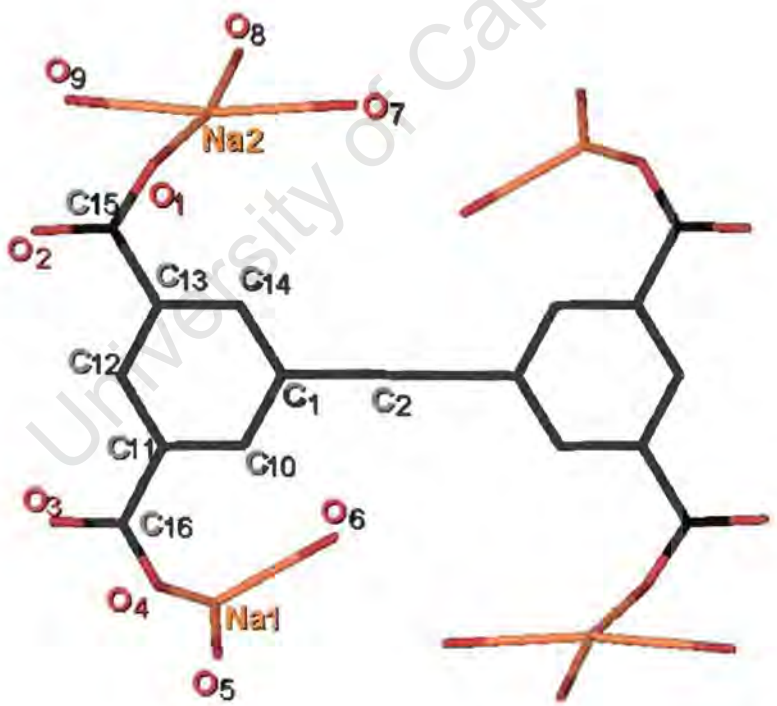

Figure 4.24: H_2 • Na numbering scheme

$H_2 \bullet Na$

The X-ray diffraction pattern of **H_2 • Na** displayed 2/m Laue symmetry. Therefore the **H_2 • Na** structure crystallises in the monoclinic crystal system. The reflection conditions observed on inspection of X-ray intensity data were:

hkl: none
h0l: l = 2n
0k0: k = 2n.

This corresponds to the space group $P2_1/c$ which is uniquely determined. The structure was solved and fully refined in this space group.

The number of reflections that were collected was 5032 with 2156 unique. After merging the data, 1482 reflections with $I_{rel} > 2\sigma I_{rel}$ were observed. Positions of all the host and guest non-hydrogen atoms were obtained by direct methods using program SHELX-86.

The positions of the host non-hydrogen atoms and metal ions in the asymmetric unit were located using direct methods. All non-hydrogen atoms were located on the electron density map and refined anisotropically. The heavy metal ions were identified immediately and both sodium ions, Na1 and Na2, were found to be bonded to carboxylate oxygens of the host. The hydrogen atoms of the water molecules were allowed to refine without constraints. Phenyl hydrogen atoms were geometrically constrained to their parent carbon atoms and refined with linked temperature factors. The structure refined successfully to $R_1 = 0.0483$.

The packing and hydrogen bonding interactions: **H_2 • Na** is a hydrated metal salt formed between the host anions, sodium ions and water molecules. There is a half-host anion with two sodium ions bonded to it and five waters of crystallisation in the asymmetric unit (Z = 2). Na1 and Na2 ions are bonded to the deprotonated oxygen that belongs to the carboxylate group of the host anion (Figure 4.24). The sodium ions are also bonded to the peripheral oxygen atoms belonging to water molecules surrounding these metal ions. The sodium ions are located in general positions, while the host anions are located on the centres of inversion, Wyckoff position b. The O9 water molecules bonded to Na2 ions are also located on the centres of inversion, Wyckoff position d.

The packing of the **H_2 • Na** structure takes on a web-like shape (Figure 4.25a)). The hydrated metal salt **H_2 • Na** packs in such a way that two of four carboxylate groups of the one host anion are connected to two of four carboxylate groups of the neighbouring host anion via the two sodium ions bonded to each carboxylate group and these ions are in turn bridged by a single water molecule. The O9 water molecules bonded to Na2 ions are located on the centres of inversion. The O9 hydrogen atoms could not be located in the electron density map. This is due to the O9 being necessarily disordered. Figure 4.25b) shows a water molecule located on the centre of inversion viewed down b-axis.

The packing of the host anions reveals that the central axis running through each host anion backbone is at a right angle to its neighbours (Figure 4.25 c), d)). However, the mean planes through the host anions positioned at the origin and at the centre of the unit cell are at a small angle to each other (Figure 4.26). The layers formed by the host anions are stabilised by hydrogen bonding network between the host carboxylate oxygen atoms, sodium ions and water oxygen atoms (Figure 4.25).

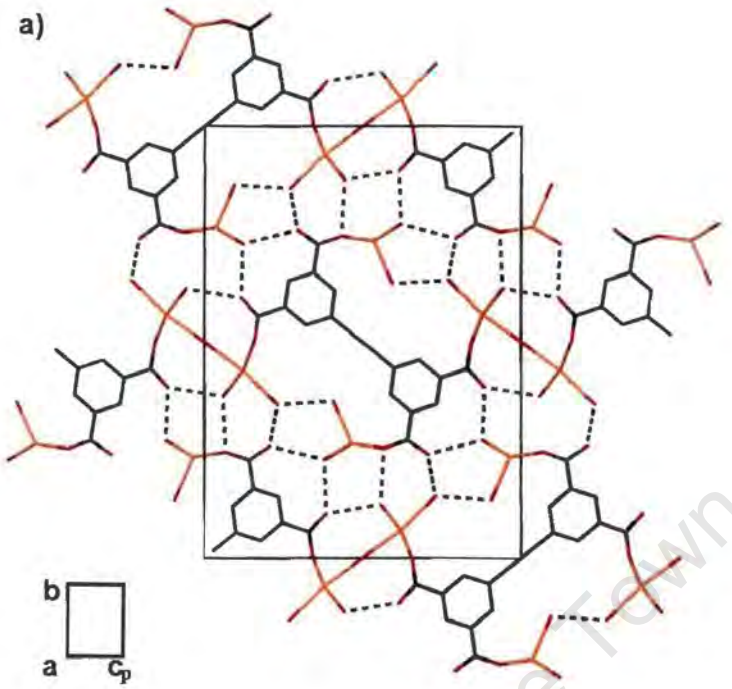

Figure 4.25: a) Packing of H_2 • **Na**, showing a single layer of metal salt complex (sodium ions are in yellow), viewed along the [100] direction. **b)** Representation of the water molecule located on the centre of symmetry viewed in the [010] direction. Host anions are omitted for clarity.

b)

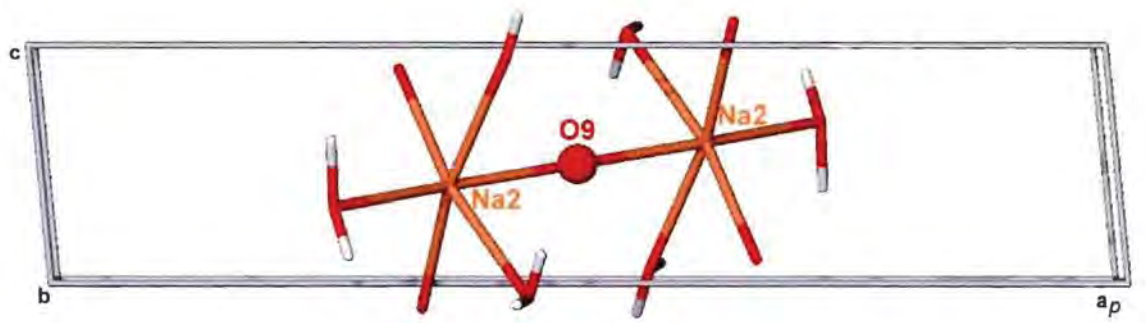

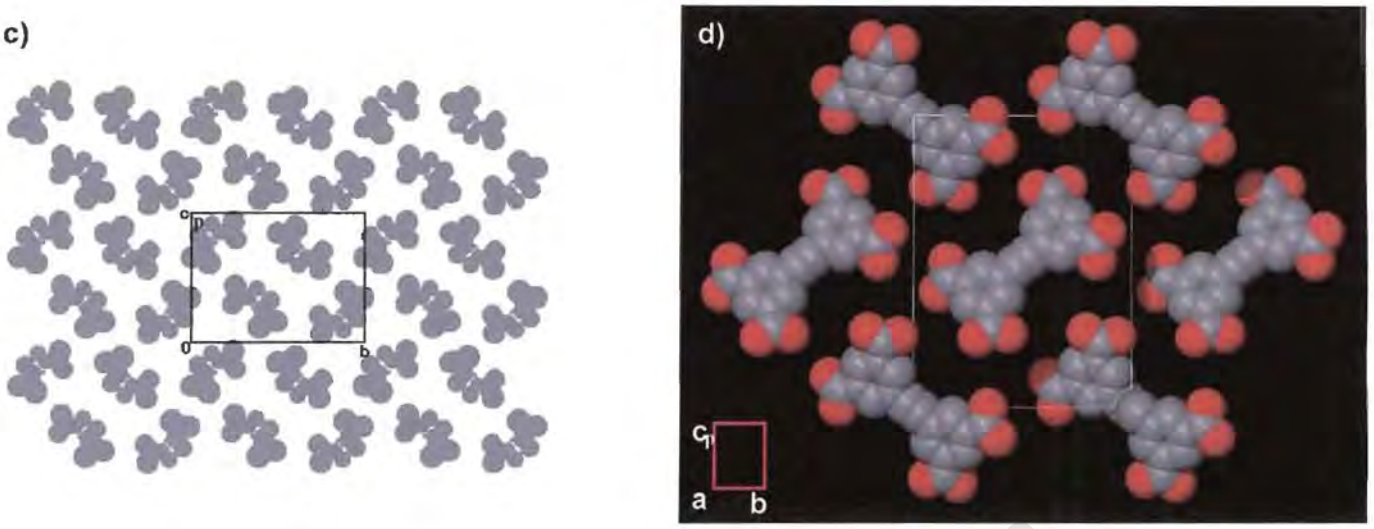

Figure 4.25: c) Space filling representation of the host anions in **H_2 • Na**, viewed along [100] at a=0Å, showing positioning of host anions relative to each other, **d)** space-filling representation of the host anions in **H_2 • Na**, viewed along a-axis.

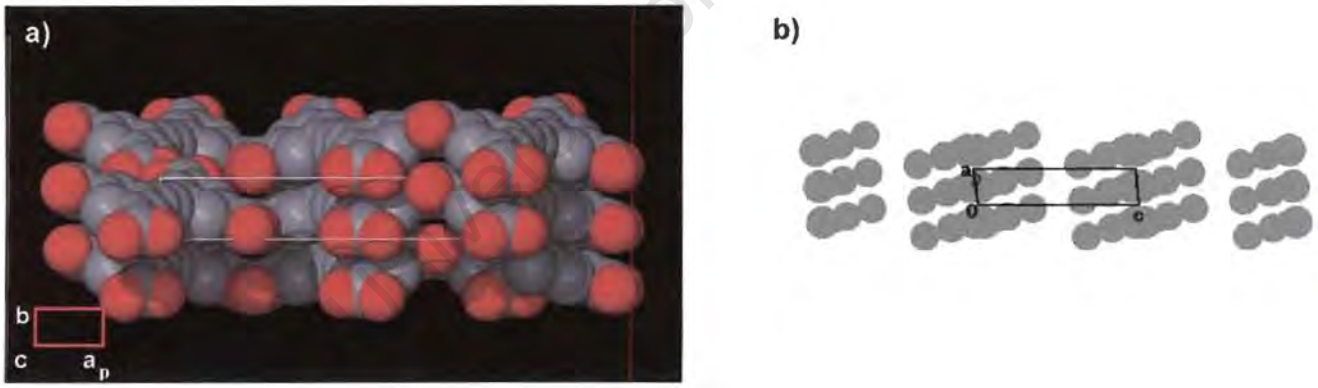

Figure 4.26: Space-filling representation of the host anions in **H_2 • Na**, **a)** viewed along the [001] direction, showing host anions positioned at an angle to each other. Metal ions are omitted for clarity. **b)** viewed along [010] at b=0Å, showing layer arrengement (host anions only).

Sodium ions, Na2, are coordinated to six oxygen atoms that lie at the vertices of an irregular octahedron. Four of these six ligands are water molecules that are a part of the hydrogen bonding network and two ligands are oxygen atoms belonging to the carboxylate groups of the host anions (Figure 4.27a).

The Na1 sodium ions however are coordinated to five oxygen atoms and in this case the ligand atoms lie at the vertices of an irregular square pyramid (Figure 4.27b). The geometry of the three water molecules around Na1 is pyramidal. The two remaining oxygen atoms belong to the host carboxylate groups.

The angles and bond distances related to the geometry of sodium ions in **H_2 • Na** are shown in Figures 4.27a and 4.27b.

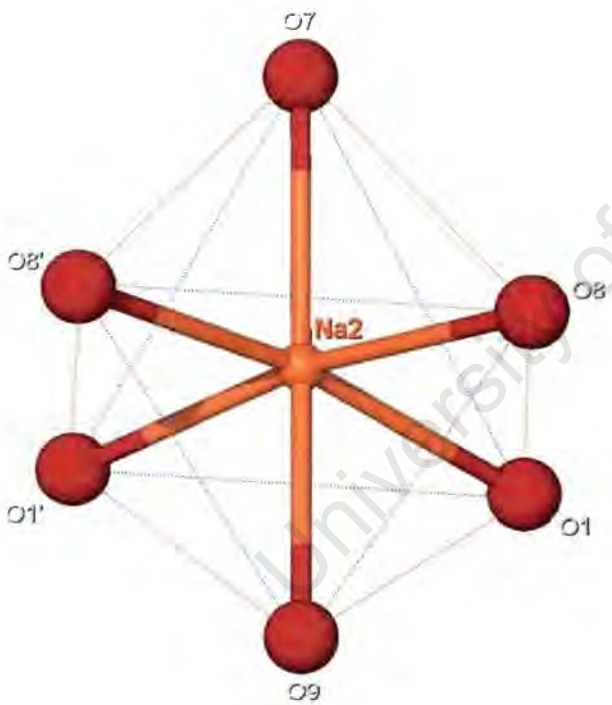

Bond angles:
O1-Na2-O9 = 78.47°
O1'-Na2-O9 = 83.49°
O9-Na2-O8 = 85.41°
O9-Na2-O8' = 90.39°
O7-Na2-O1 = 106.90°
O7-Na2-O1' = 101.47°
O7-Na2-O8 = 89.39° <89.77°>
O7-Na2-O8' = 83.98°
O1-Na2-O8 = 80.74°
O1'-Na2-O8' = 81.90°
O1-Na2-O1' = 98.45°
O8-Na2-O8' = 96.70°

O7-Na2-O9 = 171.85°
O1-Na2-O8' = 168.71° <169.78°>
O8-Na2-O1' = 168.79°

Bond distances:
O9···Na2 = 2.385Å
O1···Na2 = 2.411Å
O1'···Na2 = 2.381Å
O7···Na2 = 2.417Å <2.408Å>
O8···Na2 = 2.441Å
O8'···Na2 = 2.415Å

Figure 4.27a: Irregular octahedron geometry (shown by dotted lines) of sodium, Na2, ions in the **H_2 • Na** structure with the related geometry angles, bond distances and their average values.

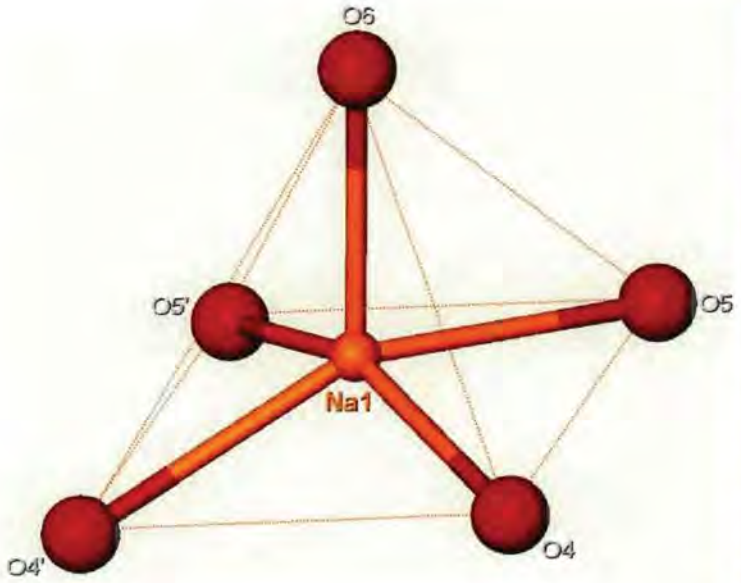

Bond angles:
O5-Na1-O4 = 78.44°
O5-Na1-O5' = 97.69°
O4-Na1-O4' = 94.99° <87.19°>
O4'-Na1-O5' = 77.64°

O6-Na1-O5 = 85.97°
O6-Na1-O5' = 102.76° <102.57°>
O6-Na1-O4 = 102.45°
O6-Na1-O4' = 119.09°

O5-Na1-O4' = 154.94°
O4-Na1-O5' = 154.14° <154.54°>

Bond distances:
O6···Na1 = 2.343Å
O5···Na1 = 2.435Å
O4···Na1 = 2.416Å <2.417Å>
O4'···Na1 = 2.506Å
O5'···Na1 = 2.384Å

Figure 4.27b: Irregular square pyramidal geometry of sodium, Na1, ions in the H_2 • **Na** structure. The related angles, bond distances and their average values are listed on the side.

MOLECULAR STRUCTURE AND CRYSTAL PACKING

H_2 • Rb

H_2: 5-(3,5-Dicarboxyphenylethynyl)-isophthalic acid

Rb: rubidium

$[C_{18}H_6O_8]^{-4} \cdot 4Rb^{+4} \cdot 6H_2O$

Space group: $P2_1/n$

Unit cell parameters: a = 4.0435(8) b = 18.991(4) c = 16.411(3) /Å

β = 95.894(2) /°

Unit cell volume = 1253.5(1) $Å^3$

Z = 2

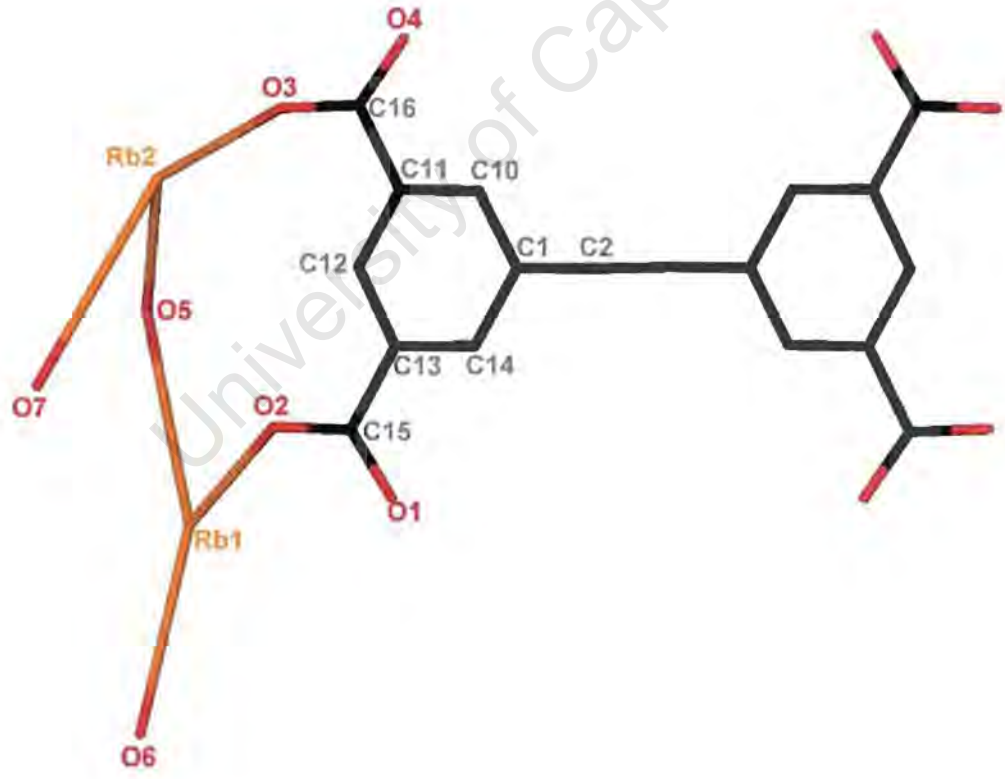

Figure 4.28: H_2 • Rb numbering scheme

H_2 • Rb

H_2 • Rb crystallises in the monoclinic crystal system, space group $P2_1/n$. The centrosymmetric space group was indicated by the mean value for the intensity data, $|E^2-1| = 0.916$. The space group, $P2_1/n$, was then indicated by systematic absences in the diffraction data. The crystal structure was successfully refined in this space group. A total of 2505 reflections were obtained by data collection of which 2505 were unique. The data were merged and 1712 reflections were observed with $I_{rel} > 2\sigma I_{rel}$. Positions of all the host and guest non-hydrogen atoms were obtained by direct methods using program SHELX-86. All non-hydrogen atoms were refined with anisotropic temperature factors. Aromatic hydrogens of the host anion were refined with an independent temperature factor and a simple bond length constraint. The rest of the hydrogen atoms were included in the model with no constraints. The structure refined to $R_1 = 0.0582$.

The packing and hydrogen bonding interactions: **H_2 • Rb** crystallises in $P2_1/n$ with Z = 2. There is a half-host anion with two rubidium ions bonded to it and three water molecules in the **H_2 • Rb** asymmetric unit (Figure 4.28). The two carboxylate groups of the host anion are bonded to Rb1 and Rb2 ions which are in turn bonded to two peripheral water oxygen atoms. The oxygen atoms belong to the waters of crystallisation that seem to have a small role in filling the space of the crystal. The host anions are located on the centre of inversion, Wyckoff position d, while the rubidium ions and water molecules are in general positions.

The packing of the **H_2 • Rb** structure takes on a web-like shape (Figure 4.29a)). The packing of the host anions reveals that the central axis running through each host anion backbone is at a right angle to its neighbours and the mean planes through the host anions are at a small angle to each other (Figure 4.29). As a result of this, Figure 4.30a) of the SECTION plot of **H_2 • Rb**, viewed along the [100] direction, shows neighbouring host anions having a slightly different shape to each other. The layers of a hydrated metal salt complex are stabilised by host···water hydrogen bonds, as shown in Figure 4.29a). In the **H_2 • Rb** structure an extensive hydrogen-bonding network is formed between the host anion carboxylate oxygen and water oxygen atoms bonded to the neighbouring rubidium ions.

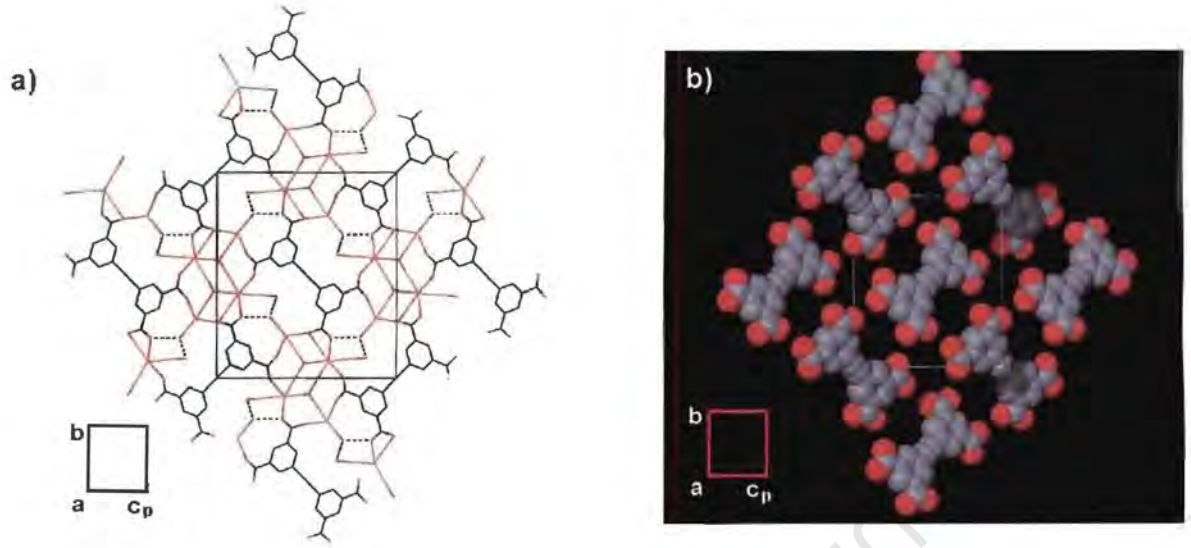

Figure 4.29: Packing diagram of H_2 • **Rb** viewed along [100]. **a)** Stick representation of host anions hydrogen bonded to waters of crystallisation. H-bonds are represented by dotted lines. **b)** Space-filling representation of host anions only, showing spaces for rubidium ions and water ligands.

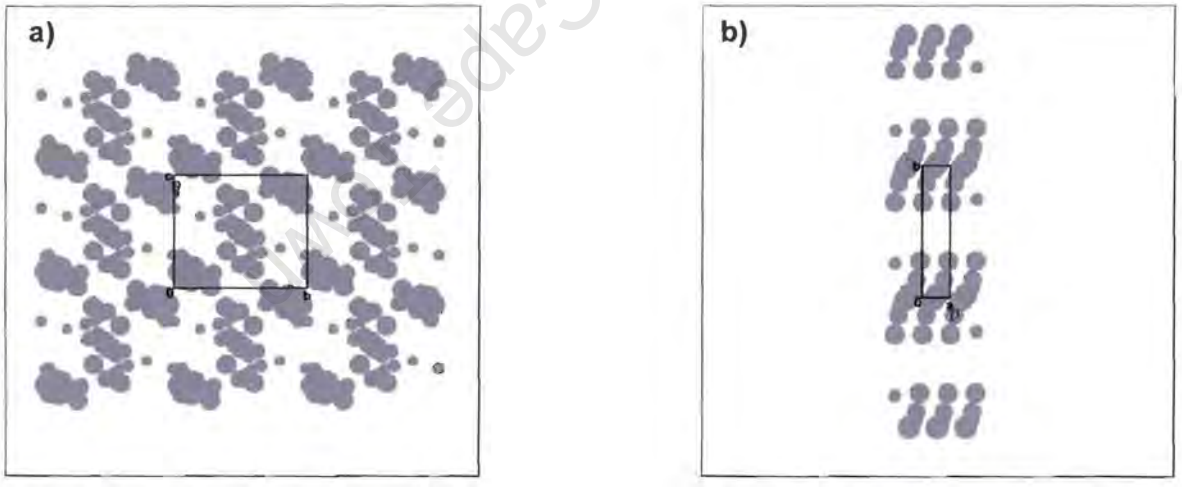

Figure 4.30: SECTION plot of the H_2 • **Rb** structure, **a)** at a=0, viewed down the a-axis, showing host anions only, **b)** at c=0, viewed along the [001] direction, showing layers of host anions stacked together, making spaces for rubidium ions and water ligands.

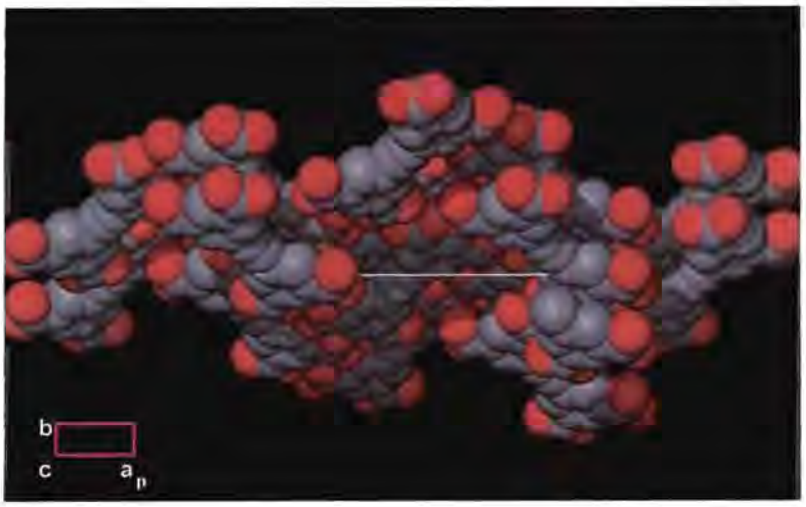

Figure 4.31: Space-filling representation of H_2 • **Rb** down the c-axis, showing host anions only forming a wave-like shape due to the fact that the mean planes through the host anions are at a small angle to each other.

Rubidium ions are able to accommodate a number of ligands due to their size. Rubidium ions, Rb2, are coordinated to eight oxygen atoms that lie at the vertices of an irregular dodecahedron (Figure 4.32). Four of these eight ligands are water molecules that take part in hydrogen bonding network and four ligands are host anion carboxylate oxygen atoms.

Rubidium, Rb1, ions are coordinated to nine oxygen atoms. There is only one symmetrical arrangement that occurs with regularity for this coordination number. It is derived from a trigonal prism, shown in Figure 4.33, by placing the three additional atoms outside the centres of the vertical faces[7]. The irregular trigonal prism geometry around Rb1 is shown in Figure 4.34. The ligands that are coordinated to the Rb1 ion comprise four water molecules and five host anion carboxylate oxygens. The irregular trigonal pyramid is the geometry of the water molecules around the rubidium ions.

The angles and bond distances related to the geometry of rubidium ions in H_2 • **Rb** are shown in Figures 4.32 and 4.34.

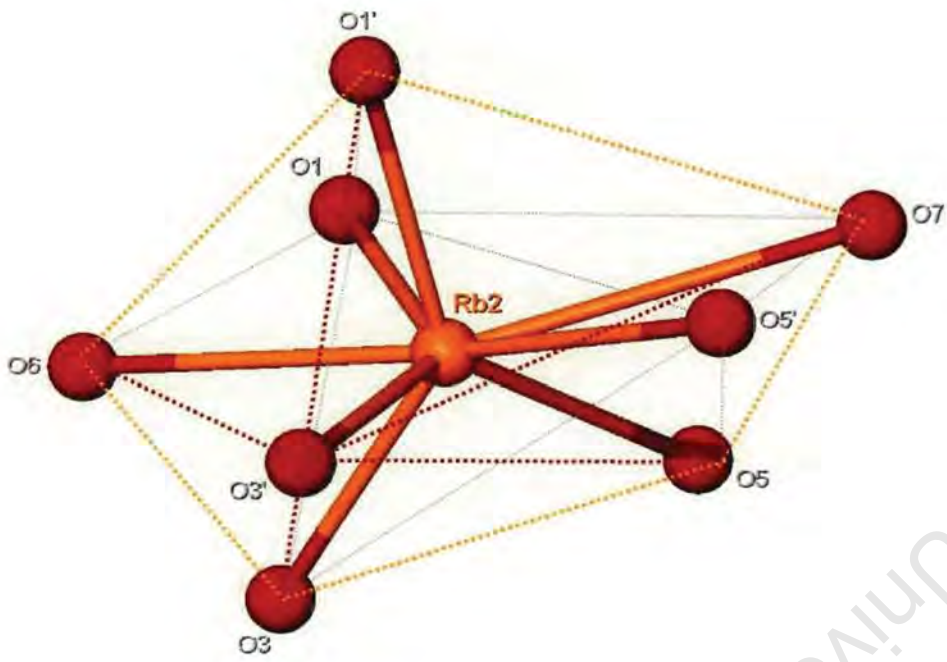

Bond angles:

O3-Rb2-O3' = 87.45°	O6-Rb2-O7 = 155.07°
O3-Rb2-O5 = 81.00°	O6-Rb2-O5' = 158.35°
O5-Rb2-O5' = 82.87°	O6-Rb2-O5 = 118.07°
O5'-Rb2-O3' = 75.86°	O3-Rb2-O5' = 136.56°
O1'-Rb2-O6 = 88.11°	O3-Rb2-O7 = 132.79°
O1-Rb2-O7 = 99.36°	O3-Rb2-O1' = 137.04°
O7-Rb2-O1' = 88.74°	
O3'-Rb2-O6 = 84.68°	Bond distances:
O6-Rb2-O3 = 49.96°	O3···Rb2 = 2.903Å
O3-Rb2-O1 = 76.52°	O3'···Rb2 = 2.947Å
O1-Rb2-O5 = 80.83°	O6···Rb2 = 3.304 Å
O5-Rb2-O7 = 52.25°	O1···Rb2 = 3.002Å
O7-Rb2-O5' = 42.98°	O1'···Rb2 = 2.831Å
O5'-Rb2-O1' = 78.91°	O5···Rb2 = 2.913Å
O1'-Rb2-O3' = 78.51°	O5'···Rb2 = 3.189Å
O1-Rb2-O1' = 87.72°	O7···Rb2 = 3.800Å
O1-Rb2-O3' = 138.67°	
O1-Rb2-O5' = 139.51°	
O3'-Rb2-O1 = 138.67°	
O3'-Rb2-O5 = 134.42°	
O3'-Rb2-O7 = 118.83°	

Figure 4.32: Stick-and-ball representation of irregular dodecahedral geometry around rubidium, Rb2, ion in **H_2 • Rb** (shown by dotted lines) with its related bond distances and angles.

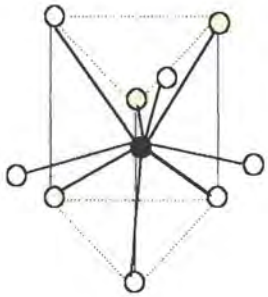

Figure 4.33: Schematic representation of the structure of many 9-coordinate complexes.

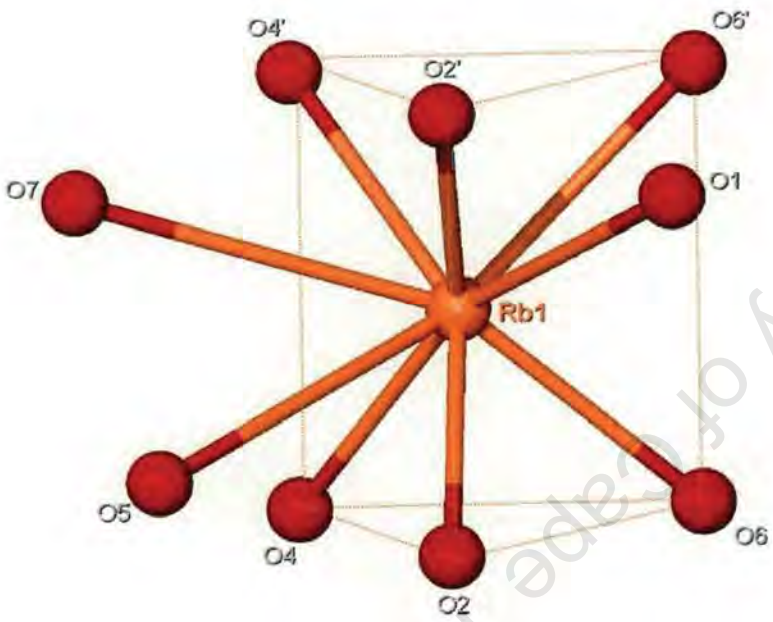

Bond angles:

O2'-Rb1-O6' = 67.80°	O4'-Rb1-O1 = 112.40°
O6-Rb1-O6' = 84.68°	O4'-Rb1-O7 = 50.72°
O6-Rb1-O2 = 71.49°	O2'-Rb1-O2 = 85.91°
O2-Rb1-O4 = 83.17°	O2'-Rb1-O6 = 124.20°
O4-Rb1-O4' = 88.93°	O2'-Rb1-O4 = 145.67°
O4'-Rb1-O2' = 81.78°	O2'-Rb1-O1 = 39.63°
O2-Rb1-O1 = 75.10°	O2'-Rb1-O5 = 75.66°
O2-Rb1-O5 = 45.79°	O2'-Rb1-O7 = 117.59°
O2-Rb1-O7 = 94.42°	O6-Rb1-O4' = 124.20°
O6-Rb1-O1 = 84.81°	O6-Rb1-O4 = 82.57°
O6-Rb1-O5 = 114.10°	O6'-Rb1-O4' = 79.20°
O6-Rb1-O7 = 157.55°	O2-Rb1-O4' = 145.13°
O6'-Rb1-O5 = 143.29°	O5-Rb1-O7 = 48.77°
O6'-Rb1-O7 = 117.59°	Bond distances:
O6'-Rb1-O1 = 53.83°	O6···Rb1 = 2.899Å
O6'-Rb1-O4 = 142.56°	O2···Rb1 = 2.926Å
O6'-Rb1-O2 = 125.40°	O4···Rb1 = 2.885Å
O4-Rb1-O1 = 157.44°	O5···Rb1 = 3.774Å
O4-Rb1-O5 = 73.42°	O7···Rb1 = 3.637Å
O4-Rb1-O7 = 78.36°	O4'···Rb1 = 2.888Å
O4'-Rb1-O5 = 99.42°	O1···Rb1 = 3.421Å
	O2'···Rb1 = 3.007Å
	O6'···Rb1 = 3.093Å

Figure 4.34: Irregular trigonal prismatic coordination of oxygen ligands about a central rubidium, Rb1, ion in $\mathbf{H_2 \bullet Rb}$ (shown by dotted lines) with the listed related bond distances and bond angles.

Distances between the host anions and rubidium ions are summarised in chapter 5.

MOLECULAR STRUCTURE AND CRYSTAL PACKING

$H_2 \bullet Cs$

H_2: 5-(3,5-Dicarboxyphenylethynyl)-isophthalic acid

Cs: caesium

$[C_{18}H_6O_8]^{-4} \cdot 4Cs^{+4} \cdot 6H_2O$

Space group: $P2_1/n$

Unit cell parameters: a = 4.2667 (9) b = 18.4341(3) c = 16.8981(1) /Å

β = 94.742(2) /°

Unit cell volume = 1324.5(5) $Å^3$

Z = 2

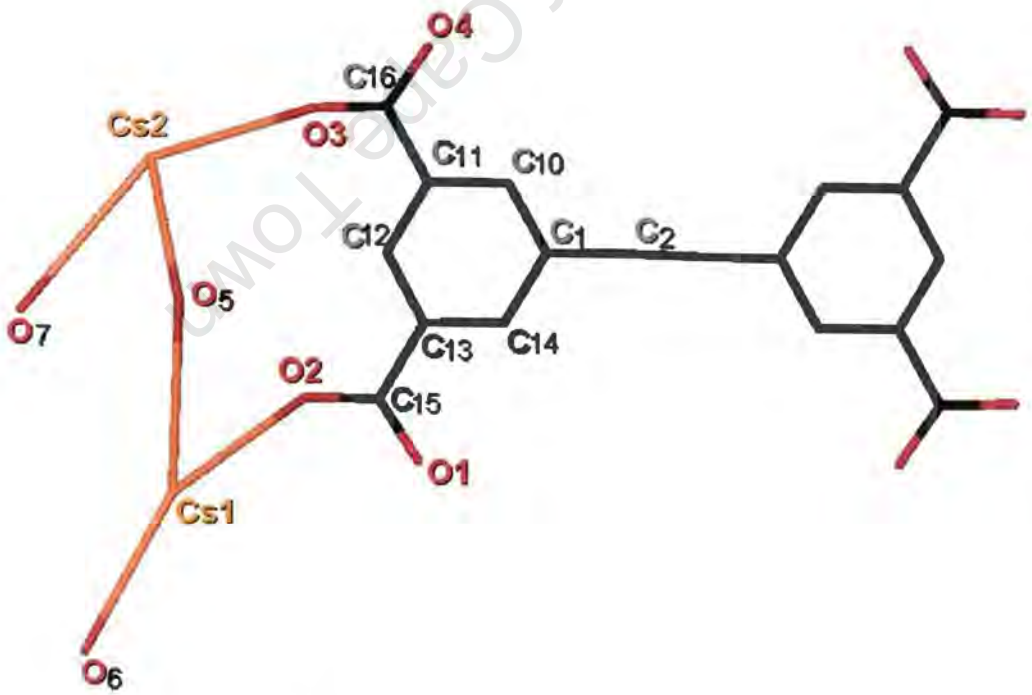

Figure 4.35: $H_2 \bullet Cs$ numbering scheme

$H_2 \bullet Cs$

H_2 • Cs hydrated metal salt crystallises in the monoclinic crystal system. The centrosymmetric space group was indicated by the mean value for the intensity data, $|E^2-1| = 0.937$. The space group, $P2_1/n$, was then indicated by systematic absences in the diffraction data. The crystal structure was solved and fully refined in this space group. The data collection yielded a total of 7608 reflections, of which 2923 were unique. The data were merged and 2531 reflections were observed. The structure was then solved by direct methods using program SHELX-86.

Positions of all non-hydrogen atoms of the host anions, guest cations and water molecules in the asymmetric unit were located by direct methods. Two caesium ions were placed with certainty, since their electron density peaks were greatest in magnitude compared to the other peaks attributed to carbon and oxygen atoms. Cs1 and Cs2, were found to be bonded to carboxylate oxygens of the host.

All of the non-hydrogen atoms were refined with anisotropic temperature factors while all of the hydrogen atoms were refined isotropically. The hydrogen atoms of the water molecules were refined with isotropic temperature factors and no bond length constraint. Aromatic hydrogens of the host anion however, were geometrically placed in idealised positions with bond length constraint and refined with linked thermal parameters. The final $R_1 = 0.0293$. The **H_2 • Cs** structure is isostructural with the **H_2 • Rb** structure with respect to the cell dimensions, space group as well as atomic coordinates. The unit cell volume of **H_2 • Cs** is slightly larger due to the bigger size of the caesium ions.

The packing and hydrogen bonding interactions: **H_2 • Cs** hydrated metal salt crystallises in $P2_1/n$ with $Z = 2$. There is a half-host anion bonded to two caesium ions and there are three water molecules in the asymmetric unit (Figure 4.35). The two carboxylate groups of the host anion are bonded to Cs1 and Cs2 ions which are in turn bonded to two water oxygen atoms and connected by a bridging oxygen atom belonging to the water molecule. The host anions of the **H_2 • Cs** hydrated metal salt are located on the centre of inversion, Wyckoff position d, while caesium ions and

water molecules are located in general positions. As was the case in the **H_2 • Rb** structure, the packing of the **H_2 • Cs** structure takes on a web-like shape (Figure 4.36a)). The hydrated metal salt **H_2 • Cs** packs in such a way that host anions of the salt are connected to each other via the caesium ions bonded to the carboxylate groups. The arrangement of host anions in the **H_2 • Cs** structure, as shown in Figure 4.36b), reveals the caesium ions to be located in spaces running parallel to the [100] direction. The aromatic rings of the host anions are stacked along the [100] direction, host anions being positioned at a small angle relative to each other (Figure 4.37a), b)).

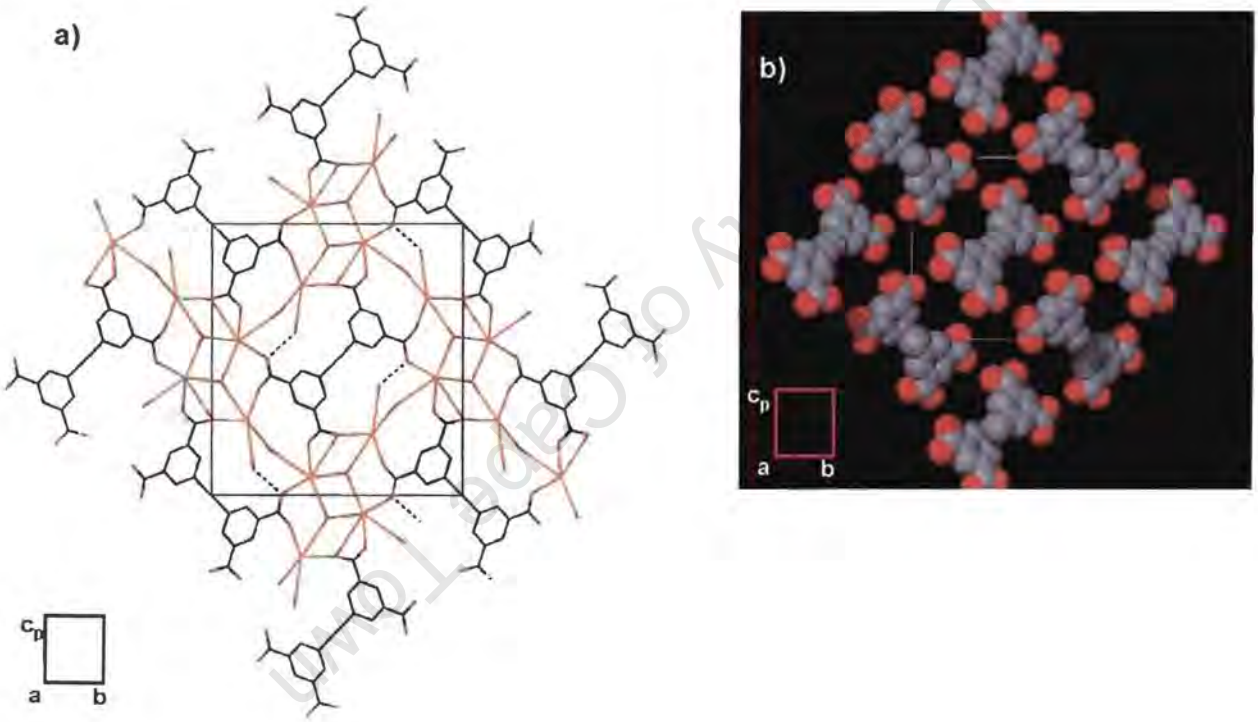

Figure 4.36: a) Packing diagram of **H_2 • Cs**, viewed down [100], showing a single layer of host anions linked by caesium ions and intermolecular hydrogen bonding interactions (shown by dotted lines), creating a web-like shape. **b)** Space-filling representation of host anions only down [100], showing the positioning of the host anions relative to each other (caesium ions are omitted for clarity).

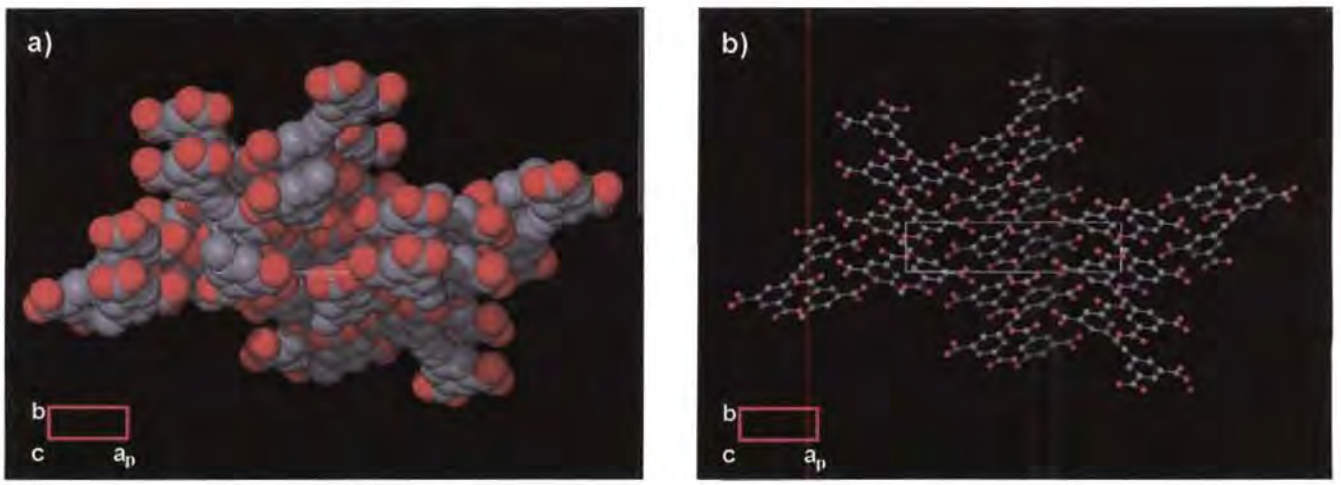

Figure 4.37: Packing of host anions in H_2 • **Cs** structure, viewed along the [001] direction: **a)** space-filling representation of host anions with caesium ions omitted for clarity, **b)** stick-and-ball representation of host molecules, with caesium ions omitted for clarity.

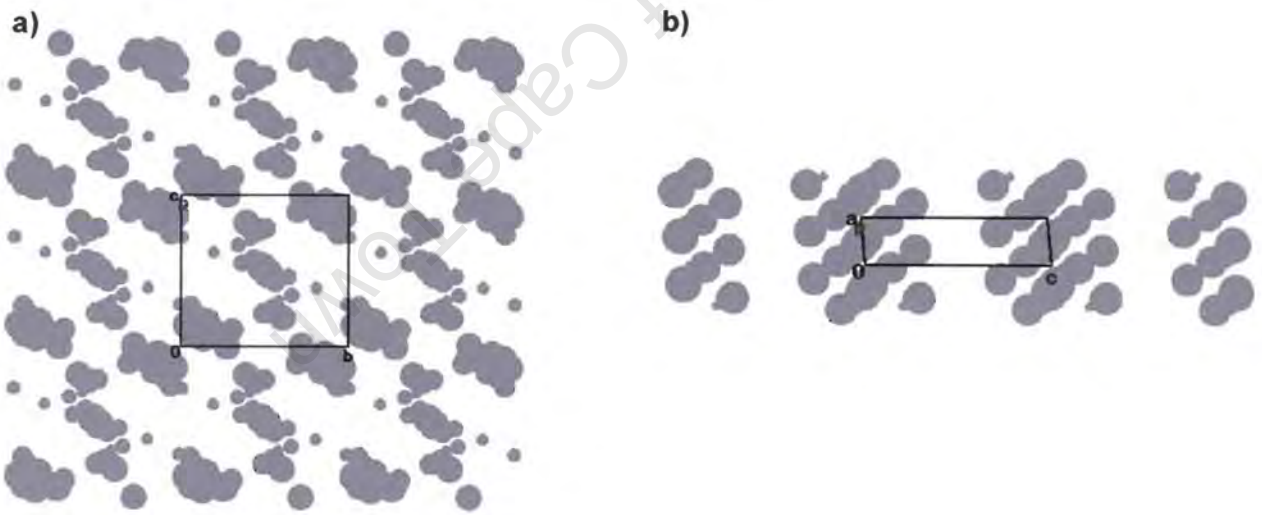

Figure 4.38: Space-filling representation of H_2 • **Cs**, **a)** at a=0Å, viewed along the [100] direction (host anions represented in grey), **b)** at b=0Å, viewed along the [010] direction, showing layers of host anions stacked together.

An extensive hydrogen-bonding network is formed between host anions and water ligands surrounding metal ions. Intermolecular hydrogen bonds include carboxylate oxygen atom bonded to carboxylate carbon and water oxygen bonded to a neighbouring caesium ion. These hydrogen-bonding interactions stabilise the **H_2 • Cs** structure.

Caesium ions can accommodate a large number of ligands due to their size. As was the case in the **H_2 • Rb** structure, **H_2 • Cs** caesium ions, Cs2, are coordinated to eight oxygen atoms that lie at the vertices of an irregular dodecahedron (Figure 4.39). Four of these eight ligands are water molecules that take part in the hydrogen bonding of the **H_2 • Cs** structure and four ligands are oxygen atoms belonging to the carboxylate groups of the host anions. The distorted trigonal pyramid is the geometry of the water molecules around the caesium ions.

Caesium, Cs1, ions are coordinated to nine oxygen atoms. This symmetrical arrangement that occurs with regularity for this coordination number is derived from a trigonal prism (Figure 4.40) by placing the three additional atoms outside the centres of the vertical faces.The irregular trigonal prism is shown by dotted lines in Figure 4.40. The ligands that are coordinated to the Cs1 ion comprise four water molecules and five oxygen atoms that belong to the host carboxylate group.

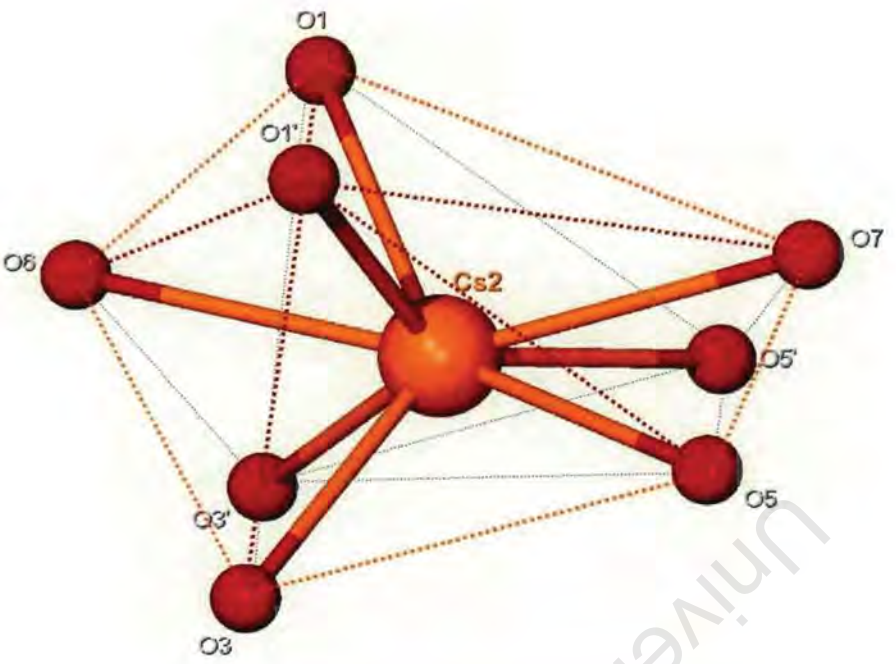

Bond angles:

O1-Cs2-O7 = 104.59°	O5-Cs2-O1' = 84.44°
O1-Cs2-O5' = 84.29°	O3-Cs2-O3' = 85.85°
O1-Cs2-O5 = 143.88°	O3-Cs2-O6 = 82.44°
O1-Cs2-O3 = 129.42°	O3-Cs2-O1' = 73.03°
O1-Cs2-O3' = 72.93°	O3'-Cs2-O6 = 48.31°
O1-Cs2-O6 = 49.06°	O3'-Cs2-O1' = 128.90°
O1-Cs2-O1' = 85.45°	O6-Cs2-O1' = 82.48°
O7-Cs2-O5' = 60.10°	
O7-Cs2-O5 = 40.75°	Bond distances
O7-Cs2-O3 = 119.81°	O1···Cs2 = 3.161Å
O7-Cs2-O3' = 140.55°	O7···Cs2 = 3.395Å
O7-Cs2-O6 = 152.79°	O5'···Cs2 = 3.189Å
O7-Cs2-O1' = 89.11°	O5···Cs2 = 3.214Å
O5'-Cs2-O5 = 83.57°	O3···Cs2 = 3.146Å
O5'-Cs2-O3 = 137.57°	O3'···Cs2 = 3.119Å
O5'-Cs2-O3' = 80.64°	O6···Cs2 = 3.435Å
O5'-Cs2-O6 = 115.39°	O1'···Cs2 = 3.127Å
O5'-Cs2-O1 = 143.54°	
O5-Cs2-O3 = 79.86°	
O5-Cs2-O3' = 137.59°	
O5-Cs2-O6 = 160.44°	

Figure 4.39: Irregular dodecahedral coordination of oxygen ligands about a central caesium, Cs2, ion in $\mathbf{H_2 \bullet Cs}$ (shown by dotted lines) with the related bond distances and bond angles.

Distances between the host anions and caesium ions are summarised in chapter 5.

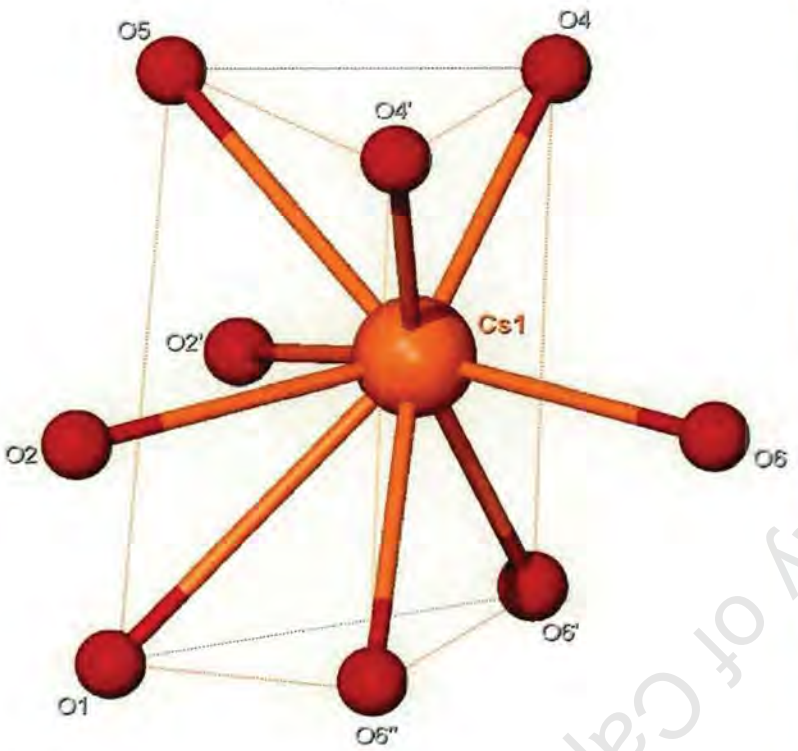

Bond angles:

O4'-Cs1-O4 = 86.92°	O4'-Cs1-O6 = 73.13°
O4'-Cs1-O6' = 162.07°	O4-Cs1-O6 = 95.97°
O4'-Cs1-O6'' = 90.99°	O4-Cs1-O6' = 94.15°
O4'-Cs1-O1 = 109.28°	O4-Cs1-O6'' = 162.88°
O4'-Cs1-O2 = 76.04°	O4-Cs1-O1 = 149.87°
O4'-Cs1-O2' = 134.38°	O4-Cs1-O2 = 135.26°
O4'-Cs1-O5 = 88.68°	O4-Cs1-O2' = 77.82°
O6-Cs1-O6' = 88.97°	O4-Cs1-O5 = 57.60°
O6-Cs1-O6'' = 67.23°	O1-Cs1-O2 = 36.67°
O6-Cs1-O1 = 112.78°	O1-Cs1-O2' = 72.73°
O6-Cs1-O2 = 117.16°	O1-Cs1-O5 = 96.45°
O6-Cs1-O2' = 150.32°	O2-Cs1-O2' = 85.20°
O6-Cs1-O5 = 149.21°	O2-Cs1-O5 = 80.61°
O6'-Cs1-O6'' = 82.73°	O2'-Cs1-O5 = 46.94°
O6'-Cs1-O1 = 78.16°	Bond distances
O6'-Cs1-O2 = 114.36°	O4'···Cs1 = 3.104Å
O6'-Cs1-O2' = 62.97°	O4···Cs1 = 3.099Å
O6'-Cs1-O5 = 107.01°	O6···Cs1 = 3.142Å
O6''-Cs1-O1 = 45.90°	O6'···Cs1 = 3.148Å
O6''-Cs1-O2 = 60.03°	O6''···Cs1 = 3.306Å
O6''-Cs1-O2' = 114.95°	O1···Cs1 = 3.691Å
O6''-Cs1-O5 = 139.38°	O2···Cs1 = 3.208Å
	O2'···Cs1 = 3.094Å
	O5···Cs1 = 3.645Å

Figure 4.40: Stick-and-ball representation of an irregular trigonal prismatic coordination around caesium, Cs1, ion in the **H_2 • Cs** structure (shown by dotted lines) with related bond distances and angles.

DISCUSSION

In this chapter the hydrated salts **H_2 • RPEA**, **H_2 • RSPEA**, **H_2 • PEA**, **H_2 • Na**, **H_2 • Rb** and **H_2 • Cs** have been described and analysed. All six structures crystallise as hydrated salts comprising the host anions, the guest cations and water molecules. In four of these structures host anions are located on the centre of inversion, while guest cations and waters of crystallisation are in general positions. However in the **H_2 • RPEA** and **H_2 • PEA** structures the host, guest and water components are all located on the general positions.

The guest components in **H_2 • RPEA**, **H_2 • RSPEA** and **H_2 • PEA** are structurally related. The **H_2 • RPEA** structure has (+)-R-1-Phenylethylamine as a guest. However, in **H_2 • RSPEA** the two enantiomers cannot be differentiated because of the disorder that is present in β-carbons of the guest cations. The **H_2 • PEA** structure contains 2-Phenylethylamine as a guest. In each of the structures the individual molecular components, are linked by an extensive series of hydrogen bonds. With the exception of the intramolecular C-H···O hydrogen bonds, all the hydrogen bonds are of N-H···O type where the nitrogen atom acts as a proton donor and the oxygen atom acts as a proton acceptor. In the two-centre hydrogen bonds, the N-H···O angles range from 160(2)° to 170(3)°. The N-O distances are in the range of 2.735(3) to 2.842(3)Å, which would describe moderately strong hydrogen bonds, since the literature values of N-O distances (oxygen atom belongs to a carboxylate group of the host anion) attain a maximum value of 3.253(7)Å[6].

The structure analysis has shown that in each of the three structures water molecules are included. These waters of crystallisation appear to play a major role in stabilising the structure, since they take part in hydrogen bonding.

In **H_2 • RPEA** the host molecules form single layers that stack in a manner of sinusoidal curves that are in a phase with each other. Guest cations are located in the interlayer spaces forming hydrogen bonds with host anions. **H_2 • RPEA** crystallises in the space group $P2_1$ (Z = 2).

H_2 • RSPEA crystallises in the centrosymmetric space group C2/c with Z = 4. The asymmetric unit contains half of the host anion and two guest cations with the host anion placed on the center of inversion, Wyckoff position b, and the guest cations occupying the general positions. The **H_2 • RSPEA** structure consists of parallel layers of host anions, with guest cations located in cross-channels generated by these layers. The planes of host and guest ions are almost perpendicular to each other.

H_2 • PEA crystallises in the orthorhombic system, space group Pbca, and has by far the largest unit cell volume of the three salt structures due to the large Z value. There is one host anion, four guest cations and five waters of crystallisation in the asymmetric unit ($H:G_1:G_2$=1:4:5) with Z = 8. The guest cations are located in channels that run in the [100] direction. The host anions form bilayers perpendicular to the b axis that in turn shape to form voids occupied by the guest cations. The structure has a large packing efficiency and is stabilised by hydrogen bonding between the host carboxylate oxygen and the guest nitrogen, which is characteristic of all three structures.

The three structures described, **H_2 • Na**, **H_2 • Rb** and **H_2 • Cs**, are examples of metal salts, solvated by water. The water plays a part in hydrogen bonding, thus stabilising the salt structure. Each host anion is bonded to the four metal ions, each *via* one O atom of the carboxylate group. Metal ions in these structures can accommodate a large number of ligands due to their size. In the **H_2 • Rb** and **H_2 • Cs** structures the metal ions are each coordinated to eight and nine oxygen atoms that lie at the vertices of an irregular dodecahedron and an irregular trigonal prism. Sodium ions, however, due to their smaller size accommodate only five and six oxygen atoms. In the case of six surrounding ligands an irregular octahedron is formed and in the case of five, an irregular square pyramidal geometry is found in the **H_2 • Na** structure.

The crystals of **H_2 • Cs** and **H_2 • Rb** hydrated metal salts are isostructural. They crystallise in the monoclinic system, space group $P2_1/n$, with Z = 2. **H_2 • Na** crystallises in the space group $P2_1/c$ (alternative setting of $P2_1/n$) with Z = 2. In all three structures metal ions are trapped in cavities created by host anions, and are also bonded to water molecules. Hydrogen bonding interactions generate a three-dimensional hydrogen bonded network. The stability of the three structures is reflected in the high onset of the complex decomposition. In the asymmetric unit of

the **H_2 • Rb** structure no H-atoms for the water molecule (O_7) could be located. This was encountered in the other two structures for some water oxygens, presumably because of disorder and/or mobility of these components.

REFERENCES for CH.3 and CH.4

1. G. M. Shedrick, SHELX-86, Crystallographic Computing 3, G. M. Shedrick, C. Kruger and R. Goddard (Eds), Oxford University Press, 1985, 175.
2. L. J. Barbour, SECTION, A computer program for the graphic display of cross sections through a unit cell, *J. Appl. Cryst.*, 32, 353, 1999.
3. J. C. Speakman, The Hydrogen Bond, Bartholomew Press, The Chemical Society, London, 1975, Chapter 1.
4. A. Bondi, *J. Phys. Chem.*, 68, 1964, 441.
5. C. M. Zakaria, G. Ferguson, A. J. Lough, C. Glidewell, *Acta Crystallographica* Section C, 57, 2001, 687-689.
6. C. M. Zakaria, G. Ferguson, A. J. Lough, C. Glidewell, *Acta Crystallographica* C57, 683-686, 2001.
7. J. E. Huheey, Inorganic Chemistry: Principles of Structure and Reactivity, Ed. 2, Harper and Row, Publishers, Inc., New York, 1978, Chapter 10.

5 HOST CONFORMATIONS

"Whatever is small, trivial or mean serves to complete the splendour of the whole."

Giordano Bruno, Dell' Infinito, Universo e Mondi (1584)

CONFORMATION OF HOST H_1

Four structures have been analysed in this thesis involving the host H_1, 1,1,6,6-Tetraphenyl-hexa-2,4-diyne-1,6-diol. The host H_1 hydroxyl groups were found to be *trans* to each other (Figure 5.1). The *trans* configuration allows tight packing of the crystal and the host molecule to be located at the inversion centre[1]. It is found that when the *trans* configuration is present the guest molecules are located in the channels formed by the packing of host molecules.

A Cambridge Structural Database[2] search showed 34 other structures involving the host H_1. The *trans* and *gauche* are the two hydroxyl group configurations characteristic of the H_1 conformation, *trans* being the more favourable one. When the *trans* conformation is adopted the guest molecules are located in channels and hydrogen bonded to host molecules.

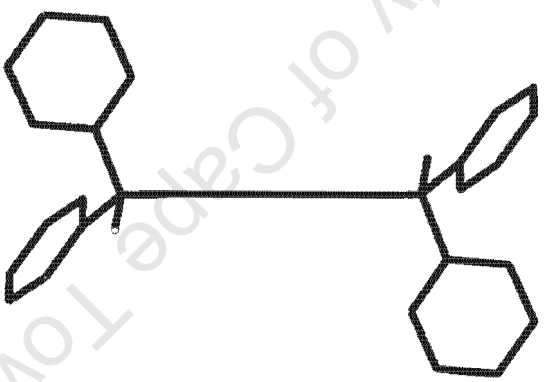

Figure 5.1: Host conformation from $H_1 \bullet$ **4PP** structure showing *trans* configuration of hydroxyl groups.

Only six structures with the *gauche* configuration were found in the search substantiating the fact that the *trans* configuration is the preferred one.

Host molecules in all four structures studied in this thesis are situated on the centrosymmetric sites. The angle between the planes of the two phenyl rings bonded to the same carbon, is the dihedral angle (Figure 5.2). Dihedral angles between the

planes of the aromatic rings are in the range 82.44(7)° to 89.8(3)°, indicating an almost perpendicular relationship between these phenyl rings. The phenyl rings of the host are essentially planar. The maximum out-of-plane deviation of all aromatic carbons from the least-squares plane is 0.0136(4)Å.

The set of three torsion angles is the second set of parameters describing the host conformation (Figure 5.2). Torsion angle τ_3 is 180° in all four structures indicating that the host molecule is situated on the centre of inversion and that the hydroxyl groups are *trans* to each other. Dihedral angles are in good agreement in all four structures. Torsion angles, τ_1 and τ_2, however vary considerably. This difference in torsion angle values is due to different packing of host and guest molecules in the crystal.

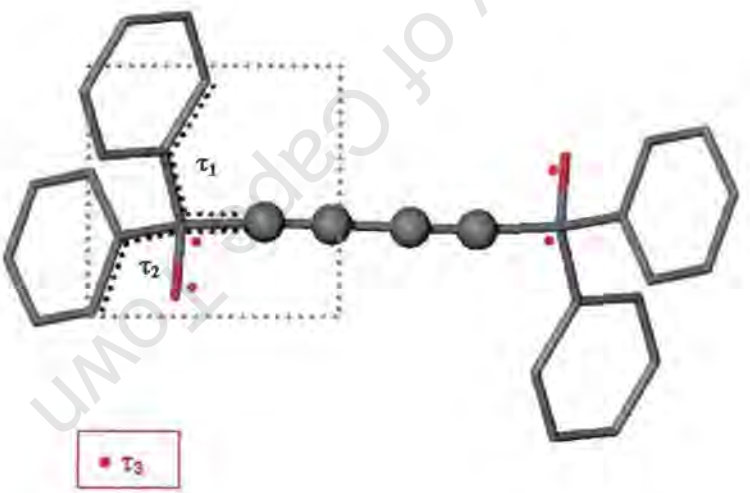

Figure 5.2: The torsion angles describing the $\mathbf{H_1}$ conformation

Table 5.1: Torsion and dihedral angles for different inclusion compounds with the same host, H_1

Complex	τ_1/°	τ_2/°	τ_3/°	*Dihedral angle/°*
H_1 • TED A	0.1(3)	63.5(8)	180	89.4(3)
H_1 • TED B	0.2(2)	64.1(8)	180	89.8(3)
H_1 • TBDA	84.3(3)	-19.1(4)	180	85.8(2)
H_1 • 4PP	-4.3(1)	-60.2(1)	180	87.99(5)
H_1 • PA	-54.9(1)	-179.1(1)	180	82.44(7)

Bond lengths for all four compounds are in close agreement with each other and compare well with the standard values[5]. Table 5.2 below shows a summary of these bond lengths. The **H_1 • TED** complex has two host molecule halves in the asymmetric unit, labelled **A** and **B**.

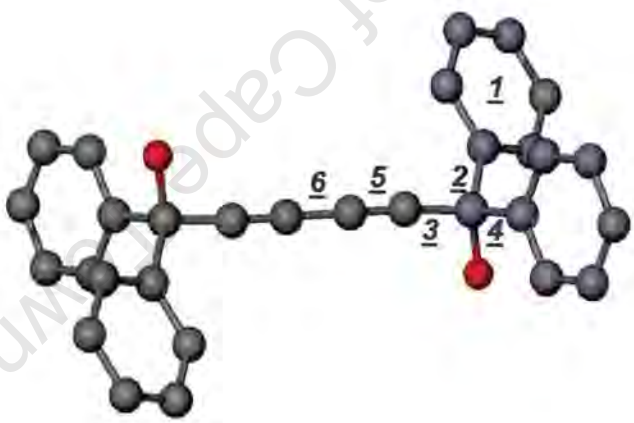

Figure 5.3: Host H_1 diagram indicating the selected bonds

Table 5.2: Bond lengths for H_1 inclusion compounds

Complex	*1 / C_{ar}~ C_{ar} /Å*	*2 / C_{ar}- C_{sp^3} /Å*	*3 / C_{sp^3}-C_{sp} /Å*	*4 / C_{sp^3}-O /Å*	*5 / C_{sp}≡C_{sp} / Å*	*6 / C_{sp}-C_{sp} / Å*
H_1• TED A	1.34(2)*	1.57(2)**	1.44(2)	1.388(9)	1.22(2)	1.47(3)
	1.43(2)*	1.53(2)**				
H_1• TED B	1.35(2)	1.58(2)	1.49(2)	1.395(9)	1.19 (2)	1.39(2)
	1.44(2)	1.53(2)				
H_1 • TBDA	1.347(5)	1.521(3)	1.486(4)	1.429(3)	1.188(3)	1.385(6)
	1.394(5)	1.531(3)				
H_1 • 4PP	1.375(2)	1.535(1)	1.488(1)	1.425(1)	1.203(1)	1.383(3)
	1.395(1)	1.538(1)				
H_1 • PA	1.358(3)	1.532(2)	1.484(2)	1.416(1)	1.203(2)	1.374(3)
	1.400(3)	1.543(2)				
Standard Values[5]	1.375-1.391 (0.013)	1.517-1.539 (0.016)	1.464-1.481 (0.012)	1.432-1.449 (0.012)	1.187-1.197 (0.010)	1.374-1.384 (0.012)

* Minimum and maximum distances between adjacent carbons in phenyl rings.

**Different bond lengths for the same type of bonding in one molecule.

The H_1 conformation has six different bond types (Figure 5.3). Their bond lengths are in good agreement with each other and with the standard values.

CONFORMATION OF HOST H_2

A Cambridge Structural Database[2] search showed that no other structures with the host H_2, 5-(3,5-Dicarboxyphenylethynyl)-isophthalic acid, have been published.

In the six hydrated salts H_2 • **RPEA**, H_2 • **RSPEA**, H_2 • **PEA**, H_2 • **Na**, H_2 • **Rb** and H_2 • **Cs** the host H_2 conformation is governed by torsion and dihedral angles as shown below in Figure 5.7 and Table 5.4. In the four out of six related structures the other half of the host molecule is generated by inversion, while in two structures, H_2 • **RPEA** and H_2 • **PEA**, the whole host molecule is present in the asymmetric unit.

Bond lengths for all six structures are in close agreement with each other (Table 5.3). Bond angles differ somewhat, between the hydrated salts comprising metal ions, H_2 • **Na**, H_2 • **Rb** and H_2 • **Cs** and the hydrated salts comprising guest cations, H_2 • **RPEA**, H_2 • **RSPEA** and H_2 • **PEA** (Table 5.4).

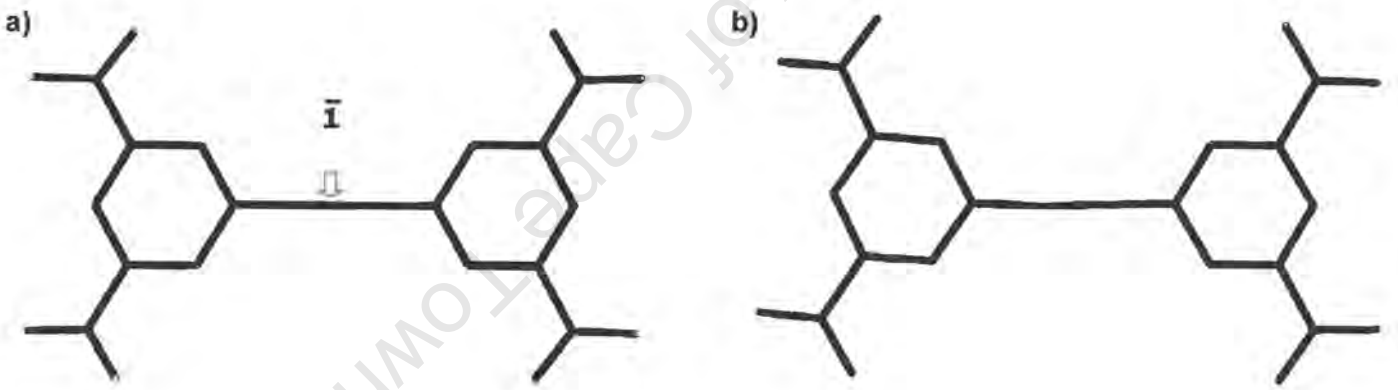

Figure 5.4: a) Conformation of host, H_2, extracted from a metal salt structure, H_2 • **Cs**, with $-COO^-$ carboxylate groups and centre of symmetry, **b)** host conformation from H_2 • **RPEA** structure with $-COO^-$ carboxylate groups involved in hydrogen bonding).

The molecular geometry of H_2 in the H_2 • **RPEA**, H_2 • **PEA** and H_2 • **RSPEA** structures is defined by five different bond types (Figure 5.5 and Table 5.3a). The bond lengths are in close agreement with the standard values[5] and compare well within the related structures. $C_{sp}{}^2$=O delocalised double bonds in carboxylate anion are in good agreement with those reported in the literature[5]. Figure 5.6 shows the host anion and guest cations extracted from the H_2 • **PEA** structure, showing the presence of carboxylate group as well as guest cations and water molecules.

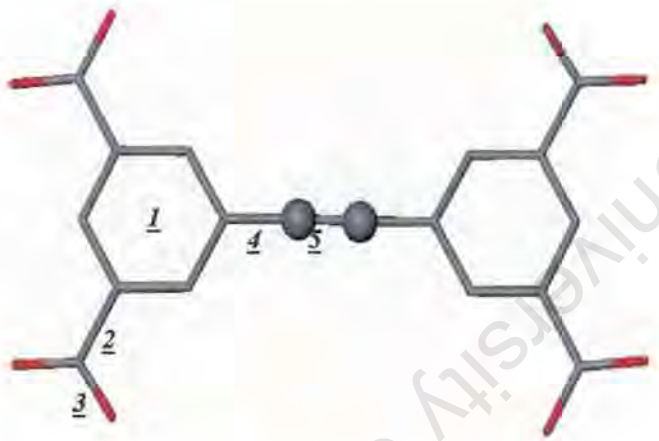

Figure 5.5: The bond lengths describing the conformation of the host.

Table 5.3a: Bond lengths for H_2 in H_2 • **RPEA**, H_2 • **PEA** and H_2 • **RSPEA**

Complex	*1 / C_{ar}~ C_{ar} /Å*	*2* / C_{ar}- $C_{sp}{}^2$ /Å*	*3 / $C_{sp}{}^2$=O*** /Å*	*4 / C_{ar}-C_{sp} / Å*	*5 / C_{sp}≡C_{sp} / Å*
H_2 • **RPEA**	1.358(6)** 1.405(6)	1.514(6) 1.530(6)	1.240(5) 1.260(5)	1.426(6) 1.445(6)	1.187(6)
H_2 • **PEA**	1.384(3) 1.399(3)	1.506(3) 1.515(3)	1.239(3) 1.269(3)	1.435(3) 1.436(3)	1.199(3)
H_2•**RSPEA**	1.379(4) 1.394(4)	1.503(5) 1.512(5)	1.244(4) 1.261(4)	1.440(4)	1.194(6)
Standard Values[5]	1.375-1.391 (0.013)	1.474-1.491 (0.014)	1.249-1.262 (0.010)	1.430-1.437 (0.006)	1.181-1.195 (0.010)

* C_{ar}-COOH

** The first line in the row reports the minimum bond length found and the second line represents the maximum bond length.

*** $C_{sp}{}^2$=O refers to delocalised double bonds in carboxylate anion,

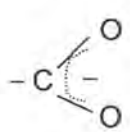

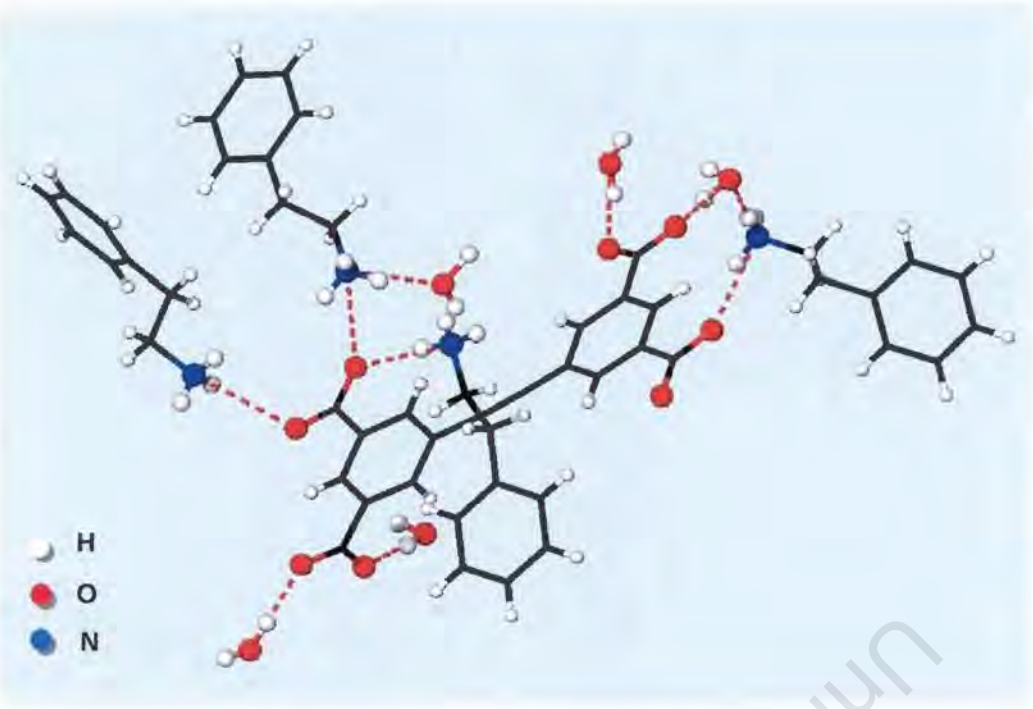

Figure 5.6: Representation of the host carboxylate groups hydrogen bonded to the guest $-NH_3^+$ groups and water molecules.

Table 5.3b: Bond lengths for H_2 in H_2 • **Na**, H_2 • **Rb** and H_2 • **Cs**

Complex	*1 / C_{ar}~ C_{ar} /Å*	*2* / C_{ar}- C_{sp}^2 /Å*	*3 / C_{sp}^2=O** /Å*	*4 / C_{ar}-C_{sp} / Å*	*5 / C_{sp}≡C_{sp} / Å*
H_2 • **Na**	1.387(5) 1.398(5)	1.506(5) 1.520(5)	1.250(4) 1.269(4)	1.432(5)	1.208(7)
H_2 • **Cs**	1.386(6) 1.399(6)	1.508(6) 1.516(6)	1.251(5) 1.262(5)	1.436(6)	1.195(9)
H_2 • ***Rb***	1.381(8) 1.403(8)	1.497(8) 1.522(8)	1.245(8) 1.266(8)	1.441(8)	1.197(12)
Standard Values[5]	1.375-1.391 (0.013)	1.495-1.512 (0.014)	1.249-1.262 (0.010)	1.430-1.437 (0.006)	1.181-1.195 (0.010)

*C_{ar}-COO^-

** C_{sp}^2=O refers to delocalised double bonds in carboxylate anion,

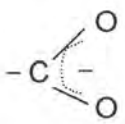

All of the aromatic rings were found to be planar with the maximum out-of-plane deviation of any aromatic carbon from the aromatic ring plane 0.0099(2)Å.

The molecular structure of H_2 in the hydrated metal salt structures, H_2 • **Na**, H_2 • **Cs** and H_2 • **Rb**, is defined by five different bond types (Figure 5.5 and Table 5.3b). The bond lengths are in close agreement with the standard values[5]and compare well within the related structures. $C_{sp}{}^2$=O is a delocalised double bond in carboxylate anion of the host.

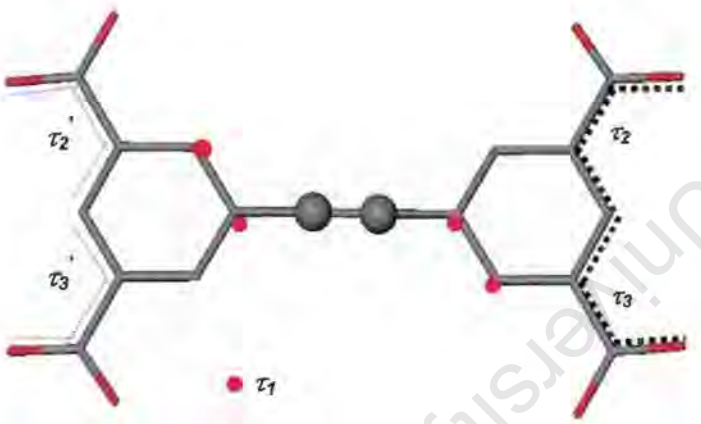

Figure 5.7: The torsion angles defining the structure conformation of the host H_2

Table 5.4: Torsion and dihedral angles defining host H_2

Complex	τ_1/°	τ_2/°		τ_3/°		*Dihedral angle/°*
H_2 • **RPEA**	-6.5	15.2	17.1*	0.6	0.7*	6.71(5)
H_2 • **RSPEA**	180	-11.7		8.3		4.41(9)
H_2 • **PEA**	8.0	-3.3	-3.6*	3.5	2.0*	8.15(4)
H_2 • **Na**	180	16.8		14.8		37.81(9)
H_2 • **Rb**	180	-9.1		12.6		27.3(4)
H_2 • **Cs**	180	-12.2		12.6		33.2(4)

* These values refer to the torsion angles marked as τ_2' and τ_3'. They are only reported for the structures with host anions located in general positions.

Dihedral angles are in the range 6.71(5)° to 37.81(9)° indicating that the planes of phenyl rings are almost parallel.

In the table below the distances within hydrated metal salt structures were summarised. These distances include the metal ion specific to the respective structure and the oxygen atom belonging to the $-COO^-$ group of the host. The bond lengths are in good agreement with the standard values. [3,4]

Table 5.5: Bond distances between metal ion and H_2 host anion

Complex	**H_2 • Na**	**H_2 • Cs**	**H_2 • Rb**
M*-O/Å	2.381(3) 2.416(3)	3.093(3) 3.169(4)	2.831(5) 2.947(6)
Standard Values	2.44(2)[5]	2.627(1) 3.066(1)[3]	2.31[4]

* M = Na, Rb, Cs respectively

REFERENCES

1. C. P. Brock, J. P. Dunitz, Chem. Mater., Vol. 6, 8, 1994, 1118.
2. Cambridge Structural Database and Cambridge Structural Database System, Version 5.22 (October 2001), Cambridge Crystallographic Data Centre, University Chemical Laboratory, Cambridge, England.
3. A. Simon, W. Bramer, H.J. Deiseroth, Inorganic Chemistry, 17, 875, 1978.
4. N. Acquista, S. Abramowitz, *J. Chem. Phys.*, 51, 2911, 1969.
5. International Tables for Crystallography, Vol. C, 691-706, 684, 1992.

6 CONCLUSION

"True sciences are those which have penetrated through the senses as a result of experience and thus silencing the tongues of disputants, not feeding investigators on dreams but always proceeding successively from primary truths and established principles, in a proper order towards the conclusion."

-Leonardo, Codex Urbinas Latinus

The crystal structures of inclusion compounds with host H_1 and hydrated salt compounds with host H_2 have been elucidated and their thermal stability analysed by monitoring decomposition reactions using different thermal techniques such as TG, DSC and HSM.

Host H_1 is described as a 'wheel-and-axle' host, by virtue of its shape. It is designed to be awkwardly shaped, bulky and highly symmetrical and also containing functional groups that are capable of hydrogen bonding to the guest. This design facilitates the inclusion of the guest compounds.[1,2]

The inclusion compounds **H_1 • TED**, **H_1 • TBDA**, **H_1 • PA** and **H_1 • 4PP** are classified as *coordinato-clathrates* due to their coordinative host-guest interactions.[3] These clathrates comprise hydrogen bonded networks throughout their crystal lattices. This is attributed to the presence of potential hydrogen bond donor and acceptor groups situated on the host and guest components. This results in clathrates that are stabilised by intermolecular host-guest interactions. In addition to host-guest hydrogen-bonding interactions the **H_1 • PA** structure is stabilised by intermolecular guest-guest π-π interactions while the **H_1 • 4PP** structure is stabilised by moderately strong intermolecular host-guest O-H···N interactions.

Host H_1 is found to form host-guest inclusion compounds, where its hydroxy moieties adopt an energetically more favourable *trans* conformation. The guest molecules are located in the channels formed by the host molecules. The ratio of the host to guest molecules in **H_1 • TED** is 1 to 1, while in the other inclusion compounds it is 1 to 2, which is the ratio generally found in the channel clathrates[4].

Thermal analysis for **H_1 • TED**, **H_1 • TBDA**, **H_1 • PA** and **H_1 • 4PP** inclusion compounds shows a high thermal stability, with the guest molecules being released only at the onset of host decomposition.

Host H_2 has a molecular backbone comprising two phenyl rings with four carboxylate groups attached to each ring. In comparison to H_1 inclusion compounds, host-guest complexation was found to be accompanied by solvation by water molecules in all six structures. Host H_2 contains all of the structural characteristics that should favour host-guest complexation, in that it is bulky and rigid and packs inefficiently allowing

for the accommodation of guests in voids. It also contains carboxylate moieties, which are efficient hydrogen bond donors and acceptors.

The stability of inclusion compounds can be determined by measuring the onset temperature of guest release using DSC. The higher the onset temperature the more stable the complex. For the salt compounds, **H_2 • RPEA**, **H_2 • PEA** and **H_2 • RSPEA**, guest release is a multistep process, therefore allowing the precise determination of stoichiometries and H:G ratios.

The clathrates, **H_2 • RPEA**, **H_2 • RSPEA** and **H_2 • PEA**, are stabilised by intermolecular host-guest interactions which comprise a hydrogen-bonded framework. The hydrogen bond framework includes symmetry related three-centre N-H···$(O)_2$ and two-centre N-H···O hydrogen bonds, with nitrogen belonging to the guest cations and oxygen atoms to the carboxylate moieties and water molecules. We find that for these clathrates, the H:G ratio is 1:4. Hence in comparison with the H_1 clathrates, the H:G ratios are in accordance with the number of functional groups of the host.

H_2 • Na, **H_2 • Rb** and **H_2 • Cs** represent self-assembled supramolecules in which metal ions are employed as links in the radiating strands. Host **H_2** acts as a stabilising agent for bound alkali metal ions. Therefore it tends to yield metal complexes that exhibit substantial thermal stability. As well as acting as centres for ligand binding and orientation, the presence of metal ions in many cases introduces electrochemical and/or photochemical properties that confer additional functionality to the final supramolecular structures[5].

Other type of interactions encountered in these structures is hydrogen bonding. These interactions are much weaker than the covalent connection of metal ions. The hydrogen-bonding network comprises two-centre hydrogen bonds between oxygens from water molecules surrounding the metal ions and host carboxylate oxygens. Each host anion is bonded to the four metal ions, each *via* one O atom of the carboxylate group. Metal ions in these structures can accommodate a large number of ligands due to their size. In the **H_2 • Rb** and **H_2 • Cs** structures the metal ions are coordinated to eight and nine oxygen atoms that lie at the vertices of an irregular dodecahedron and an irregular trigonal prism. Sodium ions, however, due to their smaller size

accommodate only five and six oxygen atoms. In the case of six surrounding ligands an irregular octahedron is formed and in the case of five, an irregular square pyramidal geometry is found in the **H_2 • Na** structure.

The thermal stability of **H_2 • Na**, **H_2 • Rb** and **H_2 • Cs** hydrated metal salts was determined by measuring the onset temperature of complex decomposition using DSC. The onset temperatures being very high (above 300°C) implies very stable structures. The hydrated metal salts **H_2 • Na**, **H_2 • Rb** and **H_2 • Cs** comprise metal ions that belong to the same group of elements and have similarities in chemical and physical properties. We find that similarities, such as decomposition onset, molecular packing and orientation together with other structural characteristics, are also present in the complexed metal salts. For consistency of these results we tried to grow the potassium salt, but we did not obtain suitable crystals, despite very many tries and differing conditions.

Thermal analysis proved to be a very useful investigative tool since precise stoichiometries could be determined and insight into the manner of decomposition and strength of host-guest binding could be derived. TG was used to detect the presence and concentration of guest components present in host-guest inclusion compounds and to study the guest release behaviour. DSC was used to detect the onset of the melting of host-guest compounds with HSM to follow both methods visually. The guest release onset or decomposition onset served as a method to examine the strength and the stability of the crystal structure.

REFERENCES

1. E. Weber, I. Csöregh, B. Stensland, M. Czugler, *J. Amer. Chem. Soc.*, 106, 1984, 3297-3306.
2. E. Weber, *J. Mol. Graphics*, 7, 1989, 12.
3. E. Weber, *Topics in Current Chemistry*, 140, 2. (1987).
4. J. Lipkowski, Inclusion Compounds, Vol. 1, ed. J. Atwood, J. E. D. Davies, D. D. MacNicol, 1984, Chapter 3.
5. L. F. Lindoy, I. M. Atkinson, Self-Assembly in Supramolecular Systems, Cambridge University Press, Cambridge, UK, 2000, Chapter 7.

APPENDIX A

The supplementary material for the crystal structures analysed in this work is stored on a CD labelled APPENDIX A.

The supplementary material comprises files for each structure named as following:

- *Structurename*.RES (e.g. H1TED.RES). These files are SHELX files and allow one to visualise the structures.
- *Structurename*.FCF (e.g. H1TED.FCF). These files comprise tables of observed and calculated structure factors.
- *Structurename*.TEX (e.g. H1TED.TEX). These files comprise tables of atomic coordinates, isotropic and anisotropic displacement parameters bond lengths and bond angles.

All files are text files and can be viewed in an editor under any of the following operating systems: DOS, WINDOWS 3.1/95/98/2000NT, APPLE MAC, Linux or UNIX.

The files are located under the directory named after the chapter in which the structure is described and subdirectory named after the structure code (e.g. \APPENDIX A\CH.3\ H1 . TED\).

Filenames for tables do not match the structurenames in the files for crystal structures. This is due to the structure codes being changed at the end of this work.